

CZECH TECHNICAL UNIVERSITY IN PRAGUE
FACULTY OF MECHANICAL ENGINEERING
DEPARTMENT OF AUTOMOTIVE, COMBUSTION AND RAILWAY
ENGINEERING



THEORETICAL AND EXPERIMENTAL ANALYSIS OF
INDUCTION MOTOR PARAMETERS

MASTER'S THESIS

Student Name: **MOHITH KUMARAN SATYAN BABU**

Personal ID Number: 491071

Study Program: Master of Automotive Engineering

Branch of Study: Advanced Powertrains

Master's Thesis Supervisor: **doc.Ing. Pavel Mindl. CSc**

Workplace of Supervisor: Department of Electric Drives and Traction, FEE



MASTER'S THESIS ASSIGNMENT

I. Personal and study details

Student's name: **Satyan Babu Mohith Kumaran** Personal ID number: **491071**
Faculty / Institute: **Faculty of Mechanical Engineering**
Department / Institute: **Department of Automotive, Combustion Engine and Railway Engineering**
Study program: **Master of Automotive Engineering**
Branch of study: **Advanced Powertrains**

II. Master's thesis details

Master's thesis title in English:

Theoretical and experimental analysis of induction motor parameters

Master's thesis title in Czech:

Teoretická a experimentální analýza parametrů asynchronního motoru

Guidelines:

Make theoretical and experimental analysis of static and dynamic parameters of electric drive with induction motor. Electric motor parameters: P=28 kW, nominal supply voltage up to 180 V, 100 Hz, nominal revolutions 2950 min⁻¹, Revolution range 0 – 3500 min⁻¹. For experimental evaluation use laboratory workplace in VTP Rožtoky.

Bibliography / sources:

L1/ A. Bosović, Š. Mašić, S. Smak: Computing and Measuring Dynamic Characteristics of the Induction Motor
https://www.researchgate.net/publication/251960998_Computing_and_measuring_dynamic_characteristics_of_the_induction_motor
/2/ Institute for Power Electronics and Electrical Drives, RWTH Aachen University Fang Qi Daniel Scharfenstein Claude Weiss Infineon Technologies AG Dr. Clemens Müller Dr. Ulrich Schwarzer
Motor Handbook, Version: 2.1, Release Date: 12.03.2019
https://www.infineon.com/dgdl/Infineon-motorcontrol_handbook-AdditionalTechnicalInformation-v01_00-EN.pdf?fileId=5546d4626bb628d7016be6a9aa637e69
/3/ Abdel-Rehim, Yousef, "Parameter identification of induction motor" (2015). Graduate Theses, Dissertations, and Problem Reports. 5018. <https://researchrepository.wvu.edu/etd/5018>
<https://core.ac.uk/download/pdf/230449802.pdf>
/4/ Robotec manual
Induction motor parameters calculation
<https://www.robotecq.com/applications/all-blogs/497-induction-motor-parameters-calculation>

Name and workplace of master's thesis supervisor:

doc. Ing. Pavel Mindl, CSc., Department of Electric Drives and Traction, FEE

Name and workplace of second master's thesis supervisor or consultant:

Date of master's thesis assignment: **29.10.2021** Deadline for master's thesis submission: **05.01.2022**

Assignment valid until:

doc. Ing. Pavel Mindl, CSc.
Supervisor's signature

doc. Ing. Oldřich Vitek, Ph.D.
Head of department's signature

prof. Ing. Michael Valášek, DrSc.
Dean's signature

CVUT-CZ-ZDP-2015.1

© ČVUT v Praze, Design: ČVUT v Praze, VIC

III. Assignment receipt

The student acknowledges that the master's thesis is an individual work. The student must produce his thesis without the assistance of others, with the exception of provided consultations. Within the master's thesis, the author must state the names of consultants and include a list of references.

09/11/2021
Date of assignment receipt

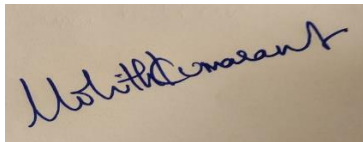
Mohith Kumaran
Student's signature

Declaration

I hereby declare that I am the sole author of the thesis titled “Theoretical and Experimental Analysis of Induction Motor Parameters”. I duly marked out all quotations. The used literature and sources are stated in the attached list of references.

Place: Prague, Czech Republic

Date: 30/12/2021

A photograph of a handwritten signature in blue ink on a light-colored surface. The signature is written in a cursive style and reads "Mohith Kumaran Satyan Babu".

Mohith Kumaran Satyan Babu

Acknowledgement:

I hereby wish to express my appreciation and gratitude to the supervisor of my thesis, doc. Ing. Pavel Mindl.CSc., for his continuous support, guidance, patience and understanding as well as for providing crucial information and assistance.

I am immensely grateful to my father, Mr. K.V. Satyan Babu, mother Mrs.V. Karpagavalli and my grandmother V. Karpagam for providing me continuous emotional and moral support and direction to bring this thesis to a successful conclusion. I would also like to thank my sister Ms. Yogitha Satyan Babu for her constant support and unwavering faith in my talents.

I would like to thank my friends Mr. Sai Kalyan Achanta, Mr. Kanishka Mathur, Mr. Rahul Jaiswal, Ms. Akshaya, Ms. Amrisha Arif and Mr. Deepak for providing me moral support and constantly encouraging.

Abstract

This diploma thesis is focused on modeling, simulation and experimental verification of electric drive with induction motor parameters using vector control of magnetic field. The aim of my work is to simulate a vector-controlled electric drive with an induction motor. Then to compare the results of stator current simulation in selected operating modes with measured values on a real drive, operated in standard mode $U / f = \text{constant}$ and in optimized mode with minimum current for required mechanical torque. Laboratory measurements were performed at the experimental workplace of CTU - VTP in Roztoky. The simulation model is created in the MATLAB - SIMULINK software environment, edition R2021b.

Keywords:

Three-Phase Induction Motor, Vector Control, Field Oriented Control, MATLAB/SIMULINK edition R2021b

Abstrakt

Tato diplomová práce je zaměřena na modelování, simulaci a experimentální ověřování parametrů elektrického pohonu s indukčním motorem využívajícím vektorové řízení magnetického pole. Cílem mé práce je simulovat vektorově řízený elektrický pohon s indukčním motorem a porovnat výsledky simulace statorových proudů ve vybraných pracovních režimech s naměřenými hodnotami na reálném pohonu, provozovaného ve standardním režimu $U/f = \text{konstanta}$ a v optimalizovaném režimu s minimálním proudem pro požadovaný mechanický moment. Laboratorní měření byla prováděna na experimentálním pracovišti ČVUT – VTP v Roztokách. Simulační model je vytvořen v programovém prostředí MATLAB – SIMULINK, verze R2021b.

Klíčová slova: Třífázový indukční motor, vektorové řízení, vektorové řízení magnetického pole, MATLAB - SIMULINK verze R2021b.

Contents

| | |
|--|----|
| Abstract..... | 5 |
| List of Figures..... | 8 |
| List of Equations..... | 11 |
| List of Tables..... | 13 |
| Introduction..... | 14 |
| Literature Survey..... | 15 |
| Three Phase Induction Machines..... | 17 |
| Construction of Three-Phase Induction Motor..... | 17 |
| Stator..... | 17 |
| Rotor..... | 18 |
| Working of a Squirrel Cage Induction Motor..... | 20 |
| Rotating Magnetic Field..... | 20 |
| Torque Production..... | 21 |
| Torque Speed Curve..... | 22 |
| Stator Inductances..... | 23 |
| Rotor Inductance..... | 25 |
| Flux Linkages..... | 26 |
| Circuit Model of a Three-Phase Induction Machine..... | 27 |
| Voltage Equations..... | 27 |
| Machine Model in qd0 Reference Frame..... | 28 |
| Voltage Equations qd0..... | 29 |
| Flux Linkage Equations qd0..... | 29 |
| Torque Equation qd0..... | 30 |
| Induction Machine Equations in Synchronous Rotating Reference Frame..... | 31 |
| Power Electronic Devices..... | 32 |
| Rectifier..... | 32 |
| Uncontrolled Rectifiers..... | 34 |
| Half Wave Rectifier..... | 34 |
| Full Wave Rectifier..... | 34 |
| Inverter..... | 35 |
| Pulse Width Modulation Inverters..... | 38 |

| | |
|---|----|
| Programmed PWM Technique | 39 |
| Sinusoidal PWM Technique | 39 |
| Space Vector PWM | 40 |
| Overmodulation | 41 |
| Motor Control | 42 |
| Scalar V/F Control Method..... | 43 |
| Vector Control | 46 |
| Direct Torque Control..... | 47 |
| PID Controllers | 47 |
| Proportional response | 48 |
| Integral Response..... | 48 |
| Derivative Response | 48 |
| Design Considerations of Control System..... | 49 |
| Selection of Bandwidth for Current Control..... | 50 |
| Speed Control Design | 51 |
| Experimental Procedure..... | 52 |
| Simulation Using MATLAB Simulink..... | 55 |
| Simulation Results | 59 |
| Steady State Analysis..... | 59 |
| Transient Analysis: | 76 |
| Conclusion | 84 |
| List of Abbreviations | 85 |
| Bibliography | 86 |

List of Figures

| | |
|--|----|
| Figure 1:Stator Components | 18 |
| Figure 2:Squirrel Cage Construction | 19 |
| Figure 3:Wound Rotor | 19 |
| Figure 4:Induction motor Complete Construction..... | 19 |
| Figure 5:mmf distribution in three phase windings of stator[3] | 20 |
| Figure 6:Torque Vs Speed Curve | 22 |
| Figure 7: Single Phase inductance in Induction machine | 24 |
| Figure 8:Ideal circuit of Induction Motor | 27 |
| Figure 9:Relationship between abc and dq0 quantities | 28 |
| Figure 10:Equivalent Circuit of IM in synchronous reference frame..... | 31 |
| Figure 11:Forward and Reverse Biased..... | 33 |
| Figure 12:Overview of Rectifiers | 33 |
| Figure 13:Half Wave Rectifier | 34 |
| Figure 14:Full wave rectifier configuration..... | 34 |
| Figure 15:Voltage Source Inverter Circuit Configuration | 36 |
| Figure 16:DC Source Short Circuit [8]..... | 36 |
| Figure 17:Circuit Configuration when both switches are OFF [8]..... | 37 |
| Figure 18:Sinusoidal PWM | 40 |
| Figure 19:SVPWM Output Vectors in complex plane [8] | 41 |
| Figure 20:Overmodulation in SPWM and SVPWM [8]..... | 42 |
| Figure 21:Overmodulation Region [8] | 42 |
| Figure 22:VFD Control Methods [1] | 42 |
| Figure 23:Voltage Vs Frequency relation in Scalar Control [16]..... | 44 |
| Figure 24:CVH Basic layout [16]..... | 45 |
| Figure 25:Closed Loop CVH System [16] | 45 |
| Figure 26:IFOC Control Architecture Layout [1]..... | 46 |
| Figure 27:DTC Layout..... | 47 |
| Figure 28:Block diagram of a typical closed loop system [12] | 47 |
| Figure 29:Basic Layout of PID controller | 49 |
| Figure 30:Gain Margin Vs Frequency [6] | 50 |
| Figure 31:Block Diagram of a synchronous frame current regulator [6] | 50 |
| Figure 32:Speed Control PI Loop [6] | 51 |
| Figure 33:Block Diagram of Test bench..... | 53 |

| | |
|---|----|
| Figure 34:Induction Motor Connected to Dynamometer | 53 |
| Figure 35:Measuring workplace with measured motor TEM 112 M04 | 54 |
| Figure 36:Measurement and Control System | 54 |
| Figure 37:Generic FOC Algorithm for IM Speed Control [9]..... | 56 |
| Figure 38:Simulink Model Outline..... | 58 |
| Figure 39:Reference Input | 59 |
| Figure 40:Motor Speed | 61 |
| Figure 41:Detailed Image showing difference between reference and simulated curve | 61 |
| Figure 42:Phase Current | 62 |
| Figure 43:Detailed Image of Phase Currents..... | 62 |
| Figure 44:phase Voltage | 63 |
| Figure 45:Phase Voltage Detailed Image | 63 |
| Figure 46:Torque | 64 |
| Figure 47:Motor Speed | 65 |
| Figure 48:Detailed Image Showing the difference between reference speed and simulated result..... | 65 |
| Figure 49:Phase current | 66 |
| Figure 50:Detailed Phase Current..... | 66 |
| Figure 51:Torque | 67 |
| Figure 52:Phase Voltage..... | 67 |
| Figure 53:Square Waves of Input Voltage | 67 |
| Figure 54:Motor Speed | 68 |
| Figure 55:Detailed Motor Speed..... | 69 |
| Figure 56:Phase Currents..... | 69 |
| Figure 57:Phase Currents during start-up | 70 |
| Figure 58:Torque | 70 |
| Figure 59:Phase Voltages | 71 |
| Figure 60:Detailed Square waves after DC-AC Conversion..... | 71 |
| Figure 61:Motor Speed | 72 |
| Figure 62:Detailed Motor Speed Figure | 73 |
| Figure 63:Motor Torque | 73 |
| Figure 64:Phase Currents during start-up | 74 |
| Figure 65:Phase Currents..... | 74 |
| Figure 66:Phase Voltage..... | 75 |
| Figure 67:Detailed Square Waves from Inverter..... | 75 |

| | |
|---|----|
| Figure 68:Transient Speed Command | 76 |
| Figure 69:Motor Speed | 77 |
| Figure 70:Detailed Motor Speed Result-Motor Start-up | 77 |
| Figure 71:Deailed Speed Difference during the first speed reduction..... | 78 |
| Figure 72:Detailed Motor speed difference while reaching the steady state | 78 |
| Figure 73:Phase Current | 79 |
| Figure 74:Detailed Image during the reduction and increment of speed..... | 79 |
| Figure 75:Torque | 80 |
| Figure 76:Phase Voltage | 80 |
| Figure 77:Speed Command for Transient Analysis-2 | 81 |
| Figure 78:Motor Speed-transient -2..... | 81 |
| Figure 79:Detailed Picture of lag between speed reference and result..... | 82 |
| Figure 80:Phase Current | 82 |
| Figure 81:Torque | 82 |
| Figure 82:Phase Voltage | 83 |
| Figure 83:Resulting Square Wave | 83 |

List of Equations

| | |
|--|----|
| Equation 1:Synchronous Speed | 17 |
| Equation 2:Currents applied to stator | 20 |
| Equation 3:Equations for Instantaneous mmf..... | 21 |
| Equation 4:Resultant mmf | 21 |
| Equation 5:Resultant mmf after substituting the phase currents in the equation 4..... | 21 |
| Equation 6:Synchronous Speed | 21 |
| Equation 7:Per Unit Slip | 22 |
| Equation 8:Torque Expression..... | 22 |
| Equation 9:Stator Self Inductance | 24 |
| Equation 10:Stator Self Inductance | 24 |
| Equation 11:Mutual Inductance of Stator per phase [11] | 24 |
| Equation 12:Stator Mutual Inductance when exciting only one phase[11] | 25 |
| Equation 13:Flux Linking phase b due to current in A-phase[11] | 25 |
| Equation 14:Mutual Inductance[11] | 25 |
| Equation 15:Mutual inductance including the effects of coupling other phases[11] | 25 |
| Equation 16:Rotor Inductance[11]..... | 25 |
| Equation 17: Flux Linkage | 26 |
| Equation 18:Stator Flux Linkage in Space Vector | 26 |
| Equation 19:Rotor Flux Linkage | 26 |
| Equation 20:Stator and Rotor Flux with respect to 'a' phase | 26 |
| Equation 21:Stator Voltage Equations [13] | 27 |
| Equation 22:Rotor Voltage Equations [13] | 27 |
| Equation 23:Transformation Angle | 28 |
| Equation 24:Rotor Angle | 28 |
| Equation 25:qd0 Transformation matrix..... | 29 |
| Equation 26:abc phase stator winding voltages | 29 |
| Equation 27:Stator Voltages in qd0 | 29 |
| Equation 28:Rotor Voltages in qd0 | 29 |
| Equation 29:Flux Linkage in terms of inductance and current..... | 29 |
| Equation 30:Flux Linkage in qd0 | 29 |
| Equation 31:Stator Flux Linkage in qd0..... | 30 |
| Equation 32:Rotor Flux Linkage in qd0 | 30 |
| Equation 33:Electromagnetic Torque | 30 |

| | |
|---|----|
| Equation 34:Expressions for machine quantities..... | 30 |
| Equation 35:Stator Voltage Equations in qd0 [13]..... | 31 |
| Equation 36:Rotor Voltage Equations in qd0 [13] | 32 |
| Equation 37:Flux Linkage Equations [13]..... | 32 |
| Equation 38:torque Equations [13] | 32 |
| Equation 39:Output Voltage [15] | 35 |
| Equation 40:Pole Voltage | 37 |
| Equation 41:Negative Pole Voltage..... | 37 |
| Equation 42:Pole Voltage based on Switch Condition..... | 37 |
| Equation 43:Pole Voltage for all three phases [8] | 38 |
| Equation 44:Phase Voltage [8] | 38 |
| Equation 45:Modulation Index [8] | 39 |
| Equation 46:Synchronous Speed [1]..... | 43 |
| Equation 47:Rotor Speed [1] | 43 |
| Equation 48:Criterion For V/F [16] | 44 |
| Equation 49:PID Controller | 48 |
| Equation 50:Proportional Gain Constant for current control..... | 59 |
| Equation 51:Integral Gain Constant for current control | 59 |
| Equation 52:Total Leakage Factor..... | 60 |
| Equation 53:Current Control bandwidth..... | 60 |
| Equation 54:proportional gain for Speed Control..... | 60 |
| Equation 55:Integral gain for Speed Control | 60 |
| Equation 56:Speed Control Bandwidth | 60 |

List of Tables

| | |
|---|----|
| Table 1:Experimental Measurements | 55 |
|---|----|

Introduction

In today's world, Induction motor is the workhorse in every industry. Therefore, the development of its performance characteristic will prove to be useful. Control of Induction motors was always a challenging topic. In many industries, scalar control of induction motor is employed but for the electric propulsion, the scalar method does not meet the required performance level.

Hence, the vector method of control is employed in the induction motor for the purpose of propulsion. The vector control method will be explained in the subsequent sections. However, a detailed explanation on construction of Induction motor and its components have been written for better understanding of the project.

The core of the thesis, is to simulate an induction motor model with Field Oriented Control in place to control the speed of the motor and try to match the parameters such as motor, current with the experimental values. The reference speed for the induction motor have been extracted from the experimental data that was performed at CVUT Laboratory near Praha.

For Simulation, MATLAB software have been used with Simulink being the simulation package and Motor Control Block-set turned out to be the most useful add-on as it had most of the blocks that was required for simulating thereby reducing the time considerably to design the blocks.

The results of the simulation are discussed presented in the penultimate part of the thesis with clear and detailed image of current, motor speed and torque.

Literature Survey

Since my thesis, consists a large part of simulation and the simulation is a block-based simulation and not an equation-based simulation, the generic Field Oriented Control layout from MATHWORKS website was used as a primary reference material.

The important challenge that I faced while doing the thesis, was controlling the PI controller as it is the primary component which controls the current and voltage that in being applied to the stator of induction motor. I studied a sufficient number of research papers to find the method in which the PI controllers can be controlled, but unfortunately, I could not find any suitable method.

Hence, I would like to state that the book 'Electric Motor Control' by Sang-Hoon Kim is my primary reference material for a large portion of this thesis as the book contained the method and the necessary mathematical formulas and required assumptions and conditions on how to control the PI Control elements for both inner current loop and outer speed loop.

The above-mentioned text book helped in understanding the actual working of the Control elements in motor control and with the solved examples for motor control and with valuable inputs from my supervisor, I was able to formulate PI gain values for a series of switching frequency and performed various iterations to land-up on the correct result.

I would also like to add another book 'Control of Induction Motors' by Andrzej M. Trzynadlowski. This book helped me to understand the basics of motor control with clear and precise explanations on scalar and vector control method. For the theoretical section of Motor control methods, this text book served as a bible.

The research paper, 'A Comparative Study between V/F and IFOC Control of three-phase Induction Motor Drives' proved to helpful in the final part of simulation when I was facing difficulty in controlling the currents. Certain changes had been done to the motor control assembly from the initially stated generic model from MathWorks. In the fifth figure of this research paper, where the layout of Indirect Field Oriented Control was presented, the reference current I_d was taken as zero and the reference I_q was taken as the output of Speed control loop as it set the required and the torque refers to the current I_q . This change proved to be highly useful in successfully simulation for the given working conditions.

The basic information on the Induction motor parameters such as voltage, flux and transformation from abc to qd0 have been referred from the textbook 'Dynamic Simulation of Electric Machinery using MATLAB/SIMULINK' by Chee-Mun Ong. This text book was proved to be helpful in understanding the derivations of motor parameters.

Three Phase Induction Machines

Induction Machines are electrical devices which convert the electrical energy into mechanical energy. The major components in the Induction motor are the stator and rotor. The stator is the stationary component connected to the primary three phase power supply and the rotor is the rotating component which produces the mechanical rotation and torque. The Induction motor is also referred to as self-starting motor because when the three-phase supply is given to the stator, it produces a rotating magnetic field with the speed of synchronous speed.

$$N_s = (120 * f) / P$$

Equation 1: Synchronous Speed

Where, f is the three-phase power supply frequency (Hz) and P is the number of poles of stator. This rotating magnetic field from the stator links to the rotor coil and induces voltage which in turn produces current, the current carrying conductor placed in a magnetic field experiences torque and hence it begins to rotate in the direction of applied magnetic field.

Construction of Three-Phase Induction Motor

The major components of an induction motor comprised of two components[4],

- Stator
- Rotor

As the name suggests, stator is a stationary part of the induction motor. For a three-phase induction motor, the primary three phase voltages are applied to the three phase stator windings. Rotor is the rotating part of the induction motor, as explained above the voltage from rotating magnetic field from stator induces voltage onto the rotor and rotor is connected to load through external shaft.

Stator

The stator of the Induction motor consists of three parts

- Stator Frame
- Stator Core
- Stator Winding

Stator Frame

Stator frame is the primary outer covering for the induction motor and its primary function is to provide constant support to the stator core and field winding. It provides mechanical protection and strength to all the inner parts of the motor. The stator can either be die-casted or fabricated steel. If the stator is not rigid, the rotor might miss its concentric alignment and will result in an unbalanced magnetic pull.

Stator Core

The primary function of the stator core is to carry the alternating three-phase flux. To reduce the eddy current losses, the stator core is laminated into individual sheets of thickness ranging up to 0.4mm. These laminated sheets are stamped together to form the stator core. Slots are made onto the core to accommodate the three phase windings

Stator winding

The slots on the stator carry the three phase windings to which the three-phase supply is given. The windings can either be given in star or delta configuration based on the requirement. These windings produce the rotating magnetic field.

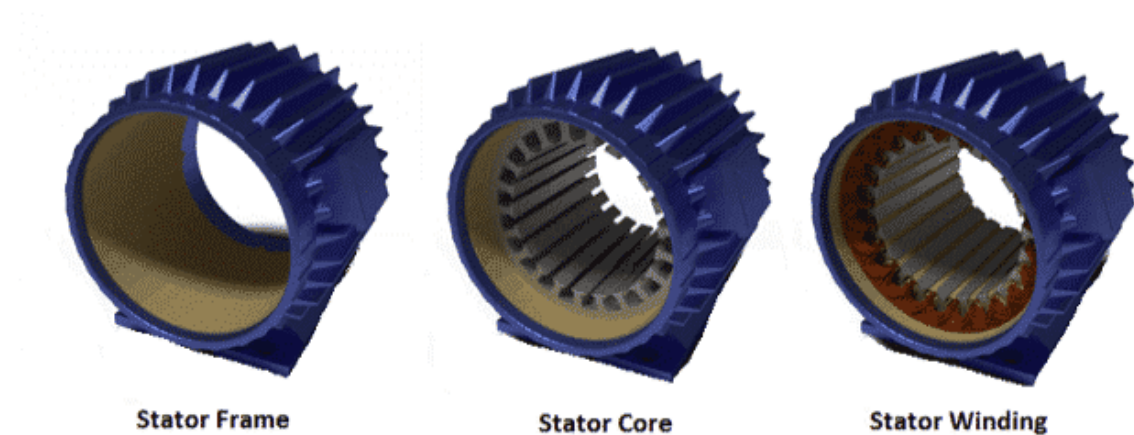


Figure 1: Stator Components

Rotor

Induction Motor is made of two types [5]

- Squirrel cage
- Wound Type

Squirrel Cage Rotor

In this type of rotor, the windings are in the form of copper or aluminium bars embedded in semi-closed slots of a laminated stator core.

To facilitate a closed path in the circuit the sides of the rotor bars are short circuited by end rings. It usually has the same number of poles as the stator. The squirrel cage has a low leakage reactance which results in low starting torque. To overcome this effect of low starting torque, the rotor bars can be skewed. By skewing the length of the rotor increases and so does the resistance and hence we can achieve high starting torque.

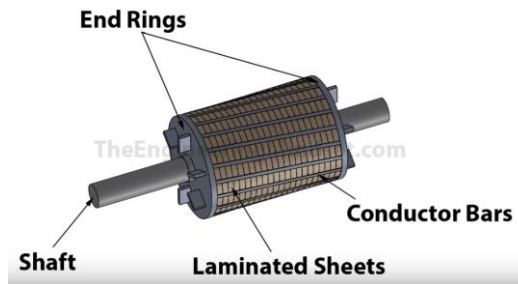


Figure 2: Squirrel Cage Construction

Wound Type Rotor

The major difference between the squirrel cage rotor and wound rotor is the presence of slip ring in the latter. In wound type rotor, the rotor windings have to be connected via star type configuration irrespective of stator winding configuration. Slip rings are made of high resistance material such as phosphorous bronze or brass. Brushes are used to make connection with external circuit. The external circuit is used to increase the resistance to improve the starting conditions of the motor.

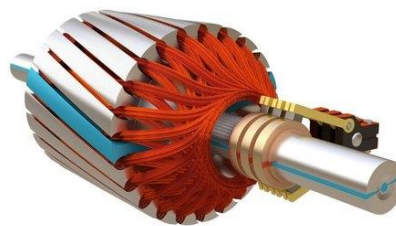


Figure 3: Wound Rotor

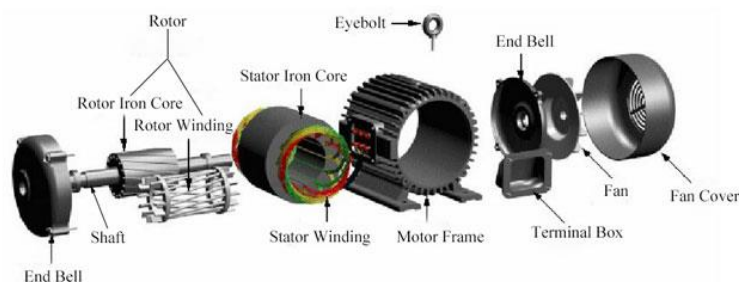


Figure 4: Induction motor Complete Construction

Working of a Squirrel Cage Induction Motor

In this thesis, a squirrel cage three phase induction motor is used. The rated three phase AC power supply is supplied to the stator windings, which in turn produces magnetic field rotating at the synchronous speed of the motor. This magnetic field induces the voltage onto the rotor the resulting voltage produces a current in the rotor. When a current carrying conductor placed in the magnetic field, the rotor experiences torque and the rotor moves in the direction of applied electric field.

Rotating Magnetic Field

The most fundamental principle involved in an induction machine is the creation of rotating and sinusoidally distributed magnetic field in the stator-rotor air gap. Consider that three-phase sinusoidal currents are supplied to the stator windings as [3],

$$i_a = I_m \cos(\omega_e t)$$
$$i_b = I_m \cos\left(\omega_e t - \frac{2\pi}{3}\right)$$
$$i_c = I_m \cos\left(\omega_e t + \frac{2\pi}{3}\right)$$

Equation 2: Currents applied to stator

Each of the phase windings will produce a sinusoidally distributed mmf (magnetomotive force) which pulsates about the respective axes.

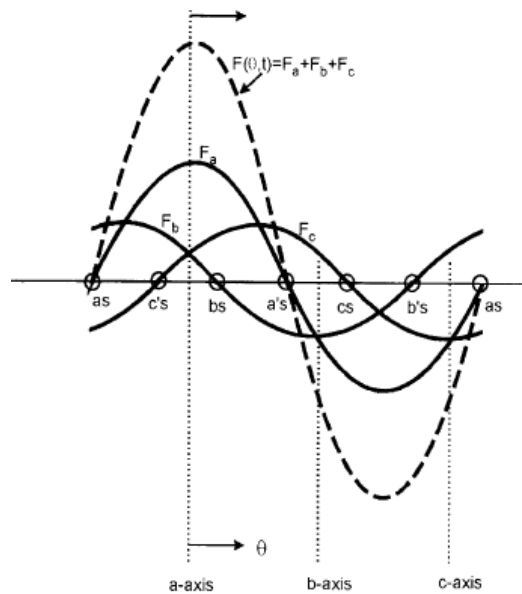


Figure 5: mmf distribution in three phase windings of stator[3]

At any spatial angle Θ , the instantaneous mmf expression can be given as,

$$F_a(\theta) = Ni_a \cos \theta$$

$$F_b(\theta) = Ni_b \cos\left(\theta - \frac{2\pi}{3}\right)$$

$$F_c(\theta) = Ni_c \cos\left(\theta + \frac{2\pi}{3}\right)$$

Equation 3: Equations for Instantaneous mmf

Where ‘N’ denotes the number of turns in the phase winding. From the above expression, we can see that the mmf’s are phase shifted by 120° . The resultant mmf can be given as,

$$F(\theta) = F_a(\theta) + F_b(\theta) + F_c(\theta)$$

Equation 4: Resultant mmf

Substituting the equations for phase current in the above equation and simplifying will give us,

$$F(\theta, t) = \frac{3}{2} NI_m \cos(\omega_e t - \theta)$$

Equation 5: Resultant mmf after substituting the phase currents in the equation 4

The above equation indicates that the sinusoidally distributed mmf wave of peak value $\frac{3}{2} NI_m$ is rotating in the airgap at a synchronous speed of ω_e . In a two-pole machine, $F(\Theta, t)$ makes one revolution per cycle of current variation. This means that for a P-pole machine, the rotational speed can be given as,

$$N_e = \frac{120 f_e}{P}$$

Equation 6: Synchronous Speed

Where N_e is the synchronous speed (rpm) and f_e (Hz) is the stator frequency given by $\omega_e/2\pi$.

Torque Production

When the rotor is stationary initially, the rotor conductors will be subjected to sweeping magnetic fields, inducing current in the short-circuited rotor at the same frequency. This interaction between airgap flux and mmf on rotor produces torque [3].

When the rotor reaches the synchronous speed, there will not be induced current therefore torque will not be generated.

At any other rotor speed due to slip between the synchronous speed and rotor speed, torque will be developed. Based on Lenz's law, the rotor moves in the same direction of induced magnetic field. The per unit slip can be defined as,

$$S = \frac{N_e - N_r}{N_e} = \frac{\omega_e - \omega_r}{\omega_e} = \frac{\omega_{sl}}{\omega_e}$$

Equation 7: Per Unit Slip

Where, N_e is the synchronous speed (rpm), N_r is the rotor speed (rpm), ω_e (rad/s) is the supply frequency, ω_r (rad/s) is the rotor electrical angular velocity and ω_{sl} (rad/s) is the slip frequency. The voltage that is being induced on to the stator is at slip frequency which results in producing currents at the same frequency. For a rotor rotating at a speed of ω_r and its current wave moving at a speed of ω_{sl} relative to the rotor, the rotor mmf waves moves at the same speed as that of airgap flux wave. The torque expression can be derived as,

$$T_e = \pi \left(\frac{P}{2} \right) l r B_p F_p \sin \delta$$

Equation 8: Torque Expression

Where P is the number of poles, l is the axial length of machine, r is the machine radius, B_p is the peak value of air gap flux density, F_p peak value of rotor mmf and δ as the torque angle given by the equation $\frac{\pi}{2} + \theta_r$

Torque Speed Curve

The torque-speed characteristic is important to gain a proper understanding of the working of induction motor.

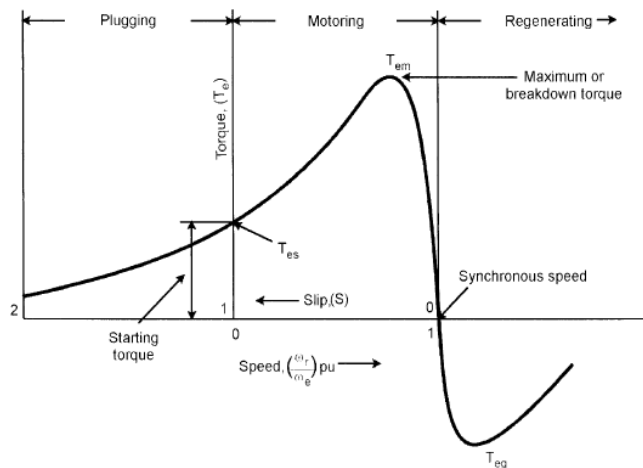


Figure 6: Torque Vs Speed Curve

In plugging regime, the rotor rotates in the opposite direction to the airgap flux. This condition may arise, if the stator supply phase sequence is reversed when rotor is moving or because of the over hauling type of load which drives the motor in the reverse direction. Since the torque is positive but the speed is negative, plugging torque appears to be braking torque. As the energy due to plugging torque is dissipated within the machine, it may cause the machine to overheat. As the name suggest, in regeneration regime the machine acts as a generator. The rotor rotates at synchronous speed in the same direction of the airgap flux, so that the slip would be negative creating a negative or regeneration torque. The positive is produced during the motoring regime. [3]

Before proceeding to the voltage equations, first we will take a look at the primary variables in the motor.

Stator Inductances

Inductance is the ability of an inductor to store energy and it stores the energy in the magnetic field that is created by the flow of current. Energy is required to setup the magnetic field and this energy needs to be released when the field fails. As a result of magnetic field interacting with current flow, inductors generate an opposing voltage to the rate of change in current in a circuit. Typical inductors can be coils of wire as the coils increases the coupling of the magnetic field and thus increasing the inductance. There are two types of inductances,

- Self-Inductance:
Self-Inductance is the property of the circuit, where a change in current causes a change in voltage due to the magnetic effect associated with the coil.
- Mutual Inductance:
Mutual Inductance is the inductive effect where a change in one circuit causes a change in voltage in another circuit as a result of magnetic field that links both circuits.

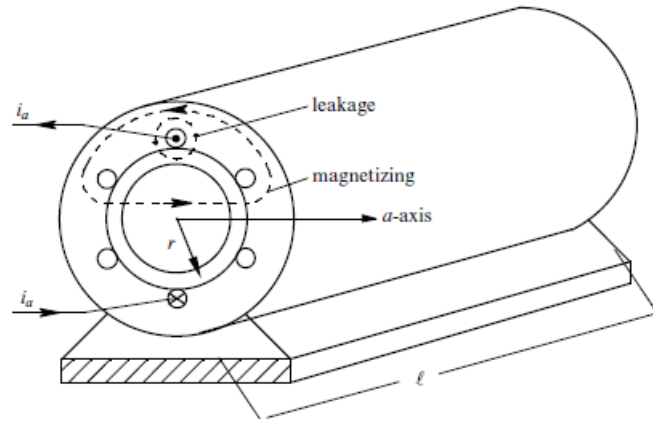


Figure 7: Single Phase inductance in Induction machine

For defining stator inductance, we will assume the induction motor circuit is open-circuited. As shown in the above picture, exciting just phase 'a' produces a magnetizing flux across the airgap which links the stator with rotor and leakage flux which links with its own phase. Therefore, the self-inductance of a stator can be given as [11],

$$L_{s,self} = \frac{\lambda_a}{i_a} \Big|_{i_a \text{ only}} = \frac{\lambda_{a,leakage}}{i_a} + \frac{\lambda_{a,magnetizing}}{i_a}$$

Equation 9: Stator Self Inductance

Where λ is the flux component and 'i' is the current component. There first term can be named as the leakage inductance and second term can be named as magnetizing inductance. Therefore,

$$L_{s,self} = L_{ls} + L_{m,1-phase}$$

Equation 10: Stator Self Inductance

The mutual inductance per phase can be easily calculated by calculating the energy stored in the airgap.

$$L_{m,1-phase} = \frac{\pi \mu_0 r l}{l_g} \left(\frac{N_s}{p} \right)^2$$

Equation 11: Mutual Inductance of Stator per phase [11]

Where, r is the mean radius at the airgap and l is the length of rotor along its shaft axis and N_s equals the number of turns per phase and p as the number of poles.

The stator mutual inductances between two stator phases can be calculated by exciting the 'a'-phase by current i_a and calculating the flux linkage with phase-b.

$$L_{mutual} = \frac{\lambda_b}{i_a} \Big|_{i_b, i_c=0, \text{open rotor}}$$

Equation 12: Stator Mutual Inductance when exciting only one phase[11]

Since the current i_a produces sinusoidally distributed flux in the airgap, therefore we can say that the flux linking the phase-b due to i_a is nothing but the magnetic flux linkage of phase-a times the cosine of the angle between two windings (120°).

$$\lambda_{b, \text{due to } i_a} = \cos(120) * \lambda_{a, \text{magnetizing due to } i_a}$$

$$\lambda_{b, \text{due to } i_a} = \frac{-1}{2} * \lambda_{a, \text{magnetizing due to } i_a}$$

Equation 13: Flux Linking phase b due to current in A-phase[11]

Therefore, we can deduce L_{mutual} to,

$$L_{mutual} = -\frac{1}{2} L_{m, 1\text{-phase}}$$

Equation 14: Mutual Inductance[11]

In the equation where $L_{m, 1\text{-phase}}$ was derived, it does not include the effect of mutual coupling from other two phases. To include this, we need to multiply the equation by 3/2

$$L_m = \frac{3 \pi \mu_0 r l}{2 l_g} \left(\frac{N_s}{p} \right)^2$$

Equation 15: Mutual inductance including the effects of coupling other phases[11]

Rotor Inductance

The magnetizing flux produced by each rotor equivalent winding has the same magnetic path in crossing the airgap and same number of turns as the stator windings. Hence, each rotor phase has the same magnetizing inductance $L_{m, 1\text{-phase}}$ as the magnetizing flux produced by the stator. Its leakage inductance L_{lr} might vary from stator.

$$L_m = \frac{3}{2} L_{m, 1\text{-phase}}$$

$$L_r = L_{lr} + L_m$$

Equation 16: Rotor Inductance[11]

Flux Linkages

To find the stator and rotor flux linkages, first we will assume the stator and rotor to be open-circuited one at a time.

Stator Flux Linkage (Rotor Open-Circuited)

According to kirchoff's current law, the currents in the stator windings sums up to be zero. Initially we assume the rotor is open-circuited. The flux linkage for each phase can be given as [11],

$$\begin{aligned}[\lambda_{a,i_s}(t) &= L_{ls}i_a(t) + L_m i_a(t)] * e^{j0} \\ [\lambda_{b,i_s}(t) &= L_{ls}i_b(t) + L_m i_b(t)] * e^{j2\pi/3} \\ [\lambda_{c,i_s}(t) &= L_{ls}i_c(t) + L_m i_c(t)] * e^{j4\pi/3}\end{aligned}$$

Equation 17: Flux Linkage

In terms of space vector, the stator flux linkage can be written as,

$$\vec{\lambda}_{s,i_s}^a(t) = L_{ls} \vec{i}_s^a + L_m \vec{i}_s^a$$

Equation 18: Stator Flux Linkage in Space Vector

Rotor Flux Linkage (Stator Open Circuited)

Assuming that rotor has currents in spite of short-circuiting the stator, the flux linkages in rotor can be expressed as [11],

$$\vec{\lambda}_{r,i_r}^a(t) = L_{lr} \vec{i}_r^a + L_m \vec{i}_r^a$$

Equation 19: Rotor Flux Linkage

Stator and Rotor Flux (Presence of stator of rotor currents)

When the stator and rotor currents are present simultaneously, the flux linking any of the stator phase is due to the stator currents as well as the magnetizing flux due to rotor currents, therefore the stator and rotor flux linkages with respect to a-phase can be given as,

$$\begin{aligned}\vec{\lambda}_s^a(t) &= L_s \vec{i}_s^a + L_m \vec{i}_r^a \\ \vec{\lambda}_r^a(t) &= L_m \vec{i}_s^a + L_r \vec{i}_r^a\end{aligned}$$

Equation 20: Stator and Rotor Flux with respect to 'a' phase

Circuit Model of a Three-Phase Induction Machine

Voltage Equations

The Ideal circuit diagram of the three-phase induction motors can be depicted as

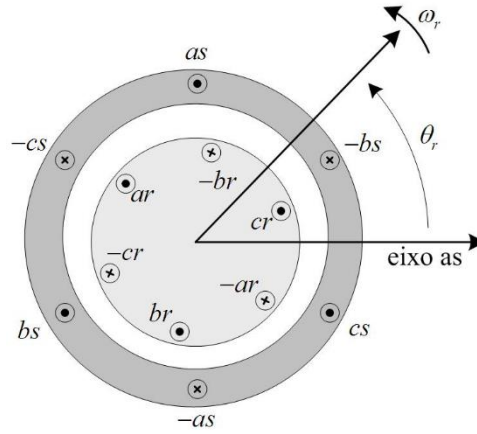


Figure 8: Ideal circuit of Induction Motor

Stator and Rotor Voltage equations for the Induction machine can be written as follows

$$\begin{aligned} v_{as} &= i_{as}r_{as} + \frac{d\lambda_{as}}{dt} \\ v_{bs} &= i_{bs}r_{bs} + \frac{d\lambda_{bs}}{dt} \\ v_{cs} &= i_{cs}r_{cs} + \frac{d\lambda_{cs}}{dt} \end{aligned}$$

Equation 21: Stator Voltage Equations [13]

$$\begin{aligned} v_{ar} &= i_{ar}r_r + \frac{d\lambda_{ar}}{dt} \\ v_{br} &= i_{br}r_r + \frac{d\lambda_{br}}{dt} \\ v_{cr} &= i_{cr}r_r + \frac{d\lambda_{cr}}{dt} \end{aligned}$$

Equation 22: Rotor Voltage Equations [13]

In the above-mentioned equations, the subscript 's' and 'r' denotes stator and rotor respectively and λ represents flux linkage. Since we have six first order differential equations one for each winding to describe an ideal Induction Machine, dq or $\alpha\beta$ transformations are used to facilitate the computation of the transient solution of the Induction Machine by transforming the differential equations with time-varying inductances to differential equations with constant inductances.

Machine Model in dq0 Reference Frame

The idealized three-phase induction machine is assumed to have symmetrical airgap. The dq0 reference frame are usually selected based on convenience. The two common reference frames used generally in the analysis of induction machine are the stationary and synchronously rotating reference frame. In the stationary rotating reference frame, the dq variable of the machine are in the same frame as those normally used for supply network. The relationship between abc and dq0 quantities can be seen in the figure below.

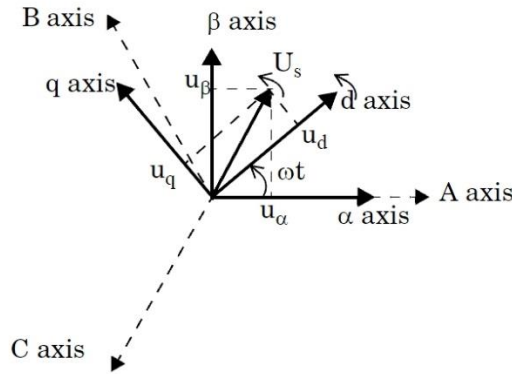


Figure 9: Relationship between abc and dq0 quantities

The transformation from abc to dq0 quantities can be given by [13]

$$\begin{bmatrix} f_q \\ f_d \\ f_0 \end{bmatrix} = [T_{qd0}(\theta)] \begin{bmatrix} f_a \\ f_b \\ f_c \end{bmatrix}$$

where, 'f' can be the phase voltages, currents or flux linkages of the machine. For an induction machine in the stationary reference frame, the equations are obtained by keeping $\omega = 0$ and for synchronously rotating reference frame, $\omega = \omega_e$. The transformation angle, $\theta(t)$, between the q-axis of the reference frame rotating at a speed of ω and the a-axis of the stationary winding can be expressed as

$$\theta(t) = \int_0^t \omega(t) dt + \theta(0) \text{ elec.rad}$$

Equation 23: Transformation Angle

Similarly, the rotor angle $\theta_r(t)$, between the axes of stator and rotor a-phase for a rotating rotor with speed $\omega_r(t)$, can be expressed as

$$\theta_r(t) = \int_0^t \omega_r(t) dt + \theta_r(0) \text{ elec.rad}$$

Equation 24: Rotor Angle

The transformation matrix for qd0 , is

$$[T_{qd0}(\theta)] = \frac{2}{3} \begin{bmatrix} \cos\theta & \cos\left(\theta - \frac{2\pi}{3}\right) & \cos\left(\theta + \frac{2\pi}{3}\right) \\ \sin\theta & \sin\left(\theta - \frac{2\pi}{3}\right) & \sin\left(\theta + \frac{2\pi}{3}\right) \\ \frac{1}{2} & \frac{1}{2} & \frac{1}{2} \end{bmatrix}$$

Equation 25:qd0 Transformation matrix

Voltage Equations qd0

The stator winding abc voltage equations can be expressed as [13],

$$v_s^{abc} = p\lambda_s^{abc} + r_s^{abc}i_s^{abc}$$

Equation 26:abc phase stator winding voltages

After applying qdo transformation and substituting back in the equation we get,

$$v_s^{qd0} = \omega \begin{bmatrix} 0 & 1 & 0 \\ -1 & 0 & 0 \\ 0 & 0 & 0 \end{bmatrix} \lambda_s^{qd0} + p\lambda_s^{qd0} + r_s^{qd0}i_s^{qd0}$$

Equation 27:Stator Voltages in qd0

Similarly for rotor voltage quantities,

$$v_r^{qd0} = (\omega - \omega_r) \begin{bmatrix} 0 & 1 & 0 \\ -1 & 0 & 0 \\ 0 & 0 & 0 \end{bmatrix} \lambda_r^{qd0} + p\lambda_r^{qd0} + r_r^{qd0}i_r^{qd0}$$

Equation 28:Rotor Voltages in qd0

Flux Linkage Equations qd0

In matrix notation, the flux linkages of stator and rotor windings, in terms of winding inductances and currents, may be written as,

$$\begin{bmatrix} \lambda_s^{abc} \\ \lambda_r^{abc} \end{bmatrix} = \begin{bmatrix} L_{ss}^{abc} & L_{sr}^{abc} \\ L_{rs}^{abc} & L_{rr}^{abc} \end{bmatrix} \begin{bmatrix} i_s^{abc} \\ i_r^{abc} \end{bmatrix}$$

Equation 29:Flux Linkage in terms of inductance and current

By applying the transformation to the stator quantities, we get,

$$\lambda_s^{qd0} = [T_{qd0}(\theta)](L_{ss}^{abc}i_s^{abc} + L_{sr}^{abc}i_r^{abc})$$

Equation 30:Flux Linkage in qd0

$$\lambda_s^{qd0} = \begin{bmatrix} L_{ls} + \frac{3}{2}L_{ss} & 0 & 0 \\ 0 & L_{ls} + \frac{3}{2}L_{ss} & 0 \\ 0 & 0 & L_{ls} \end{bmatrix} i_s^{qd0} + \begin{bmatrix} \frac{3}{2}L_{sr} & 0 & 0 \\ 0 & \frac{3}{2}L_{sr} & 0 \\ 0 & 0 & 0 \end{bmatrix} i_r^{qd0}$$

Equation 31: Stator Flux Linkage in qd0

Similarly for rotor,

$$\lambda_r^{qd0} = \begin{bmatrix} L_{lr} + \frac{3}{2}L_{rr} & 0 & 0 \\ 0 & L_{lr} + \frac{3}{2}L_{rr} & 0 \\ 0 & 0 & L_{lr} \end{bmatrix} i_r^{qd0} + \begin{bmatrix} \frac{3}{2}L_{sr} & 0 & 0 \\ 0 & \frac{3}{2}L_{sr} & 0 \\ 0 & 0 & 0 \end{bmatrix} i_s^{qd0}$$

Equation 32: Rotor Flux Linkage in qd0

Torque Equation qd0

The Electromagnetic Torque can be expressed in any of the following terms [13],

$$T_{em} = \frac{3P}{2} (\lambda'_{qr} i'_{dr} - \lambda'_{dr} i'_{qr})$$

$$T_{em} = \frac{3P}{2} L_m (i'_{dr} i_{qs} - i'_{qr} i_{ds})$$

$$T_{em} = \frac{3P}{2} (i_{qs} \lambda_{ds} - i_{ds} \lambda_{qs})$$

Equation 33: Electromagnetic Torque

Oftentimes, machine quantities are expressed in terms of flux linkages per second, ψ 's and reactances, χ 's instead of λ and L . These are related simply by base or rated values, ω_b , that is

$$\psi = \omega_b \lambda$$

$$\chi = \omega_b L$$

Equation 34: Expressions for machine quantities

Where, $\omega_b = 2\pi * f_{rated}$ in elec.rad per sec. Usually for power system studies, Induction machine loads along with other types of power system components, are often simulated on a system's synchronously rotating reference frame. The voltage and other relevant quantities of the synchronously rotating reference frame Induction machine can be easily obtained by setting the speed of the arbitrary reference frame to ω_e

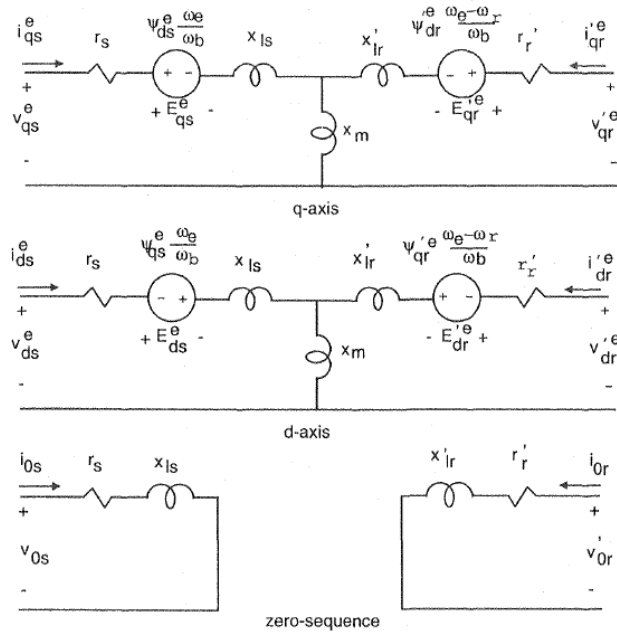


Figure 10: Equivalent Circuit of IM in synchronous reference frame

Induction Machine Equations in Synchronous Rotating Reference Frame

Stator and Rotor Voltage Equations

$$v_{qs}^e = \frac{P}{\omega_b} \psi_{qs}^e + \frac{\omega_e}{\omega_b} \psi_{ds}^e + r_s i_{qs}^e$$

$$v_{ds}^e = \frac{P}{\omega_b} \psi_{ds}^e - \frac{\omega_e}{\omega_b} \psi_{qs}^e + r_s i_{ds}^e$$

$$v_{0s}^e = \frac{P}{\omega_b} \psi_{0s}^e + r_s i_{0s}^e$$

Equation 35: Stator Voltage Equations in qd0 [13]

$$v_{qr}^{'e} = \frac{P}{\omega_b} \psi_{qr}^{'e} + \left(\frac{\omega_e - \omega_r}{\omega_b} \right) \psi_{dr}^{'e} + r_r' i_{qr}^{'e}$$

$$v_{dr}^{'e} = \frac{P}{\omega_b} \psi_{dr}^{'e} - \left(\frac{\omega_e - \omega_r}{\omega_b} \right) \psi_{qr}^{'e} + r_r' i_{dr}^{'e}$$

$$v_{0r}^{'e} = \frac{P}{\omega_b} \psi_{0r}^{'e} + r_r' i_{0r}^{'e}$$

Equation 36: Rotor Voltage Equations in qd0 [13]

Flux Linkage equations

$$\begin{bmatrix} \psi_{qs}^e \\ \psi_{ds}^e \\ \psi_{0s} \\ \psi_{qr}^{'e} \\ \psi_{dr}^{'e} \\ \psi_{0r}^{'e} \end{bmatrix} = \begin{bmatrix} \chi_{ls} + \chi_m & 0 & 0 & \chi_m & 0 & 0 \\ 0 & \chi_{ls} + \chi_m & 0 & 0 & \chi_m & 0 \\ 0 & 0 & \chi_{ls} & 0 & 0 & 0 \\ \chi_m & 0 & 0 & \chi_{lr}' + \chi_m & 0 & 0 \\ 0 & \chi_m & 0 & 0 & \chi_{lr}' + \chi_m & 0 \\ 0 & 0 & 0 & 0 & 0 & \chi_{lr}' \end{bmatrix} \begin{bmatrix} i_{qs}^e \\ i_{ds}^e \\ i_{0s} \\ i_{qr}^{'e} \\ i_{dr}^{'e} \\ i_{0r}^{'e} \end{bmatrix}$$

Equation 37: Flux Linkage Equations [13]

Torque Equation

$$T_{em} = \frac{3}{2} \frac{P}{2\omega_b} (\psi_{qr}^{'e} i_{dr}^{'e} - \psi_{dr}^{'e} i_{qr}^{'e})$$

$$T_{em} = \frac{3}{2} \frac{P}{2\omega_b} (\psi_{ds}^e i_{qs}^e - \psi_{qs}^e i_{ds}^e)$$

$$T_{em} = \frac{3}{2} \frac{P}{2\omega_b} \chi_m (i_{dr}^{'e} i_{qs}^e - i_{qr}^{'e} i_{ds}^e)$$

Equation 38: torque Equations [13]

Power Electronic Devices

Rectifier

A Rectifier is an electrical device, comprised of one or more diodes that allow the flow of current only in one direction. In principle a rectifier converts the sinusoidal alternating current into direct current. It uses a PN Junction to rectify the AC current. A PN diode permits electric current in only one direction. If the diode is forward biased it will allow the current to flow and if it is reverse biased it block the current.



Figure 11: Forward and Reverse Biased

In the above figure, the arrow head of the diode indicates the conventional direction of current when the diode is forward biased. The conventional direction of current is from anode to cathode.

The process of applying the external voltage to p-n junction diode is called the biasing. External voltage can be applied in two ways:

- Forward Biasing
- Reverse Biasing

If the p-n junction diode is forward biased, it allows the current to flow. Under forward biased condition, the p-type semiconductor is connected to the positive terminal of the battery, the n-type of the semiconductor is connected to the negative terminal of battery.

When the p-n junction diode is reverse biased, it blocks the current flow. Under reversed biased condition, the p-type is connected to negative terminal of the battery and the n-type is connected to the positive terminal of battery.

Rectifiers can be primarily classified based on the type of supply voltage,

- Single Phase Rectifier
- Three Phase Rectifier

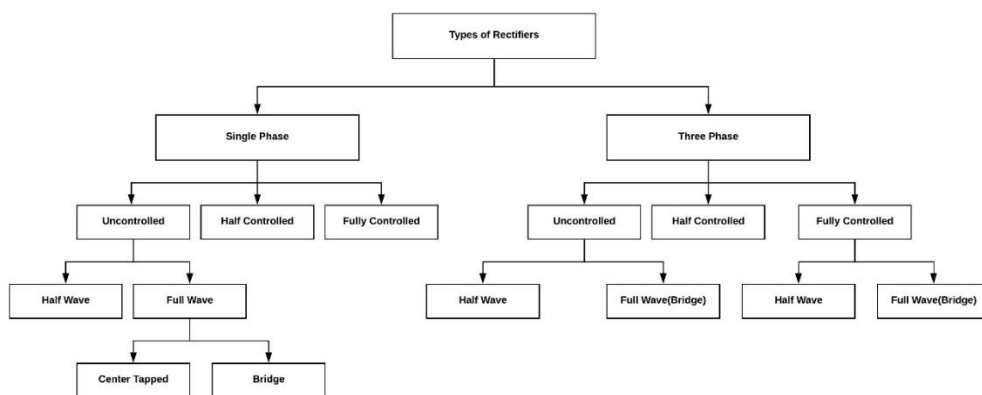


Figure 12: Overview of Rectifiers

Uncontrolled Rectifiers

The output voltage of a rectifier that cannot be controlled is known as an uncontrolled rectifier. A two-terminal component like diode is a unidirectional device and the main function is to allow the flow of current in one direction. A diode device cannot be controlled because it will perform only if it is connected in forward biased. The uncontrolled rectifiers are further divided into half wave and full wave rectifiers

Half Wave Rectifier

In this type of rectifier, only the positive half of the cycle is rectified and the negative half is covered up. For a single-phase supply, single diode will be sufficient to do a half wave rectification while for a three-phase supply it needs three diodes to perform the same function.

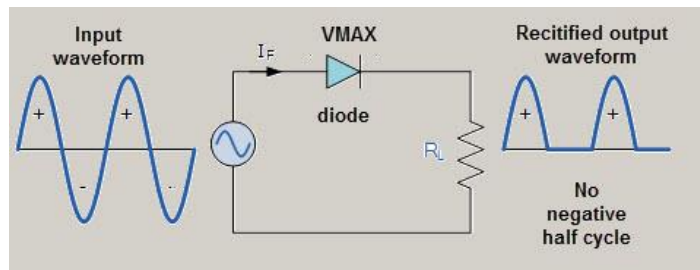


Figure 13: Half Wave Rectifier

Full Wave Rectifier

A full wave rectifier is a type of rectifier where the rectification process happens to both the positive and the negative half of an AC current converting it to pulsating DC signal. For a three-phase supply, six diodes will be needed in a closed loop configuration to perform the rectification.

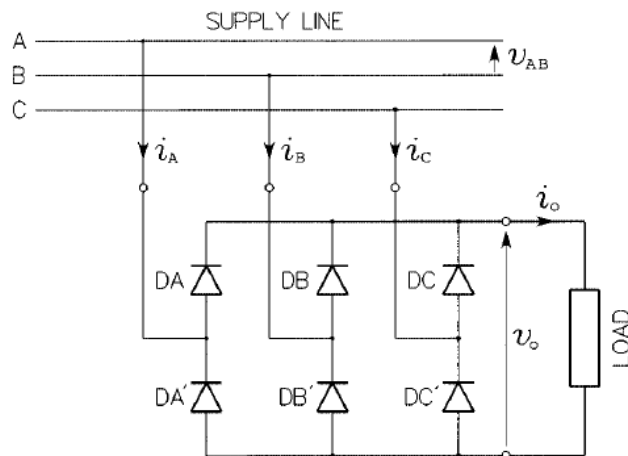


Figure 14: Full wave rectifier configuration

These diodes are subjected to the highest line-line input voltage. Due to this factor, we get the highest line-line voltage at the output of the rectifier, the output voltage is the envelope of all six line-line voltages of the supply line. The output voltage is not ideally of the dc quality, but it has a high dc component. To keep the voltage constant, a capacitor of high capacitance is connected parallelly to the output of rectifier.

$$V_0 = \frac{3}{\pi} V_{LL,m} = 0.955 V_{LL,m}$$

Equation 39: Output Voltage [15]

Where, $V_{LL,m}$ denotes the peak value of line-line input voltage.

Inverter

Inverters are electrical devices that aids in conversion of pulsating DC current to AC current. Similar to rectifiers, primarily inverters are categorized based on the type of power supply namely single-phase and three-phase supply. Further the inverter can be divided in terms of the shape of the output wave form namely sinus wave, square wave and modified square wave.

For the purpose of electric drivetrain, the inverters are usually divided as the Constant frequency Constant Voltage and Variable frequency Variable voltage inverter. Due to the demand of varying frequency in electric drives the latter is used for electric vehicle purposes. Pulse Width Modulation technique is used to vary the voltage with respect to the load requirements. Further down the line, the inverter can be divided into two types [15],

- Voltage Source Inverter
- Current Source Inverter

The primary difference between the two is the type of source that is fed to inverter. In this thesis, Voltage source inverter is used. For three phase inverter, six IGBT transistors which are connected in a similar fashion with the above-mentioned figure. IGBT transistors are operated by means of gate signals.

The magnitude of the voltage given by the inverter depends strongly on the gate signal intensity which is again dependent on the switching frequency of the inverter. Usually for Induction motor drives, the switching frequency can be up to 20kHz. It should also be noted that the increase in switching frequency increases the switching the losses, hence there is always a compromise between the losses and switching frequency

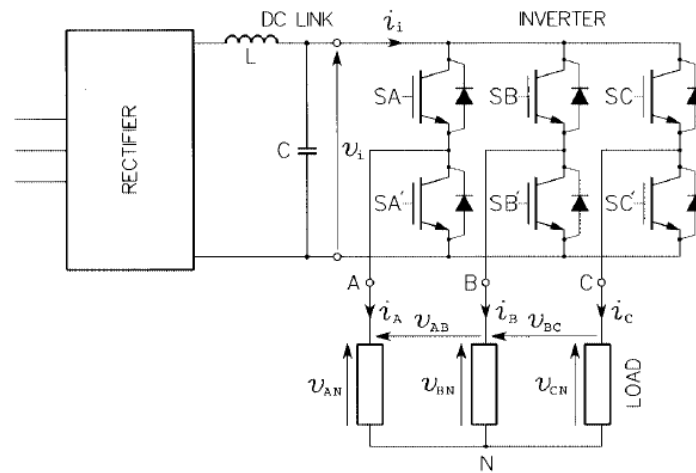


Figure 15: Voltage Source Inverter Circuit Configuration

To simulate the switching frequency in any simulating software, a sawtooth comparator is used and assumed that the frequency of the sawtooth is equivalent to the switching frequency of the inverter. Normalized sinus or space vector waves are compared with the sawtooth waves which produces the gate signals to generate the required AC voltage. The output voltage form of the inverter is usually a square wave and hence time averaging would give us the accurate voltage sinus curve. When these square waveform voltages are applied to inductive loads like motors, the harmonics are filtered and delivered as a sinus waveform voltage.

The output voltage of the basic inverter circuit is determined by the switching states of the switches. The main operating condition is to turn ON the switches in an alternating pattern. The DC source is short circuited when both the switches of the same phase are switched ON [fig.16]. Hence if one switch is turned ON, the other should be switched OFF.

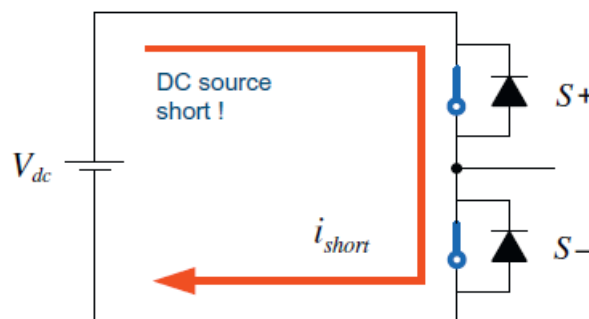


Figure 16: DC Source Short Circuit [8]

When the upper switch is turned ON, then the pole voltage becomes a positive voltage,

$$V_p = \frac{V_{dc}}{2}$$

Equation 40: Pole Voltage

When the lower switch is turned ON, then the pole voltage becomes a negative voltage,

$$V_p = -\frac{V_{dc}}{2}$$

Equation 41: Negative Pole Voltage

Finally, even if both the switches are turned OFF, the pole voltages can still be produced is the current is flowing through the load.

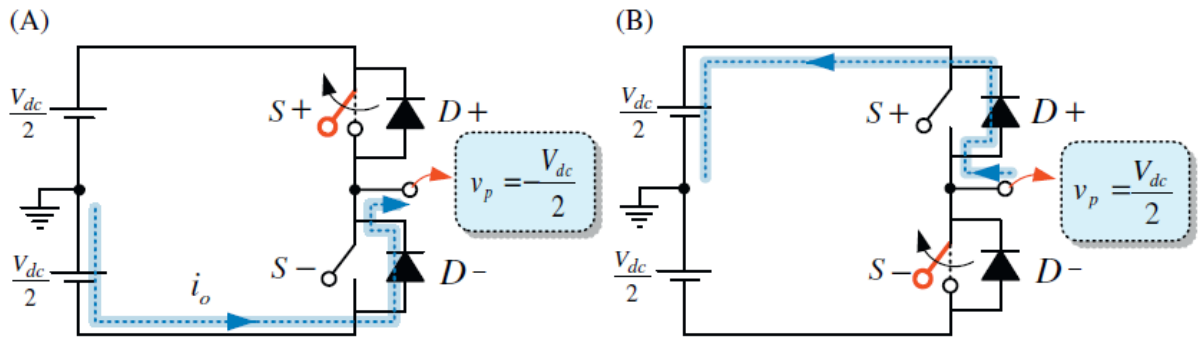


Figure 17: Circuit Configuration when both switches are OFF [8]

In the above case, the pole voltages depend on the direction of current. If the upper switch is turned OFF when a positive current is flowing through, hence the pole voltage will be $-\frac{V_{dc}}{2}$. On the other hand, if the lower switch is tuned OFF when a negative current is flowing through the circuit then the current through the upper diode becomes $\frac{V_{dc}}{2}$. From these switching situations, we can derive a simple equation to describe the state of the pole voltage which is,

$$V_p = V_{dc} \left(S - \frac{1}{2} \right)$$

Equation 42: Pole Voltage based on Switch Condition

Here, the switching function S is defined as '1' when upper switch is turned ON and '0' when lower switch is turned ON. An inverter operates in powering mode when the current flow through the switching device and regeneration mode when the current flows through the diode.

During the regeneration mode, the AC power is returned into DC source from the load. Using the corresponding switch function, pole voltage for each phase can be given by

$$V_{an} = V_{dc}(S_a - \frac{1}{2})$$

$$V_{bn} = V_{dc}(S_b - \frac{1}{2})$$

$$V_{cn} = V_{dc}(S_c - \frac{1}{2})$$

Equation 43: Pole Voltage for all three phases [8]

The expressions of phase voltages in a three-phase inverter can be given as,

$$V_{as} = \frac{V_{dc}}{2}(2S_a - S_b - S_c)$$

$$V_{bs} = \frac{V_{dc}}{2}(2S_b - S_c - S_a)$$

$$V_{cs} = \frac{V_{dc}}{2}(2S_c - S_a - S_b)$$

Equation 44: Phase Voltage [8]

Pulse Width Modulation Inverters

In a square wave inverter where only the frequency can be controlled, not its amplitude. For Induction motor drives, there is a necessity to change both frequency and amplitude. For these purposes, PWM technique can be employed. By using PWM we can linearly control the fundamental output voltage, control the frequency of the fundamental output component, control the harmonics present in the output component.

The aim of the PWM is to generate the gate signals which control the IGBT transistors in the inverter assembly. The switching patterns in the inverter is used to control the harmonics or to minimize the switching losses as mentioned in the previous topics. Ever since the introduction of Sinusoidal PWM in 1964, a variety of PWM techniques have been introduced which has its own advantages and disadvantages.

In this diploma thesis, Sinusoidal PWM has been employed to create the reference voltage signals. There are some important performance criteria that needs to be assessed while employing any PWM technique, these are

- Range up to which the output voltage can be linearly controlled, this criterion is important as a larger range can give us better utilization of dc voltage.
- Harmonics in the output voltage. In square wave inverter, the output form which is square wave, has many harmonics included and it is filtered using the machine inductance. Hence, we need to reduce the harmonic level that is injected in the wave.
- Finally, the switching frequency. Higher the switching frequency lesser the harmonics but as mentioned there is always a compromise between the final output waveform and switching losses.

Modulation Index is an important term to define before describing about the PWM methods. Modulation Index indicates the voltage utilization level as,

$$\text{Modulation Index: } MI = \frac{V_{peak}}{\left(\frac{V_{dc}}{2}\right)}$$

Equation 45: Modulation Index [8]

Programmed PWM Technique

In this technique, the PWM switching patterns for generating an output voltage with desired amplitude of the fundamental component are pre calculated off-line and then stored in memory for on-line access. Inverters which operate by this method, read the PWM switching patterns in accordance with stored operating conditions from memory. This technique is called Programmed PWM technique. [8]

Sinusoidal PWM Technique

Sinusoidal PWM is a typical PWM technique. In this method, the sinus reference voltages are compared with high frequency triangular carrier waves to determine the gate signals for IGBT switches in the Inverter. As mentioned earlier, the frequency of the carrier wave is assumed as the switching frequency of the inverter. A comparator is used to extract the signal in terms of 1's and 0's required for the switching process.

Before comparing the reference wave with the triangular signal, it is first normalized with respect to the V_{dc} , or as an alternate method without normalizing, we can directly compare reference wave with carrier wave where the carrier wave maximum amplitude would denote the V_{dc} .

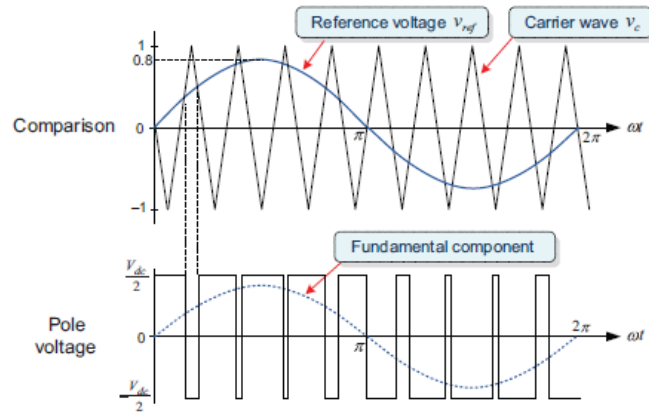


Figure 18: Sinusoidal PWM

After comparing, based on the below mentioned rule, switching states will be determined

- Voltage Reference $V_{ref} >$ Triangular carrier: Upper switched is turned ON
- Voltage Reference $V_{ref} <$ Triangular carrier: Lower switched is turned ON

In Sinusoidal PWM, the necessary condition for linear modulation of voltages is that the amplitude of reference should be less than the carrier wave ($0 \leq MI \leq 1$). Since this PWM requires a very high carrier frequency, this method is also called as carrier based PWM Technique.

Space Vector PWM

Usually, the three phase voltage reference waves are modulated individually. Space Vector PWM is a concept where the three-phase references are represented as a space vector v_{abc} in the complex plane and this reference vector is modulated by an output voltage from the inverter.

The Space Vector PWM concept, currently widely being used in many three-phase inverter applications including electric drives, since it produces 15.5% of the fundamental output voltage component more than what sinusoidal PWM can produce. Space Vector Modulation also reduces the number of harmonic disturbances in the output waveform.

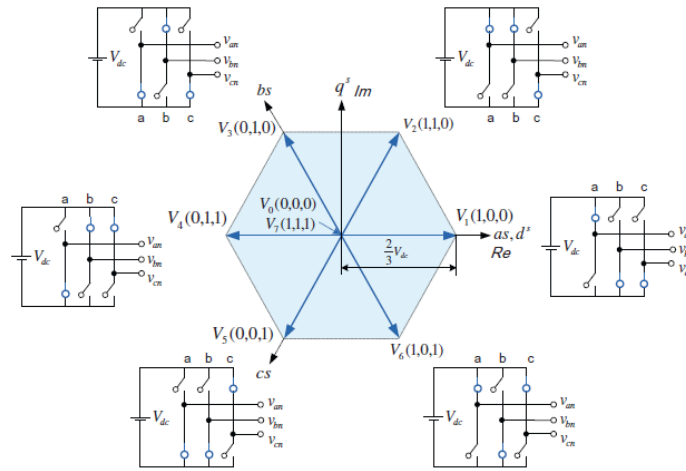


Figure 19: SVPWM Output Vectors in complex plane [8]

Six of these vectors from $V_1 - V_6$ are called active voltage vector, these vectors offer effective voltage on the load. The magnitude of all these active vectors is equal to $2V_{dc}/3$. Each vector is shifted by a phase difference of 60° . The two null vectors V_0 and V_7 cannot effectively yield output voltage.

In Space Vector PWM, a voltage reference is given as a space vector as mentioned previously and this reference is generated from the output of the inverter. By using the active voltage vectors and arranging them in an hexagon shape and assuming that the reference voltage vector is between any two adjacent active voltage vectors, the space vector method produces a fundamental volt-second average as the given voltage reference over a modulation time period T_s . [8]

Overmodulation

A PWM inverter can generate the output voltage with respect to the reference voltage, but this is highly limited to the factor of Modulation Index. In Sinus PWM technique, if the reference wave peak is higher than carrier wave peak or in Space vector concept, when the voltage vector lies outside the hexagon it can lead to non-linear increase in fundamental output voltage and current from the output of inverter. [8]

Nonlinearity also induces unnecessary injection of disturbance such as odd harmonic injection which results in noise.

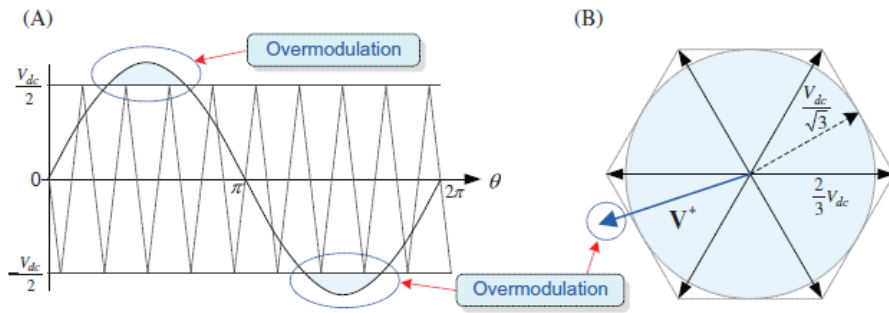


Figure 20: Overmodulation in SPWM and SVPWM [8]

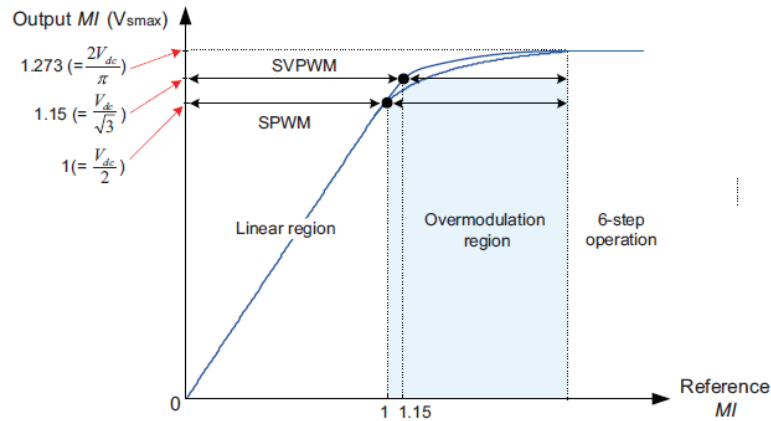


Figure 21: Overmodulation Region [8]

The beginning of overmodulation depends on which type of PWM technique we use, for instance in Sinus PWM, the overmodulation region starts at 78.5% and for Space Vector PWM, the overmodulation starts at 90.7%.

Motor Control

Controlling the Induction motor is an important aspect for both steady state and transient cases. Improper control can lead to a significant drop in power output from the motor. Scalar and Vector Control methods are usually employed to control the speed.

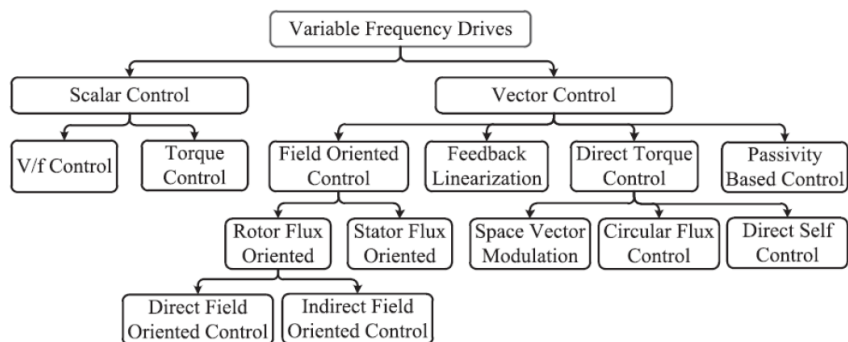


Figure 22: Variable Frequency Drives Control Methods [1]

V/F method represents the scalar method and it is one of the popular methods in motor control. It has both open and closed loop control system. It is used in many industrial process mainly due to its simplicity. The V/F ratio is kept constant in the process by keeping the magnetic flux at the rated value. For steady state conditions, this scalar method works well but it is not useful for transient conditions due to its slow response time and hence fails in control of speed during transient response.

For these reasons, Field Oriented Control (FOC) became a popular alternative to scalar control. FOC is commonly used in control of motors due to its higher performance with fast response and high control over precision. This method is based on obtaining the phase and magnitude of currents or voltages. In this thesis, I have employed FOC method to control the speed of the Induction Motor. The position of voltage, current and flux vectors are estimated using the popular mathematical transformations such as Park and Clark transformation. Therefore, the torque and flux are generated correctly.

Scalar V/F Control Method

The Three-phase IM considered generally to be self-starting constant speed because of the rotor speed alteration in proportional to the frequency change of the source voltage.

$$N_s = \frac{120f}{P}$$

Equation 46: Synchronous Speed [1]

Where, N_s is the synchronous speed, f is the supply frequency and P is the number of pole. In addition, the rotor speed is given by

$$N_r = (1 - S). N_s$$

Equation 47: Rotor Speed [1]

Where 'S' is the slip and N_r is the actual rotor speed. In scalar method of motor control, the stator voltage should be adjusted in proportion to the supply frequency in order to maintain the flux at a constant level.

For low-speed operations, the voltage drop across the stator resistance should be taken into account, hence a small proportion of boost voltage is provided during the start-up conditions to overcome this voltage drop. At high speeds, exceeding the rated frequency, the same condition to increase the voltage cannot be implemented as it would lead to overvoltage.

Therefore, if the operating condition reaches the rated frequency, the voltage supply is restricted to constant rated voltage supply. The above mentioned can be put it as a simple rule as,

$$V_s = \begin{cases} (V_{s, \text{rated}} - V_{s,0}) \frac{f}{f_{\text{rated}}} + V_{s,0} & \text{for } f < f_{\text{rated}} \\ V_{s, \text{rated}} & \text{for } f \geq f_{\text{rated}} \end{cases}$$

Equation 48: Criterion For V/F [16]

Where, $V_{s,0}$ is the rms value of the stator voltage at zero frequency.

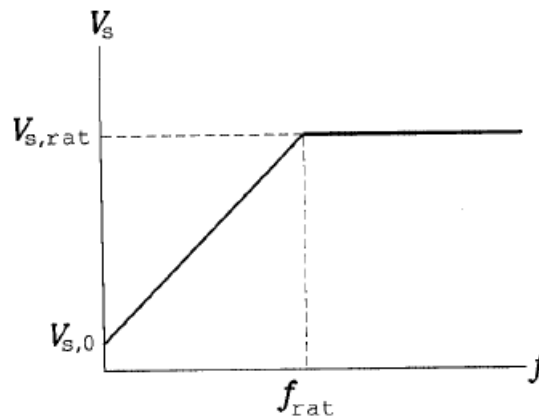


Figure 23: Voltage Vs Frequency relation in Scalar Control [16]

Frequencies higher than the rated frequency of the machine results in reduction of developed torque which is caused by the reduction in magnetizing current. This is known as field weakening mode. The motor is said to operate in field weakening mode. The region to the right of the rated frequency is the constant power area and to the area left of the rated frequency is constant torque area. [16]

As the torque reduces when the speed increases, the product between these two variables remains constant. A simple version of constant velocity to frequency drive system is shown in the below diagram. A fixed value of slip velocity ω_{s1} is added to the reference velocity ω_m^* of the motor to obtain the reference synchronous frequency ω_{syn} . To obtain the output frequency of the inverter, the reference frequency is multiplied with the number of pole pairs, p_p . This reference frequency is used as the input signal to the voltage controller. When the motor is current is too high, a current limiter is added to saturate the current beyond the peak value.

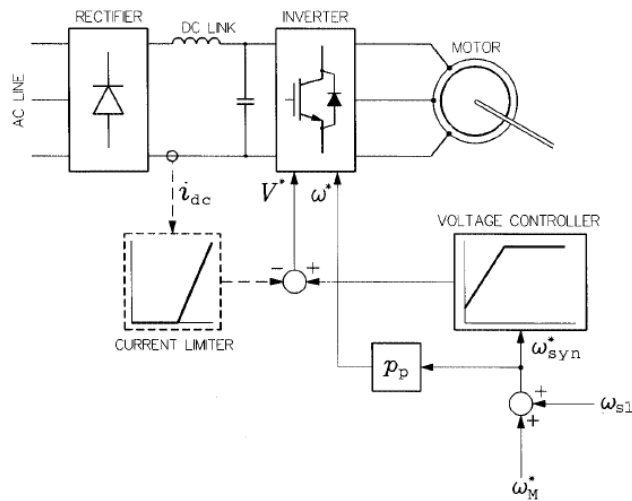


Figure 24: CVH Basic layout [16]

As the actual slip varies with the load of the motor, high speed control is not possible. Hence the simple CVH model is used in low-speed applications like pumps, fans, mixers or grinders where the application of highspeed control is not necessary.

To improve the control of the scalar system, the basic open-loop structure can be converted into a closed-loop by adding PI controller to measure the slip speed which is further summed up with the feedback rotor speed to result in reference frequency and similar to open loop process, this frequency is used as an input in voltage controller and sent to inverter as a reference voltage signal. The slip speed resulting from the PI controller must be limited for the purpose of stability and over current protection, hence a saturation tool is used to limit the slip speed similar to current limiter in open loop system.

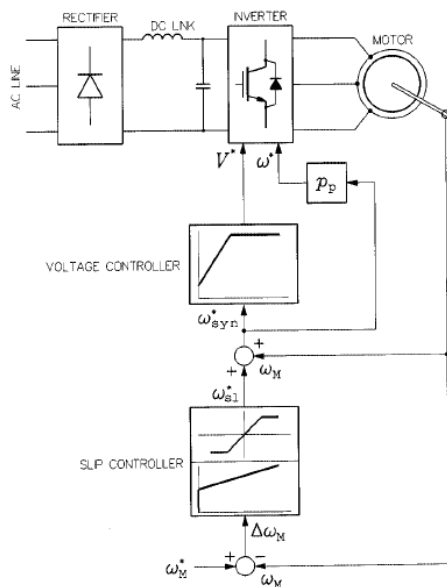


Figure 25: Closed Loop CVH System [16]

Vector Control

Scalar control is simple and offers good steady state response. However, for transient states, the dynamics are too slow. Hence to obtain a high precision and good dynamics, vector control with closed loop feedback systems is used. At the beginning of 1970's the principle of flux control was introduced by F. Blaschke and Hasse. The Field oriented control or vector control of Induction Motors works like a separately excited DC motor. The same performance of a DC motor can be achieved if the Induction motor control is considered in synchronous rotating reference frame where its sinus components appear dc-like quantities in steady state. The two stator currents can be used to control the vector control inverter. The Field Oriented Control is classified as Direct FOC and Indirect FOC. The Direct FOC depends on measuring the flux in stator- rotor gap directly while the Indirect FOC estimates the magnetic flux from the applied voltages and resulting currents through the motor. In this thesis, I have used Indirect FOC to control the speed of the Induction Motor.

Indirect FOC overcomes the problems in the scalar V/F method by adding a constant reference values for the torque and flux components of the Induction motor. Current I_q controls the Torque while I_d controls the flux.

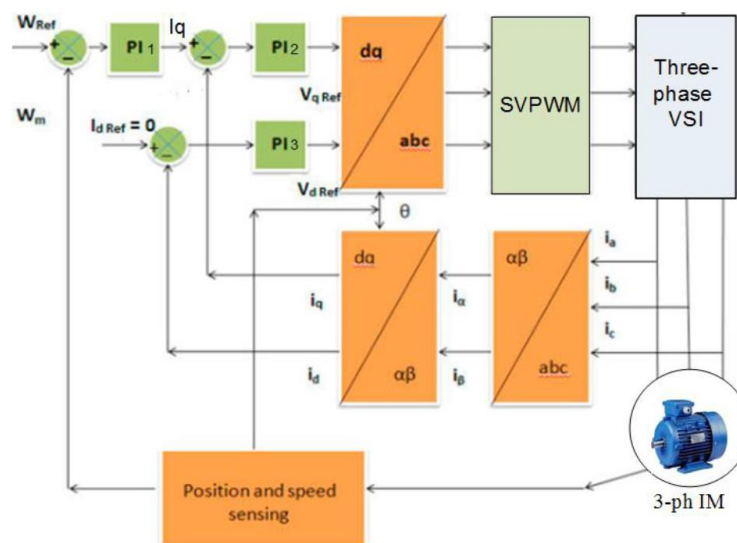


Figure 26:IFOC Control Architecture Layout [1]

In Indirect FOC there are two control loops namely outer and inner control loop. The outer control loop is the speed control loop and it sets a required torque setpoint and this torque setpoint is taken as the reference value for one of the inner control loops which controls the current I_q .

Further the output of the inner PI control is transformed from the direct and quadrature axis to three phase abc axis, and these phase voltages are taken as the reference sinusoidal voltages for Voltage Source Inverter, with the help of PWM technique the desired voltages are supplied to the Induction machine.

Direct Torque Control

Direct torque control was described first by Takahashi in 1984 in Japan and it was presented to everyone by Depenbrock in Germany. Unlike FOC, Direct Torque Control does not demand any co-ordinate transformation, control regulators, PWM and position encoders. DTC strategy works principally by choosing one of the inverter's six voltage vectors and two null vectors to keep the stator flux and torque within the hysteresis band around the command or reference flux and torque magnitudes. But some of the drawbacks of DTC control are, sluggish response during start-up, large and small or flux mistakes are not distinguished. [14]

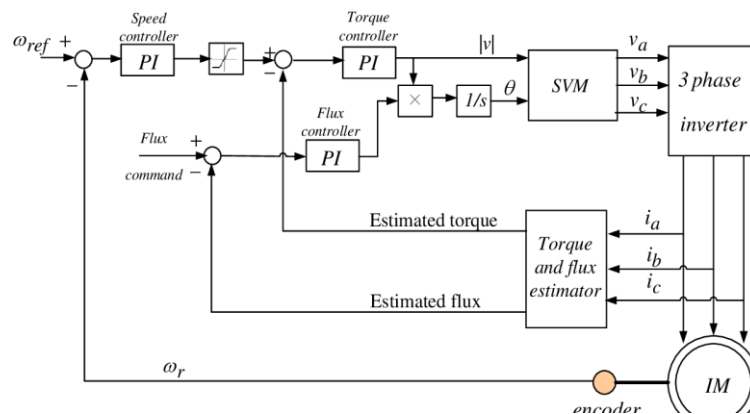


Figure 27:DTC Layout

PID Controllers

PID controllers are the typical control elements found in feedback system in any process where there is a need for automation. P stands for Proportional and I stand for Integral and D stands for Derivative.

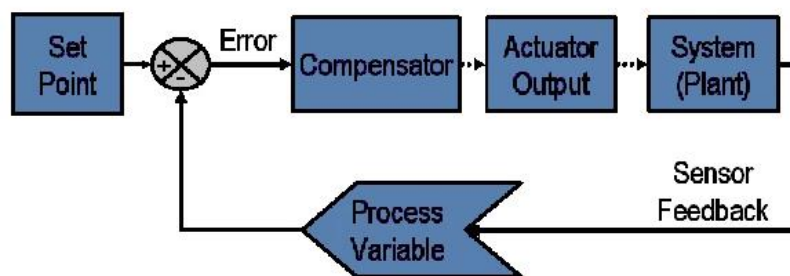


Figure 28:Block diagram of a typical closed loop system [12]

Some of the terminologies used in the control systems are,

- Set point - Desired Reference value
- Process Variable – Measured output
- Error – The difference between the setpoint and process variable

Proportional response

The proportional component depends only on the difference between the setpoint and process variable (i.e), the error term. The proportional gain constant (K_c) determines the ratio of output response to the error signal. In general, increasing the proportional gain will increase the speed of the control system [12]. However, if the proportional gain is too large, the process variable will begin to oscillate and if the gain value is increased further the system might become unstable and may even oscillate out of control.

Integral Response

The Integral component sums the error over time. The result is that even a small error term will cause the integral component to increase slowly. The integral response will continually increase over time unless the error is zero, so the effect is to drive the steady state error to zero. Steady state error is final difference between the process variable and setpoint. A phenomenon called Integral windup results when the integral action saturates a controller without the controller driving the error signal towards to zero. To avoid this Integral Anti windup constant is used along with the necessary saturation point as one of the required values to initiate the anti-windup process. The gain for Integral Anti-windup is given as the inverse value of Proportional gain.[12]

Derivative Response

The derivative component causes the output to decrease if the process variable is increasing rapidly. The derivative response is proportional to the rate of change of process variable. Increasing the derivative time (T_d) will cause the system to react more strongly to the changes in error term and will increase the speed of the overall control system response [12]. If the sensor feedback is too noisy or if the process is too slow, this can cause the derivative term to make the system unstable.

$$u(t) = K_p e(t) + K_i \int e(t) dt + K_p \frac{de}{dx}$$

Equation 49:PID Controller

Where K_p is the proportional gain, K_i is the Integral gain, $e(t)$ is the error value , $u(t)$ is the PID control variable.

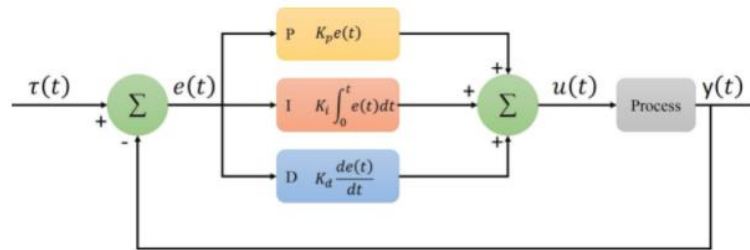


Figure 29: Basic Layout of PID controller

Design Considerations of Control System

The PI control has been widely used in the control of current, speed and flux of AC motors, The performance of PI controller heavily depends on the gain value of the individual parameters, hence good care should be given while selecting the variables.

The variables which should be considering while designing a PID controller are [6]

- Stability

In general, the whole system must be stable in order to get satisfying results. Unstable systems provide oscillatory response. The stability of the system can be assessed by checking the poles of the transfer function of the system.

- Response Time

Response time denotes how quickly the system responds to a change in input. The response speed may be proportional to its control bandwidth. In general, wider the control bandwidth, faster the speed of response. If the control bandwidth is too large, it might lead to unstable response. This control bandwidth is mainly dependent on the proportional gain of the controller.

- Steady State Error

A steady state error is defined as the difference between the process variable and the set point of the system once the system reaches the steady state.

The bandwidth of a system is a measure of a feedback system's ability to follow the input signal.

Sinusoidal inputs with a frequency less than the bandwidth frequency are followed reasonably well by the system, whereas inputs greater than the bandwidth frequency are attenuated by a factor of 1/10 or greater.

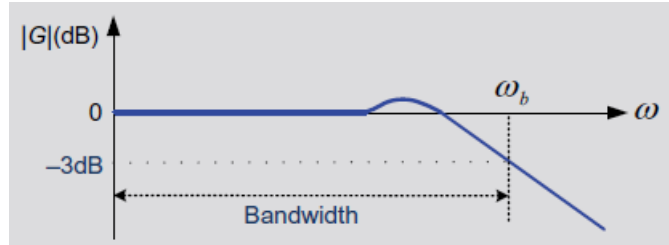


Figure 30: Gain Margin Vs Frequency [6]

For the control of Induction Motors, the current control is being done in the synchronous reference frame which is rotating at an electrical frequency of ω_e corresponding to the operating frequency of the three phase currents.

Since dq component resembles the waveform of dc component, we can assume the current of an induction motor can be controlled the same way for a dc motor.

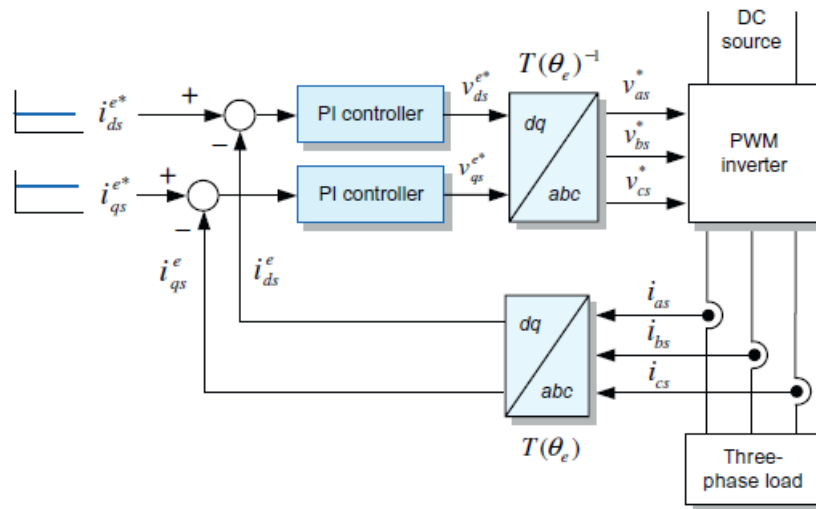


Figure 31: Block Diagram of a synchronous frame current regulator [6]

Selection of Bandwidth for Current Control

The value of proportional gain constant determines how fast the system responds whereas the integral gain constant determines how fast the steady state error is eliminated. When these gain values are larger, the system's response time is better, but beyond the threshold value the gain values would make the system unstable. Gain values are determined by its bandwidth, ω_{cc} . [6]

The bandwidth of the current controller ω_{cc} are determined by using two factors,

- Switching frequency of power converter element (inverter)
- Sample time for detecting current for feedback

Since, the motor cannot switch beyond its switching frequency, it is the main limiting point for choosing bandwidth for current control. If the current is twice sampled every period, as a rule of thumb, the maximum available frequency can be upto $1/10^{\text{th}}$ of the switching frequency. Whereas if the current is sampled for once every switching frequency, then the maximum available bandwidth is $1/20^{\text{th}}$ of switching frequency. The procedure for gain selection for PI current controller are as follows [6] ,

- Find the switching frequency of the power converter
- Select the control bandwidth ω_{cc} of the current controller to be within $1/10 - 1/20$ of the switching frequency and $1/25$ of the sampling frequency.
- Calculate the gain values using the below mentioned formula
 - Proportional gain (K_P) = $\sigma L_s \omega_{cc}$
 - Integral Gain (K_I) = $\left[R_s + R_r \left(\frac{L_m}{L_r} \right)^2 \right] \omega_{cc}$
 - Where L_s, R_s, R_r are stator inductance , resistance and rotor resistance.
 - And $\sigma = 1 - \frac{L_m^2}{L_s L_r}$
- Select the Integral Anti-Windup controller if needed, $K_a = 1/K_P$
- The first two procedures are repeated until the performance is satisfactory

Speed Control Design

Speed control of an induction motor is done on the outer loop of the control block. In this case if the bandwidth of the current controller is sufficiently wider than speed control, then current control will not have any influence on speed control and the stability of speed control can be improved.

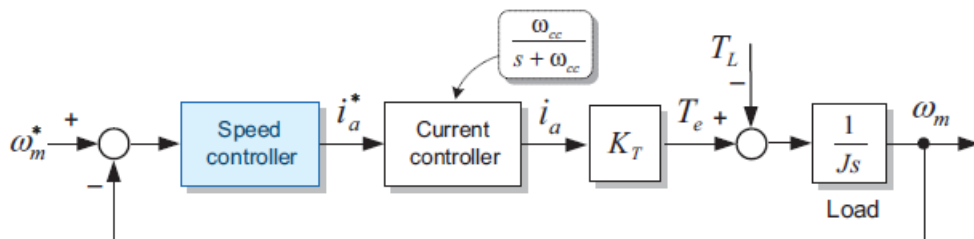


Figure 32: Speed Control PI Loop [6]

The speed control bandwidth ω_{cs} that determines the dynamic performance of speed controller, is limited by the bandwidth of current controller and the sampling time of speed. The bandwidth of speed control should be atleast 5 times less than the bandwidth of current control. The procedure to be followed while selecting the gain values for PI controller are [6],

- Identify the bandwidth of the current controller.
- Select the bandwidth of speed controller to be five times less than the current controller and ten times less than the sampling frequency of speed.
- Calculate the gain values using the below mentioned formula.
 - Proportional Gain : $K_{PS} = \frac{J\omega_{cs}}{K_T}$
 - Integral Gain : $K_I = K_{PS} * \omega_{pi} = K_{PS} * \frac{\omega_{cs}}{5} = \frac{J\omega_{cs}^2}{5K_T}$
- Select the Integral Anti windup gain if necessary : $K_A = 1/K_{PS}$
- K_T is a machine parameter called Torque constant and the expression for finding K_T is Nominal Torque / Nominal current , and J is the moment of inertia of the machine. Hence if these machine parameters are incorrectly used we might get incorrect gain values.

Experimental Procedure

The experiments on Induction Motor was conducted at the VTP Roztoky Facility near Praha. The specifications of the motor are,

- Maximum Power: 28kW
- Nominal Frequency: 100Hz
- Nominal Voltage: 180V, Star Connected
- Stator Resistance: 0.016 Ω
- Stator Leakage Reactance: 0.091 Ω
- Stator Leakage Inductance: 0.14mH
- Rotor Resistance re-calculated to stator: 0.018 Ω
- Rotor Leakage Reactance: 0.126 Ω
- Rotor Leakage Inductance: 0.20mH
- Magnetizing Inductance: 2.9mH

The above-mentioned parameters were given as machine parameter during the simulation.

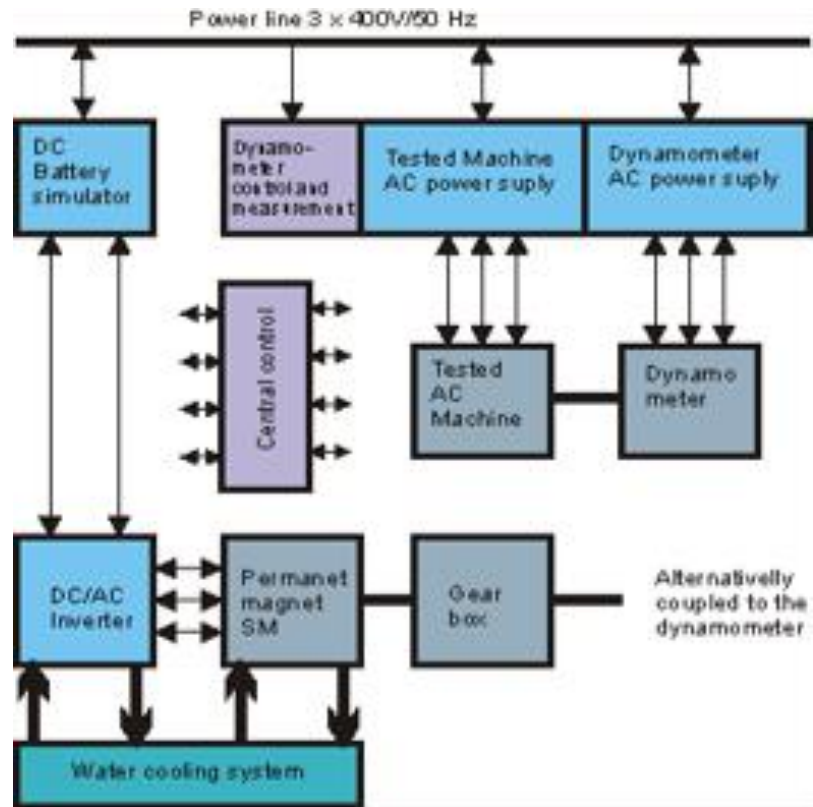


Figure 33:Block Diagram of Test bench

During Testing, some pictures of the test bench were captured for reference.



Induction Motor

Figure 34:Induction Motor Connected to Dynamometer

Dynamometer



Figure 35: Measuring workplace with measured motor TEM 112 M04

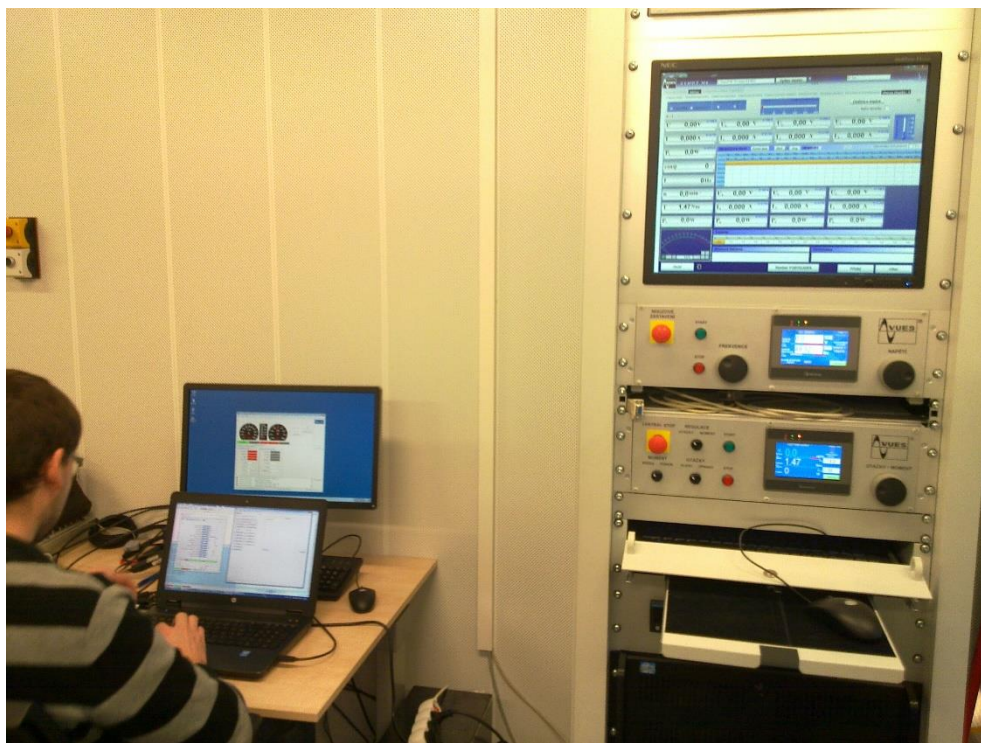


Figure 36: Measurement and Control System

The experiments were performed using Scalar method of motor controlling by controlling the frequency using the control system. Performing a closed loop experiment was not possible as the required instruments were not at disposal, hence the experiment was performed using an open loop scalar V/F method and these results were validated in Simulation using a closed loop Field Oriented Control. Thereby studying on how a closed loop system works and observing the parameters affiliated with the closed loop simulation.

The experiments were done by selecting a specific working point and running the motor for that specific working point for 10 seconds and the parameters were observed. Motor's output speed was taken as a working point. The measurements were taken for 4 working points which are 1000,1500,2500,3000 rpm. Multiple measurements were taken for the same working point and I selected one measurement for each working point with Voltage/Frequency ratio to be 1.8 or closer to 1.8.

The simulations were done for both steady state and transient state. The reference input for induction motor model was chosen as speed reference from the experimental readings.

| S.No | Speed | Torque | Voltage | Current | Frequency | Cos ψ | Power |
|------|-------|--------|---------|---------|-----------|------------|-------|
| | rpm | Nm | V | A | Hz | | W |
| 1 | 1000 | 89 | 62 | 128 | 36 | 0.85 | 9418 |
| 2 | 1500 | 115 | 91 | 163 | 53 | 0.85 | 18166 |
| 3 | 2500 | 64 | 150 | 98 | 84 | 0.74 | 16990 |
| 4 | 3000 | 83 | 180 | 120 | 100 | 0.79 | 26353 |

Table 1: Experimental Measurements

Simulation Using MATLAB Simulink

The Simulation part of this thesis was performed on the platform Simulink by the MATLAB. In general, the simulation can either be equation-based environment or block-based environment. As the latest edition of MATLAB R2021b had all the necessary block sets to perform a simulation of this kind, block-based environment was adapted. This also makes the simulation considerably less complicated.

This simulation is based on the Vector control of the Induction motors with the rotor shaft speed, as the preferred input or the variable to control. We can also provide, Load torque as an input or the variable to control but due to the difficulties faced with controlling the current, I had to switch the focus from torque control to speed control.

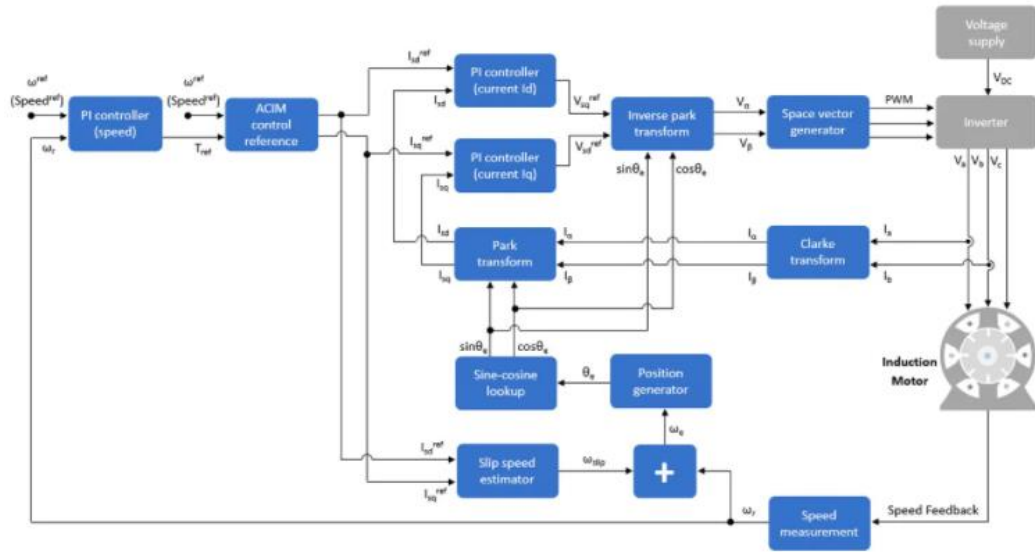


Figure 37: Generic FOC Algorithm for IM Speed Control [9]

After deciding the control method in which the simulation had to be performed, I took the above-mentioned image as a generic reference layout for speed-controlled simulation of Induction Motor. All the blocks that were necessary for performing the simulation were available under the add-on ‘Motor Control Block set’ in Simulink. Unfortunately, this ‘Motor Control Block Set’ is only available from the release year 2021.

The primary components/blocks that have been used in this simulation are [10],

- Inner Current Control Loop

There are two inner PI blocks employed to control the current and deliver it as the direct and quadrature voltage reference to generate the reference sinus voltage curves for PWM. The Q-axis current control helps in regulate the electrical torque applied to the motor whereas the D-axis current control regulates the current to reduce the D-axis flux and allow the motor to rotate above its baseline speed at the expense of torque.

- Outer Speed Control Loop

The outer PI loop is used to generate a torque setpoint. In this simulation, the torque setpoint from the Speed control loop is directed to the Q-axis current control as the reference value for the current control PI. This speed control generally has a lower sampling rate than Inner current loop so that the influence of speed control will not be higher over the current control.

- Slip Speed Estimation

In order to find the rotating angle for the mathematical transformations like park and inverse park transformation we need to know the information about slip speed. As we know that Induction Machine rotates less than its synchronous speed. This block takes the D and Q axis reference current and by mentioning the machine parameters, we will be able to calculate the slip speed which is further used to find the angle of rotation for the above-mentioned purposes.

- Position Generator

The position generator is used to find the angle θ either in radians, degrees or per.unit. This block takes the summed value of rotor output speed from a sensing device, Speed measurement block for example and the slip speed. By multiplying the summed value of slip speed and rotor shaft speed with a sample time, we can obtain the θ in the shape of sawtooth ranging from -1 to 1 for radian scale.

- Space Vector Generator

The Space vector block generates the necessary sinus voltage curves or sinus curve with third harmonics injected for PWM of the inverter.

Simulation Results

In total, six simulations were carried out. 4 simulations for steady state and 2 transient simulations. As mentioned above, since these were selected working points during steady simulations the speed input was given in the below-mentioned way.

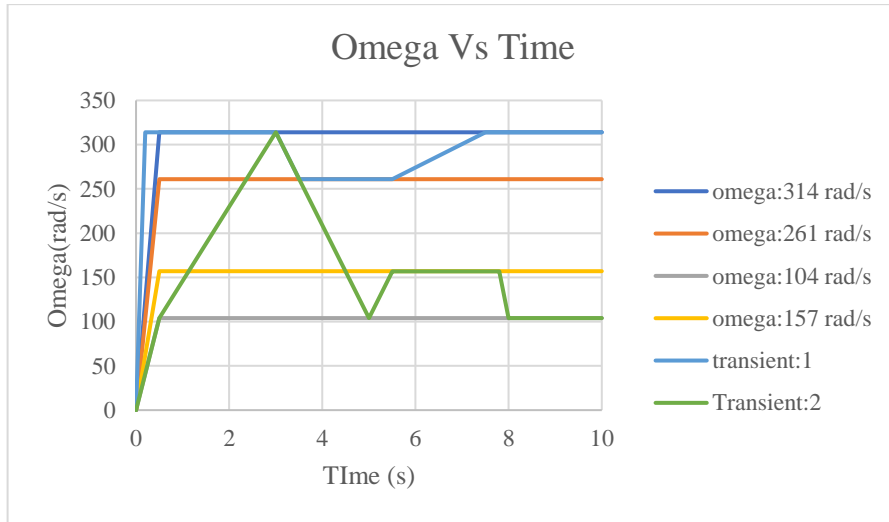


Figure 39:Reference Input

Steady State Analysis

Case 1:

Reference Output Speed- 104 rad/s

Inverter Switching frequency: 9500 Hz : 59690 rad/s

Inner Current Control Loop:

Initial iterations were performed by PI controller for calculations based on current control bandwidth to be $1/10^{\text{th}}$ of the switching frequency (rad/s). Resulting phase current was high and the use of Integral Anti-Windup as a part of saturation tool was found to be ineffective. After further iterations with the assumption that the current control bandwidth will be $1/20^{\text{th}}$ of the inverter switching frequency, the phase currents and the time required to reach the steady state for motor output speed synchronised with the experimental values.

$$\text{Proportional Gain: } K_P = \sigma L_S \omega_{CC}$$

Equation 50:Proportional Gain Constant for current control

$$\text{Integral Gain: } K_I = \left[R_S + R_R \left(\frac{L_m}{L_r} \right)^2 \right] * \omega_{CC}$$

Equation 51:Integral Gain Constant for current control

$$\sigma = 1 - \left(\frac{L_m^2}{L_S L_R} \right) = 0.108$$

Equation 52: Total Leakage Factor

Where L_m is the magnetizing inductance (2.9mH), L_S is the stator inductance (3.04mH), L_R is the rotor inductance (3.10mH), R_S is the stator resistance (0.016 Ω) and R_R is the rotor resistance (0.018 Ω)

$$\omega_{CC} = \frac{1}{20} * 9500 = 475 \text{ Hz} \triangleq 2 * \pi * 475 = 2984 \text{ rad/s}$$

Equation 53: Current Control bandwidth

Substituting these values in the above equation, the proportional gain was calculated to be 0.9798 and the Integral gain as 94.7652.

Outer Speed Control Loop

The speed control loop should be designed in such a way that it does not have a major impact on the current control loop. The bandwidth of the speed control loop should be at least 5 times less than the current control loop and within the limit of 1/10th -1/20th of the current control bandwidth.

For the reasons of stability as mentioned in the current control design, the gain values are calculated for 1/20th of current control frequency. The PI gains can be calculated as,

$$\text{Proportional Gain: } K_P = \frac{J\omega_{SC}}{K_T}$$

Equation 54: proportional gain for Speed Control

$$\text{Integral Gain: } K_I = \frac{J\omega_{SC}^2}{5K_T}$$

Equation 55: Integral gain for Speed Control

Where J is the moment of inertia (0.04 kgm²) and K_T is the torque constant (0.72).

$$\omega_{SC} = \frac{1}{20} * 475 = 23.75 \text{ Hz} \triangleq 2 * \pi * 23.75 = 149 \text{ rad/s}$$

Equation 56: Speed Control Bandwidth

After substituting the values in the above equations, the proportional gain constant was found to be 8.29 and integral gain constant as 247.42.

Sample Time

Sample time for speed and measurement and for finding the angle θ is taken as the inverse value of inverter switching frequency. For this case, the sample time is $1.67e^{-5}$ s. Incorrect value of sample time may also lead to unstable/incorrect results. Hence due care should be given to this constant.

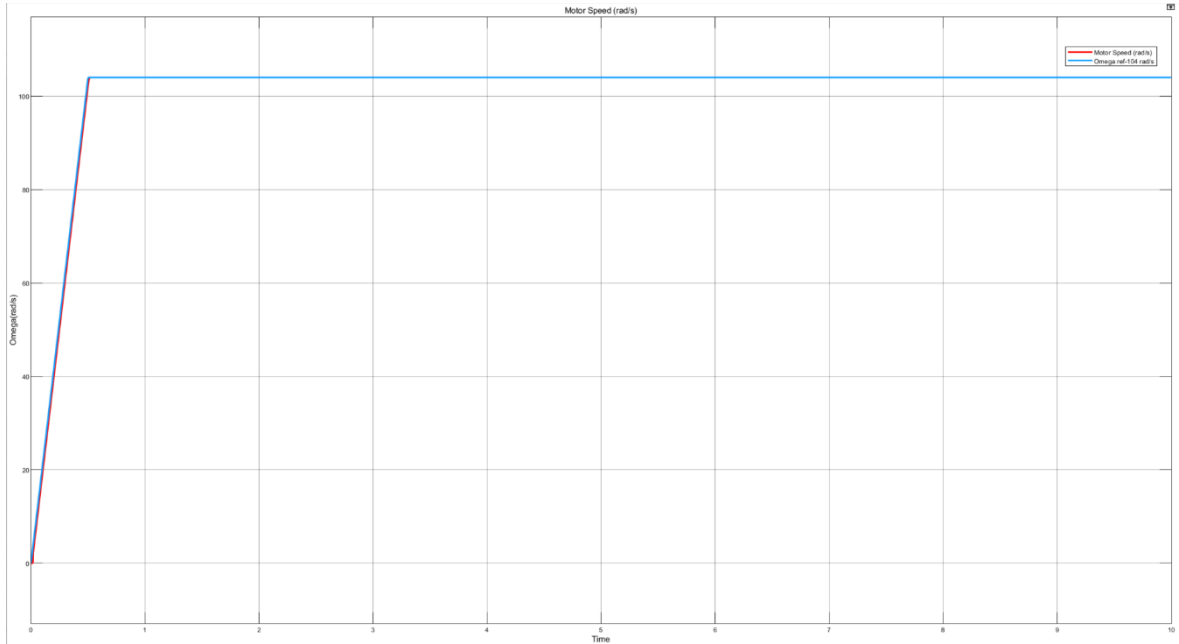


Figure 40:Motor Speed

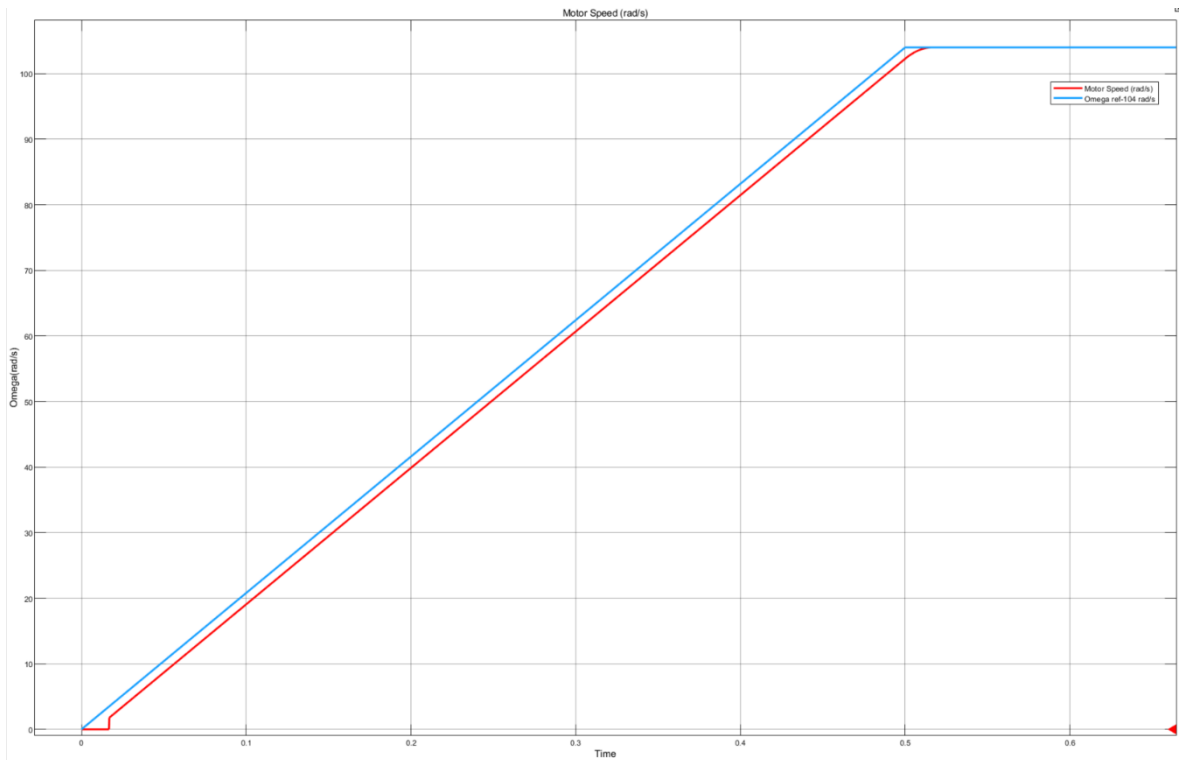


Figure 41:Detailed Image showing difference between reference and simulated curve

The above image shows the extent to which the simulated speed curve lags behind the reference speed command. As per the reference command, the motor speed should reach 104 rad/s at 0.5s.

In this result we can see that, the simulated curve lags a few tenths of a second from the speed reference. From the global point of view in the first image, the difference is not evident. Hence speed control function is achieved.

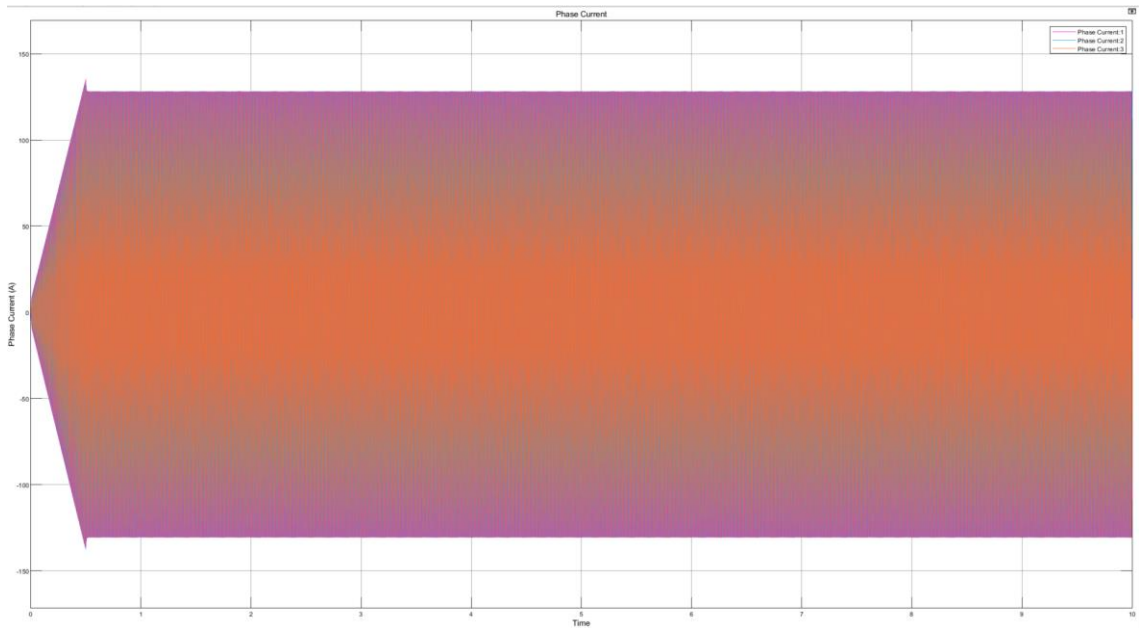


Figure 42:Phase Current

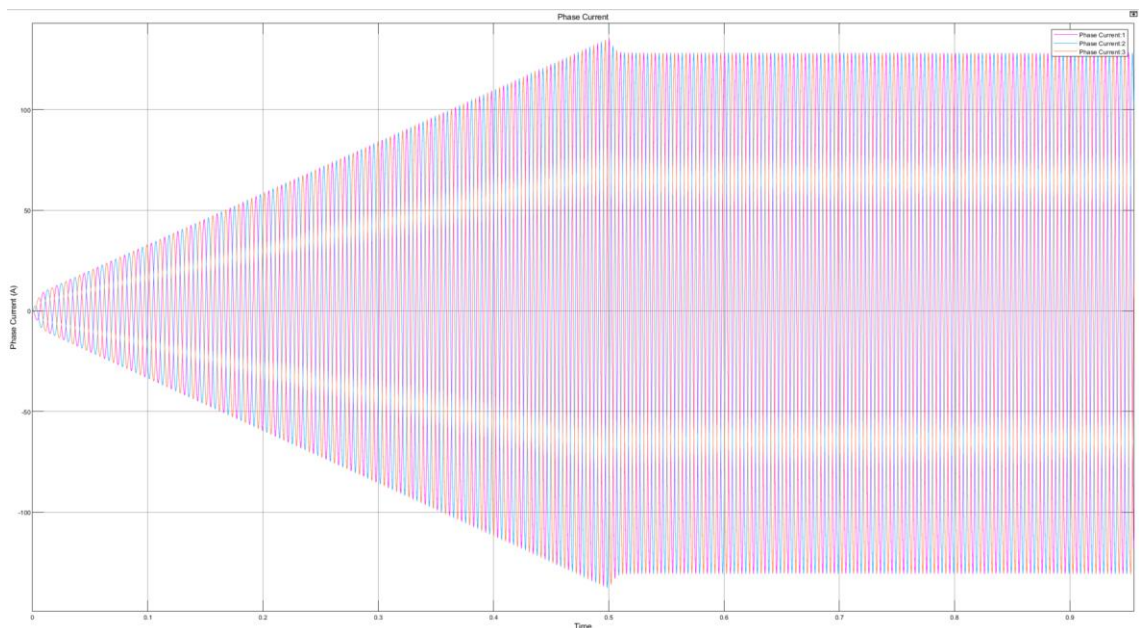


Figure 43:Detailed Image of Phase Currents

With reference to the experimental values, the required phase current of 128A was simulated once the speed reaches the steady state at 0.5s

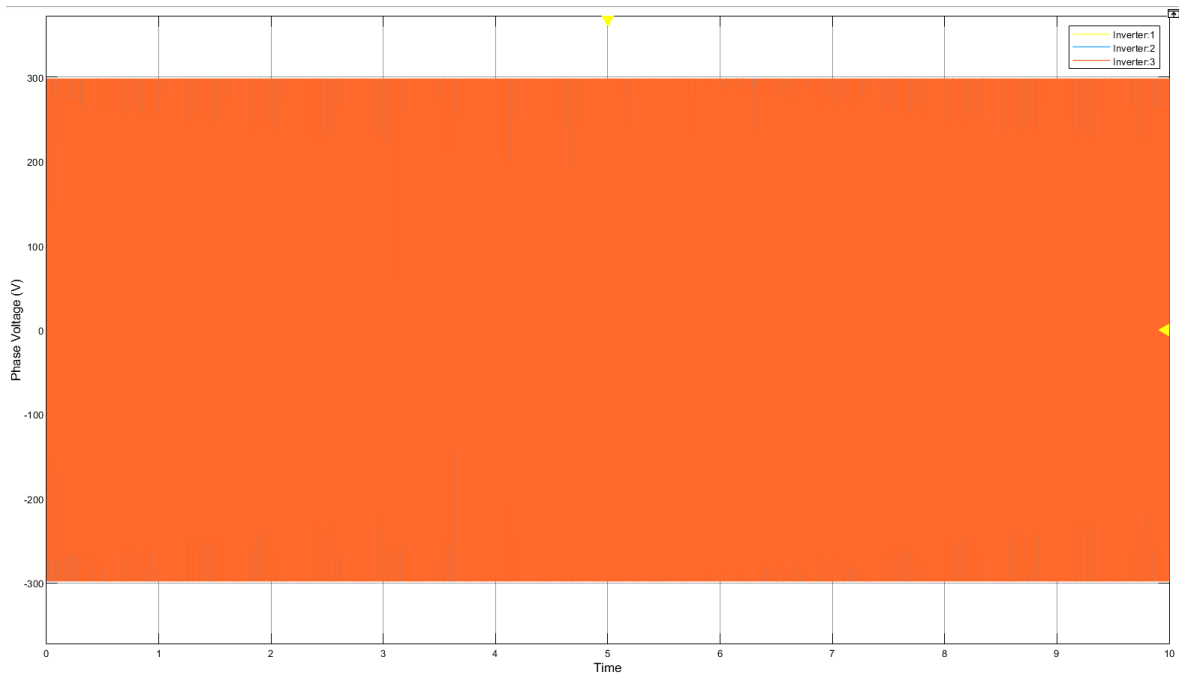


Figure 44: phase Voltage

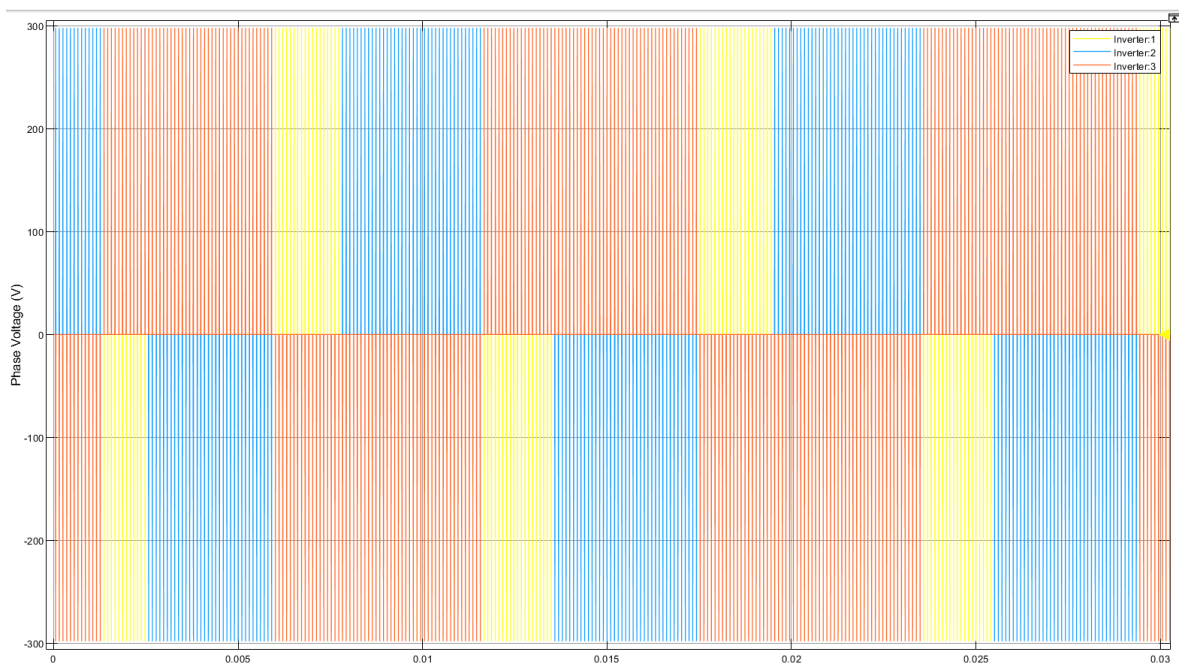


Figure 45: Phase Voltage Detailed Image

The output of the inverter is a square wave thus making it as a square wave inverter. The peak voltage remains same throughout the simulation. To find the sinusoidal amplitude of the voltage, time averaging can be performed.

The square waves are usually converted into sinusoidal waves with the help of inductance of the induction motor's stator. The square wave to sinusoidal conversion can also be done with the help of a R-C or R-L Low pass filter.

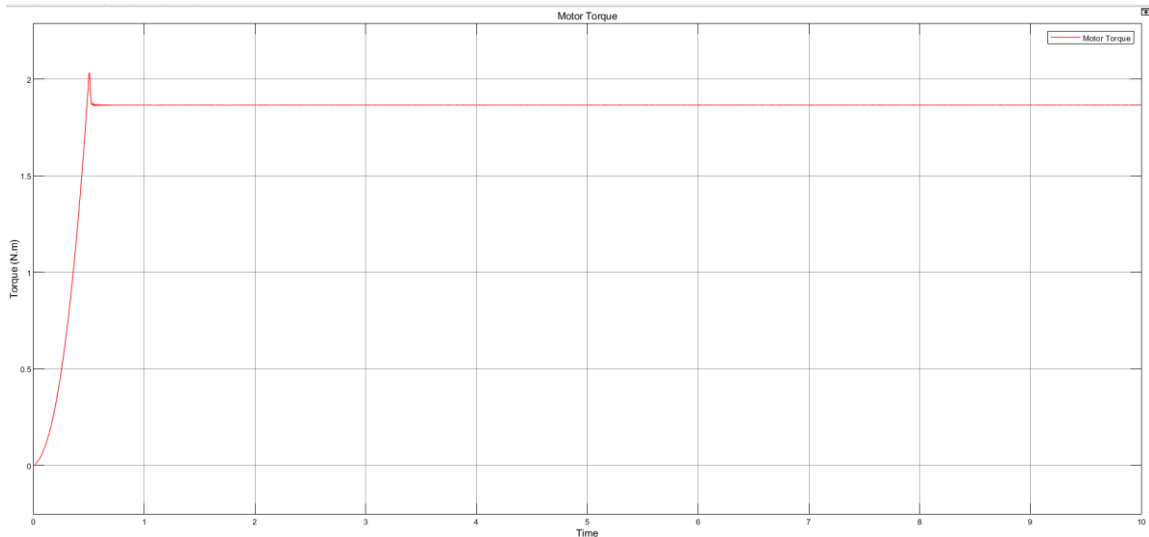


Figure 46: Torque

As the current increases, the torque also increases and once the steady state is reached, the torque settles at 1.8Nm and constant until the end.

Case 2:

Reference Output Speed- 157 rad/s

Inverter Switching frequency: 8700 Hz: 54663 rad/s

The process for calculating the gain values of PI controller for both inner current loop and outer speed loop remains the same and for the purpose of stability and easier current control. The current controller bandwidth is taken as $1/20^{\text{th}}$ of switching frequency and the bandwidth of speed controller is taken as $1/20^{\text{th}}$ of current controller.

Inner Current Controller:

Proportional Gain: $K_P = 0.8973$

Integral gain: $K_I = 86.7850$

Outer Speed Controller:

Proportional Gain: $K_P = 7.59$

Integral gain: $K_I = 207.508$

Sample Time: $1.829e^{-5}$ s

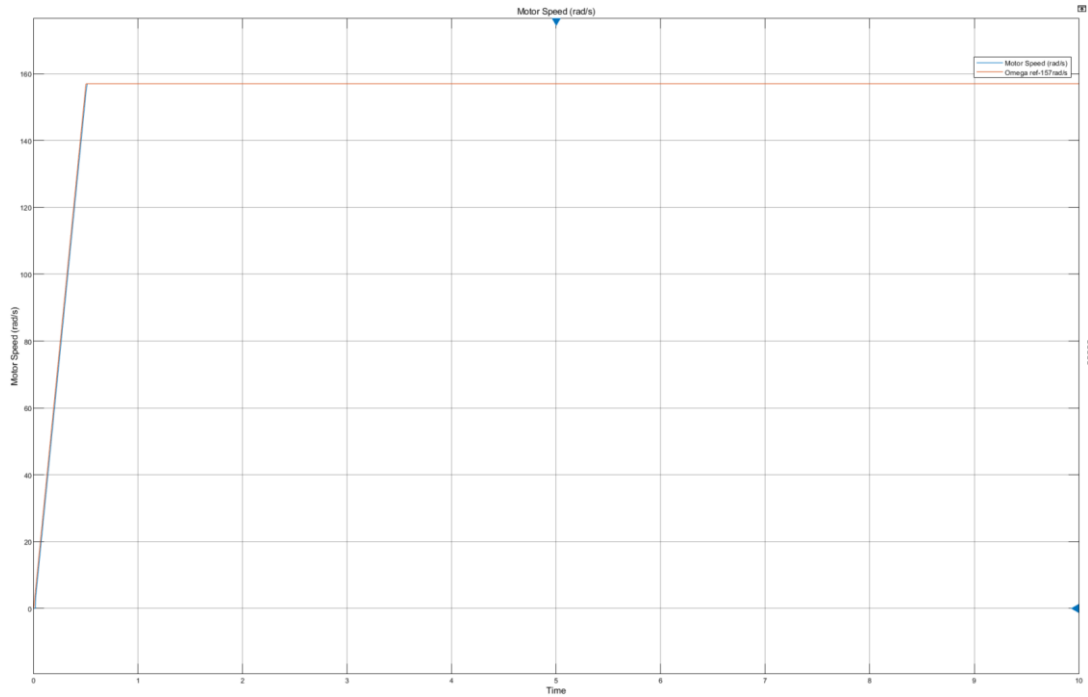


Figure 47: Motor Speed

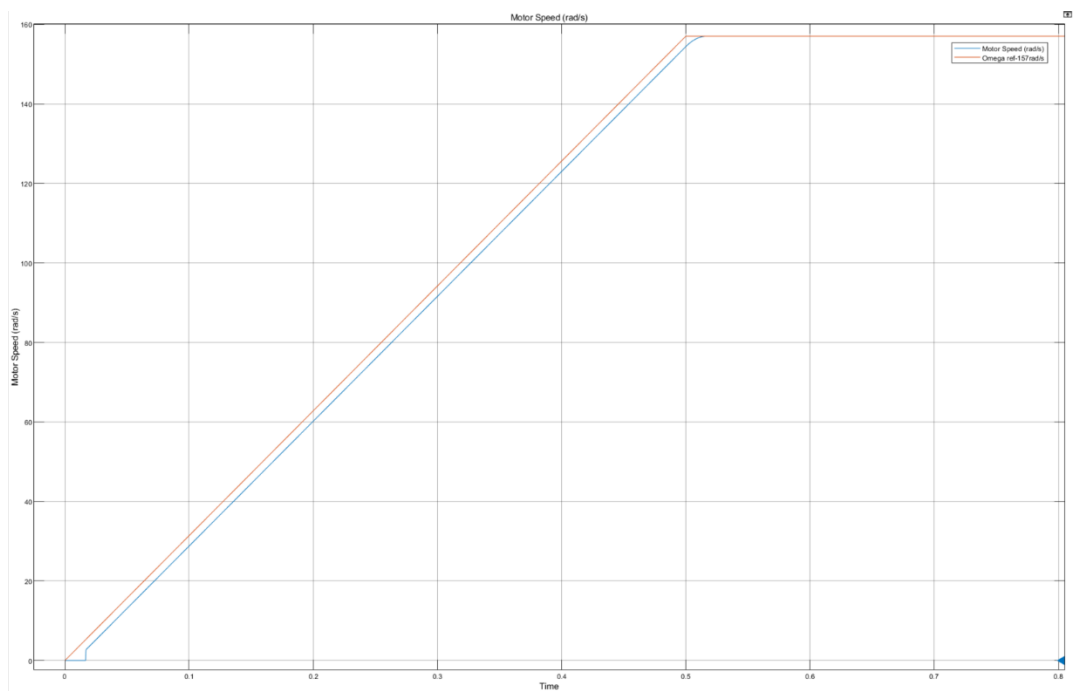


Figure 48: Detailed Image Showing the difference between reference speed and simulated result

The above picture depicts the difference on how the motor model reacts to the speed command. Similar delay at the start of the simulation can be seen when compared with the previous case of 104 rad/s. The time required to reach the steady state is few tenths more than the reference speed.

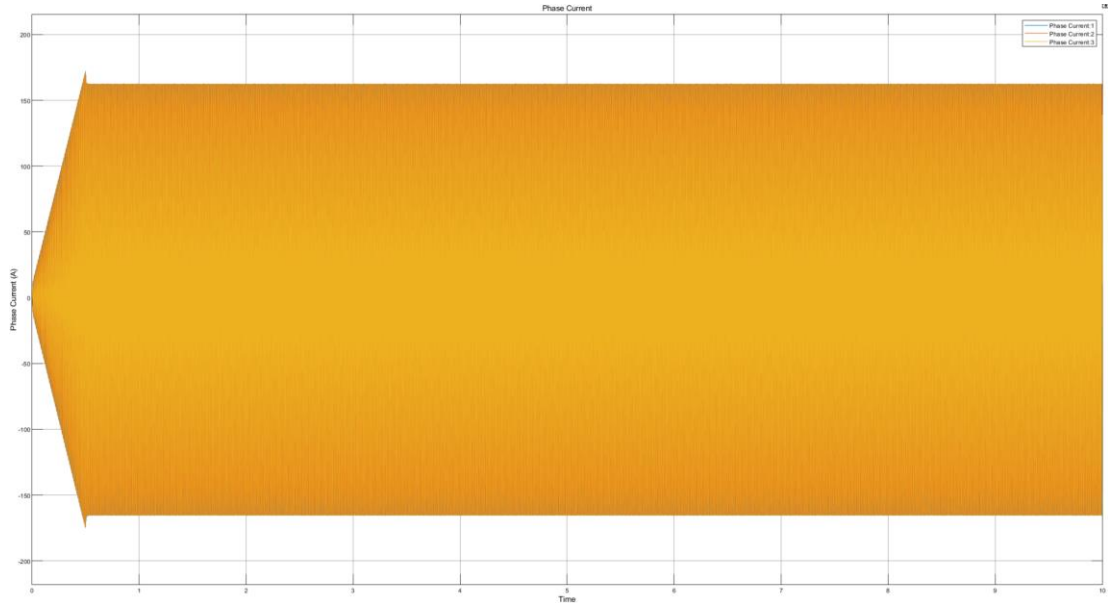


Figure 49:Phase current

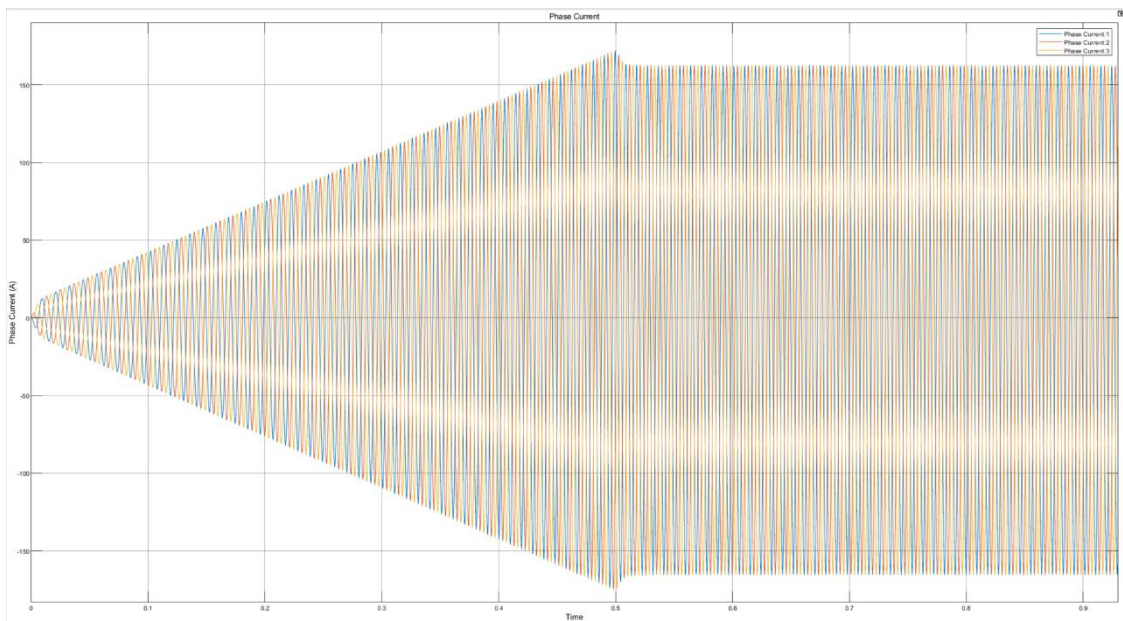


Figure 50:Detailed Phase Current

The controllers were fine tuned to match the experimental values, which was 163A with the simulation. In the simulation, once the speed reached its steady state, the current also came to the steady state condition and settled at 163A which equals to the experimental result.

As the current increases initially , torque also increases and reaches a peak of 3.7Nm and the torque reached the steady state with the magnitude of 3.4Nm.

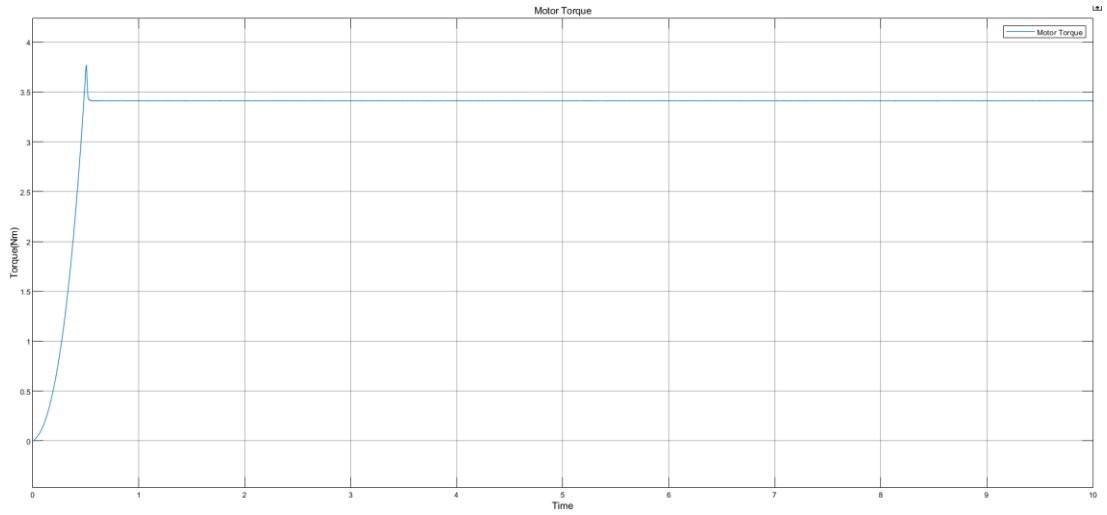


Figure 51: Torque

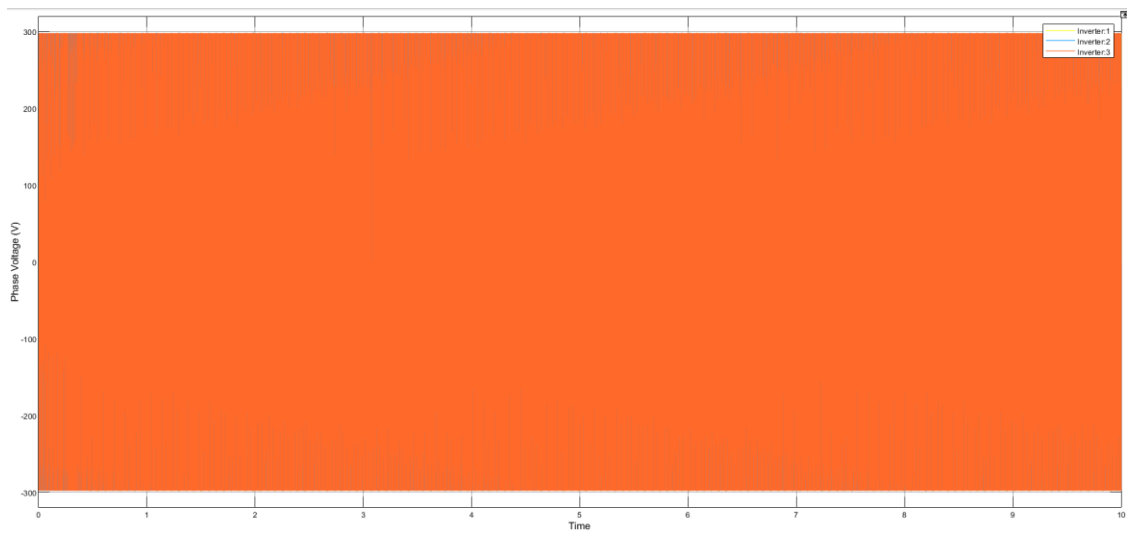


Figure 52: Phase Voltage

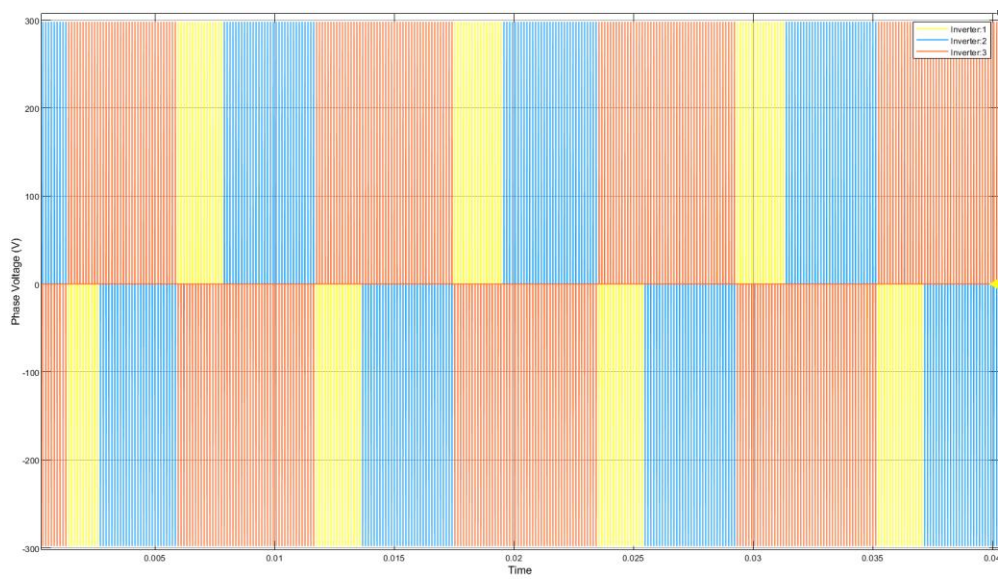


Figure 53: Square Waves of Input Voltage

Case 3:

Reference Output Speed- 261 rad/s

Inverter Switching frequency: 5200 Hz: 32672 rad/s

The process for calculating the gain values of PI controller for both inner current loop and outer speed loop remains the same and for the purpose of stability and easier current control. The current controller bandwidth is taken as $1/20^{\text{th}}$ of switching frequency and the bandwidth of speed controller is taken as $1/20^{\text{th}}$ of current controller.

Inner Current Controller:

Proportional Gain: $K_P = 0.5363$

Integral gain: $K_I = 51.871$

Outer Speed Controller:

Proportional Gain: $K_P = 4.537$

Integral gain: $K_I = 74.131$

Sample Time: $3.060e^{-5}$ s

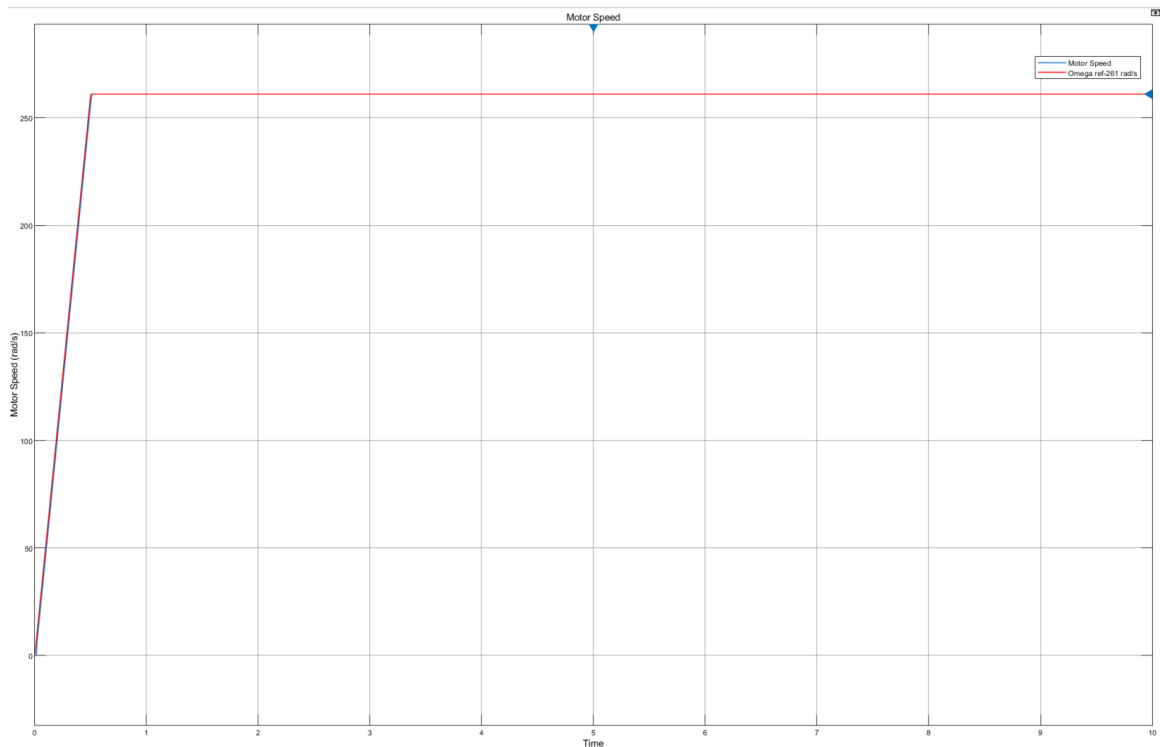


Figure 54: Motor Speed

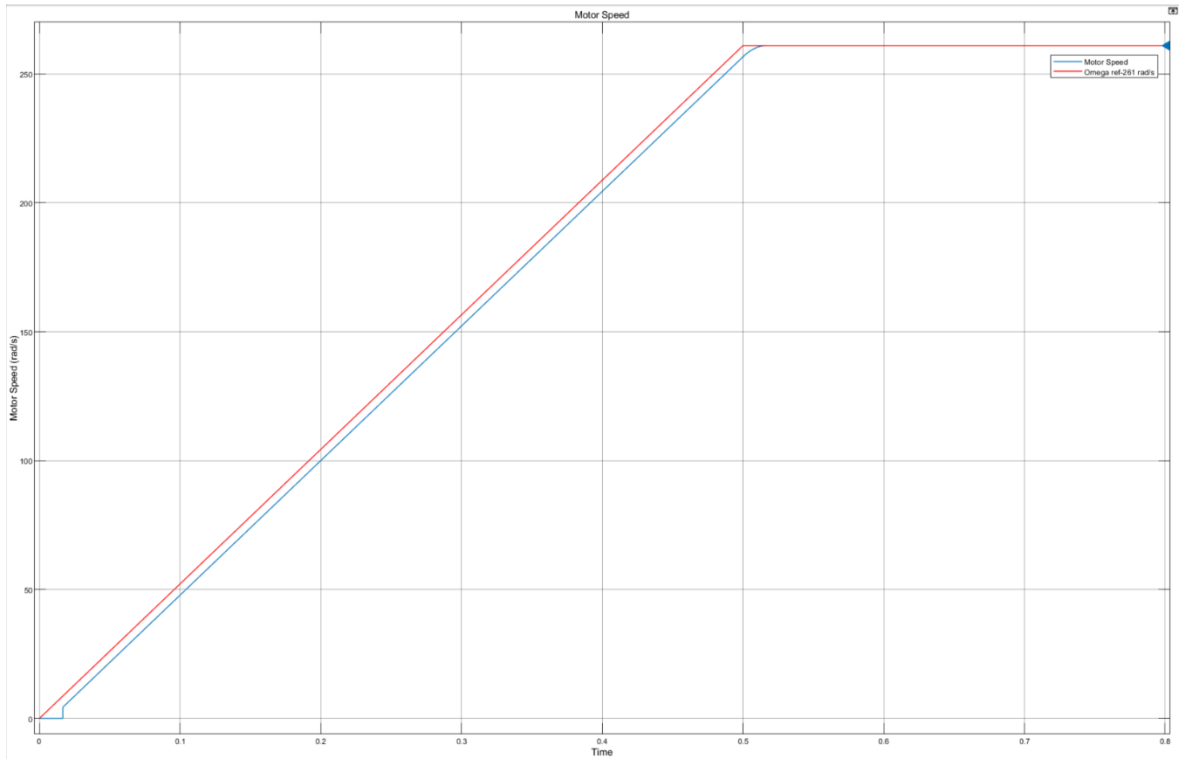


Figure 55: Detailed Motor Speed

Similar to the previous results, the lag between the reference speed command and simulated curve is only few tenths of a second.

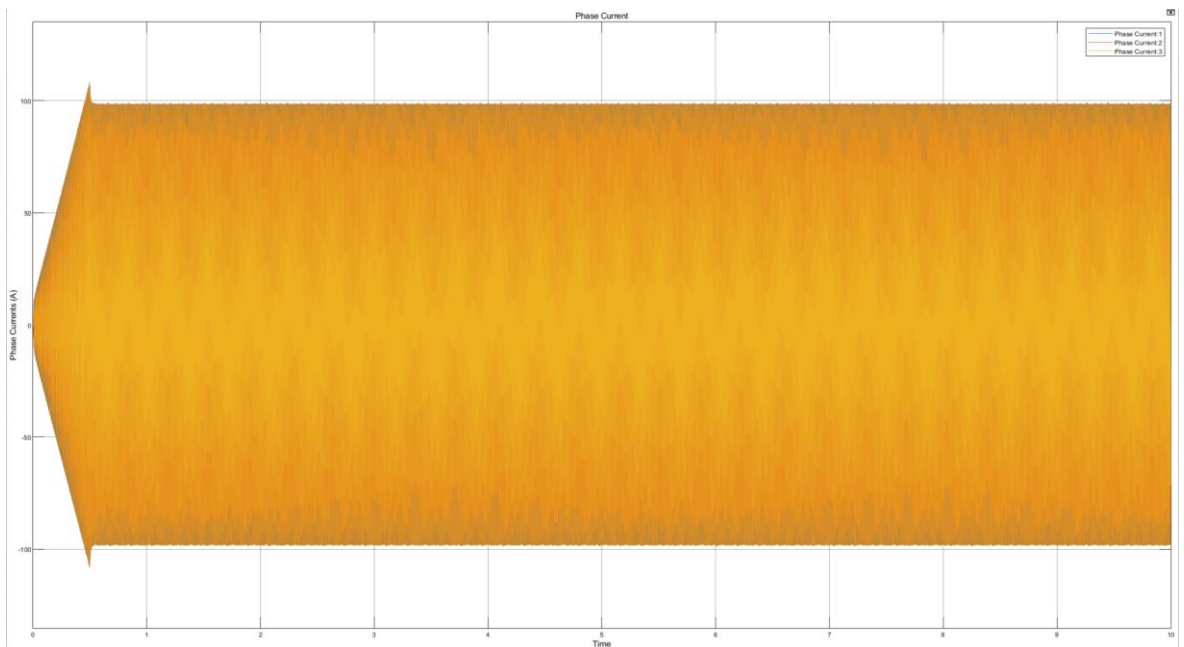


Figure 56: Phase Currents

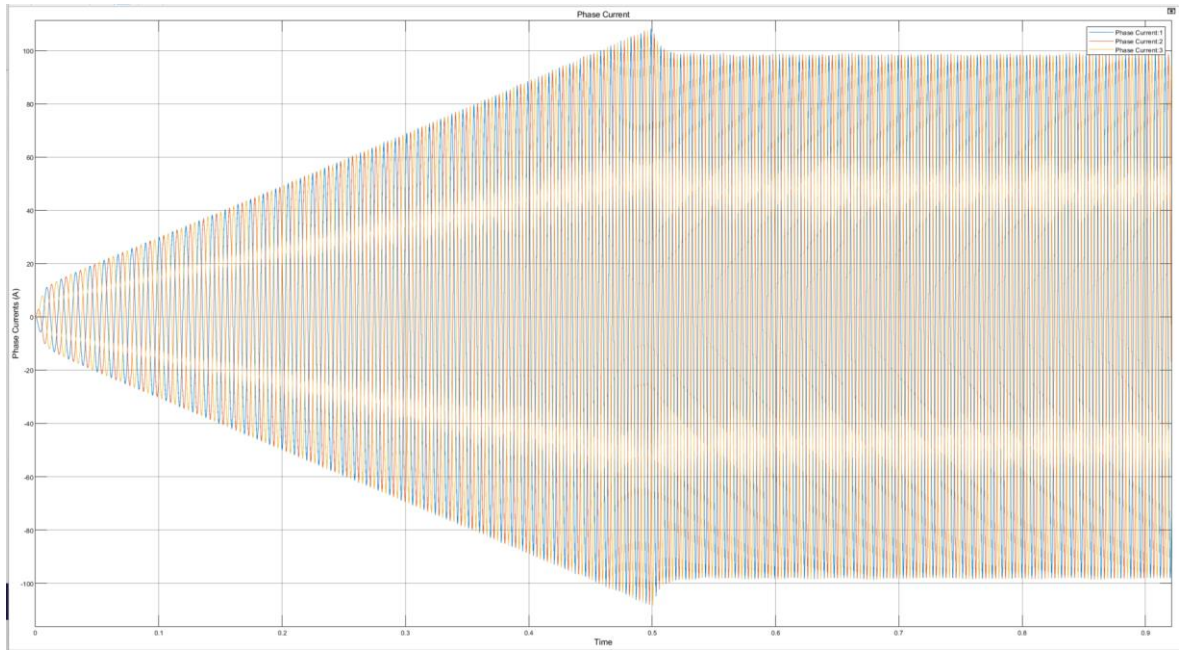


Figure 57:Phase Currents during start-up

The required current magnitude is 98A as per the experiments, by fine tuning the control system, the currents were kept in order after reaching the steady state.

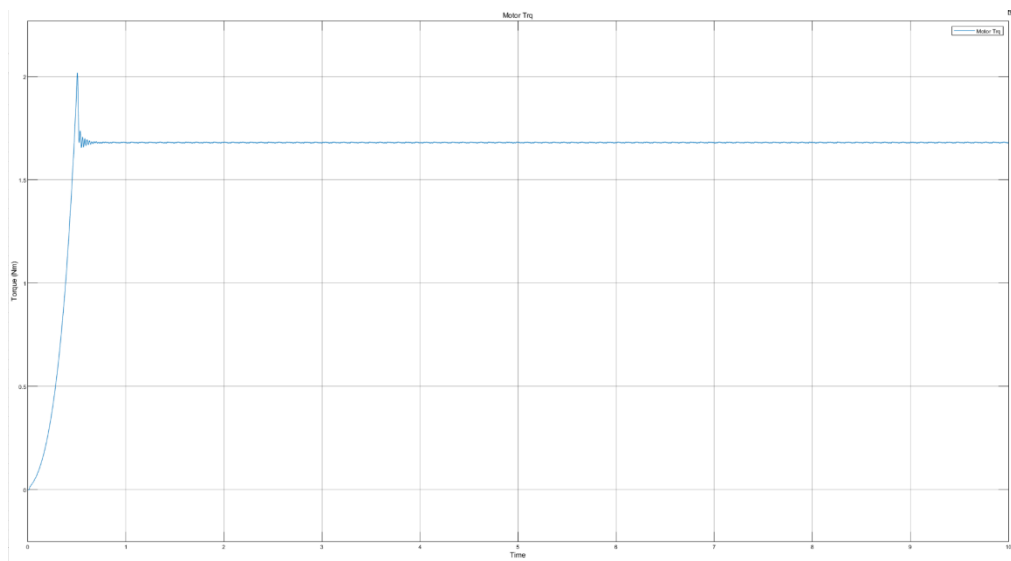


Figure 58:Torque

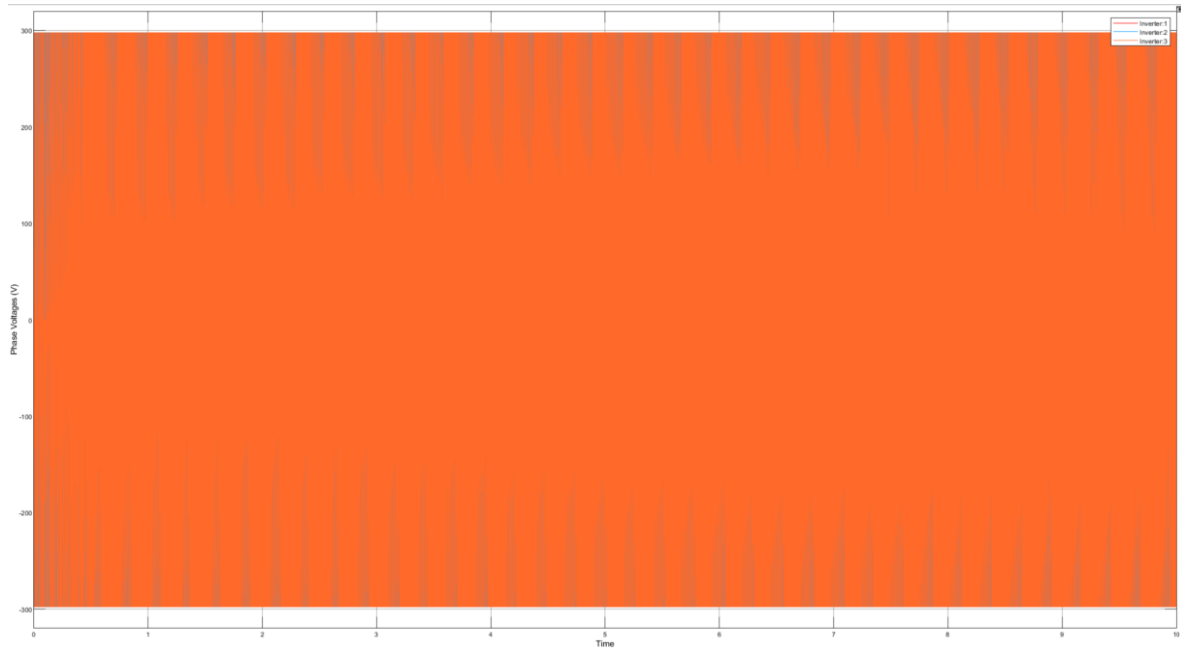


Figure 59: Phase Voltages

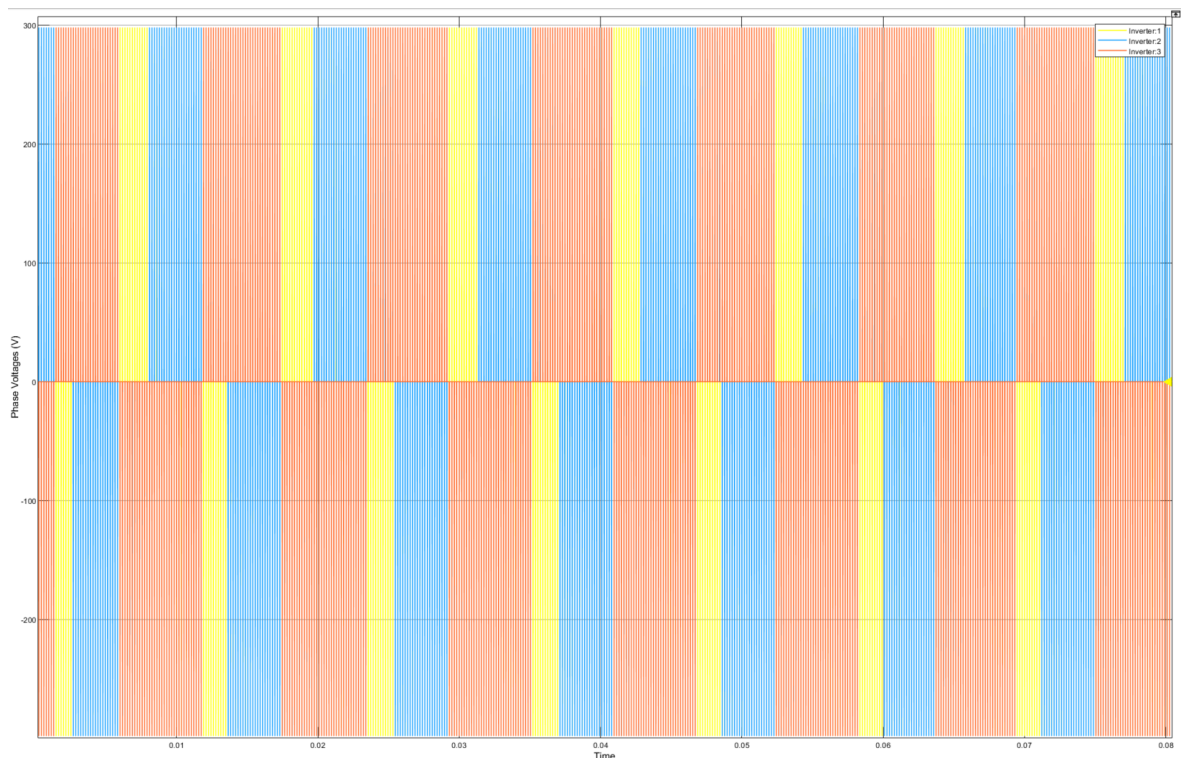


Figure 60: Detailed Square waves after DC-AC Conversion

Case 4:

Reference Output Speed- 314 rad/s

Inverter Switching frequency: 5250 Hz: 32986 rad/s

The process for calculating the gain values of PI controller for both inner current loop and outer speed loop remains the same and for the purpose of stability and easier current control. The current controller bandwidth is taken as $1/20^{\text{th}}$ of switching frequency and the bandwidth of speed controller is taken as $1/20^{\text{th}}$ of current controller.

Inner Current Controller:

Proportional Gain: $K_P = 0.54151$

Integral gain: $K_I = 57.370$

Outer Speed Controller:

Proportional Gain: $K_P = 4.581$

Integral gain: $K_I = 75.564$

Sample Time: $3.031e^{-5}$ s

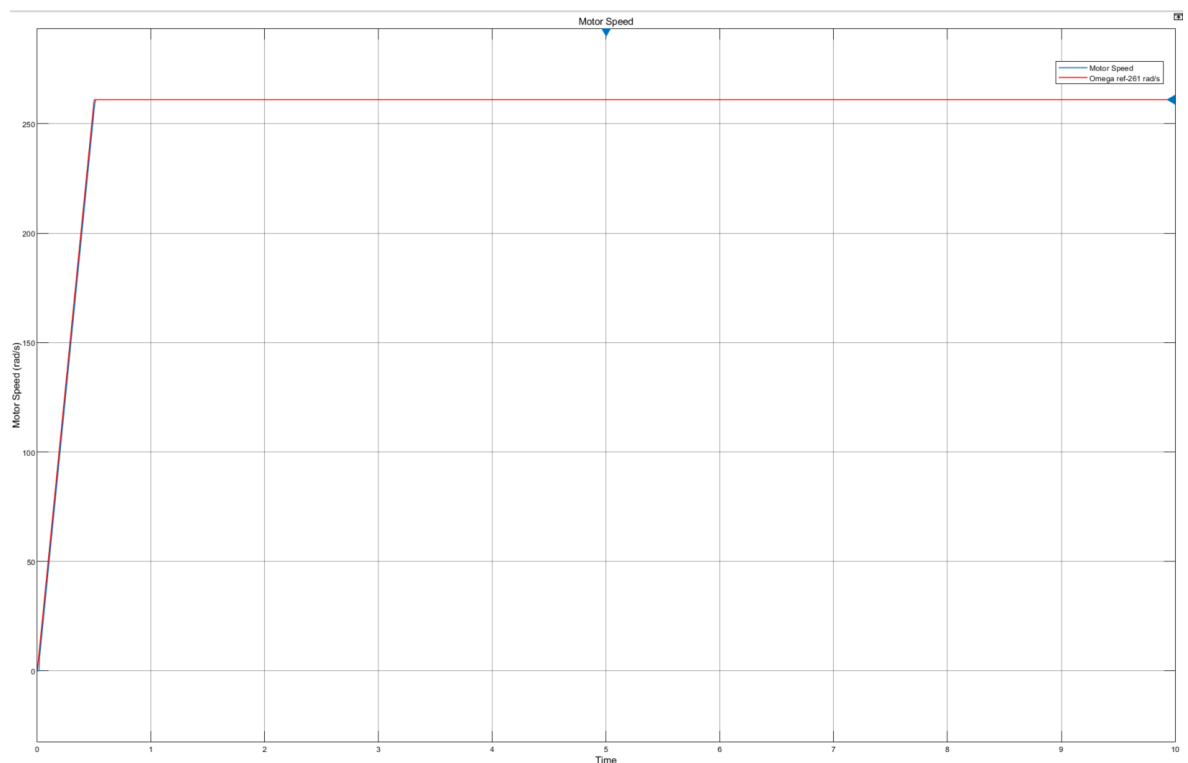


Figure 61: Motor Speed

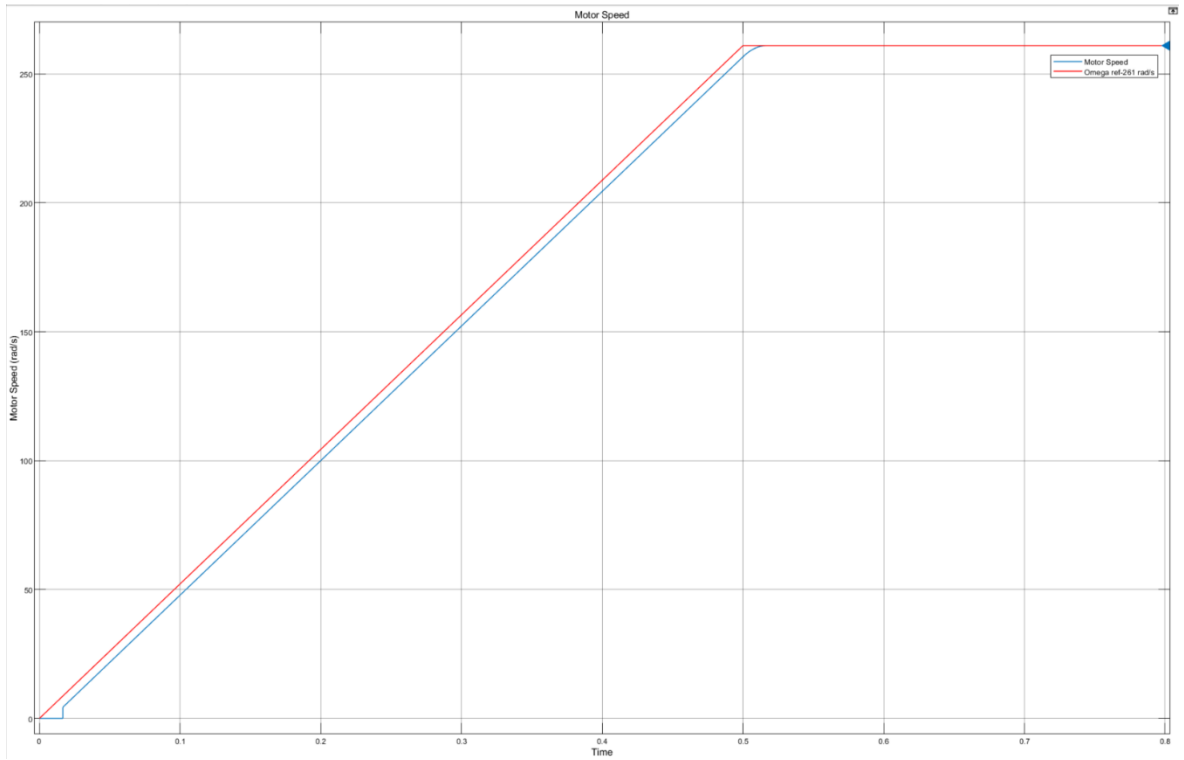


Figure 62: Detailed Motor Speed Figure

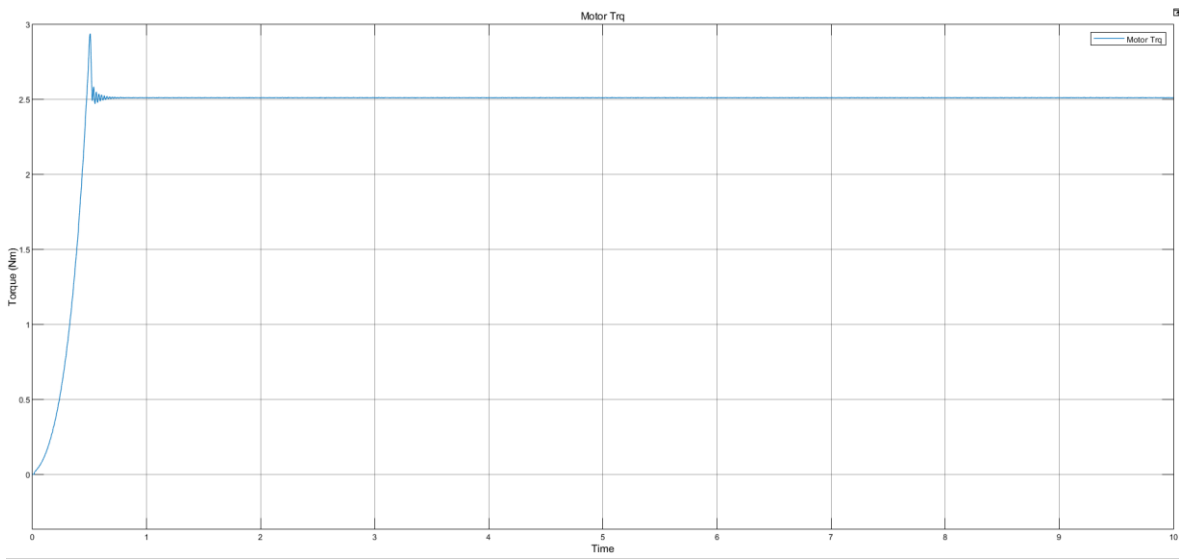


Figure 63: Motor Torque

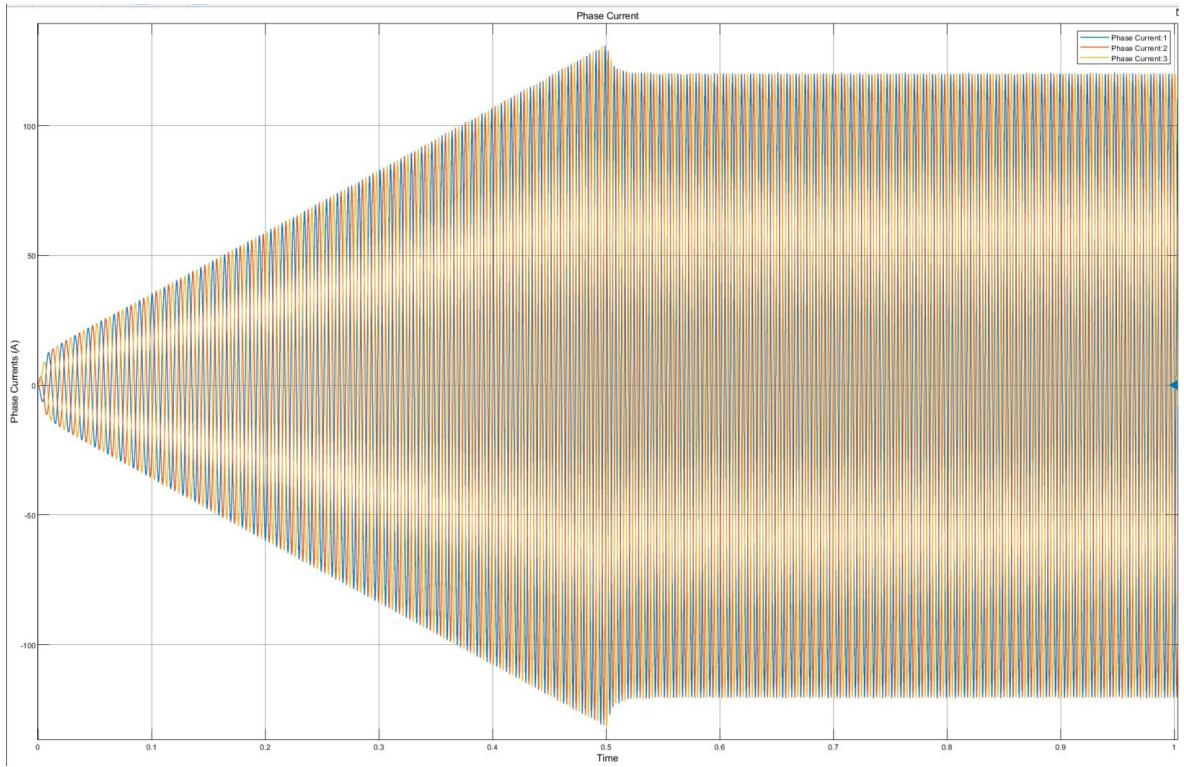


Figure 64: Phase Currents during start-up

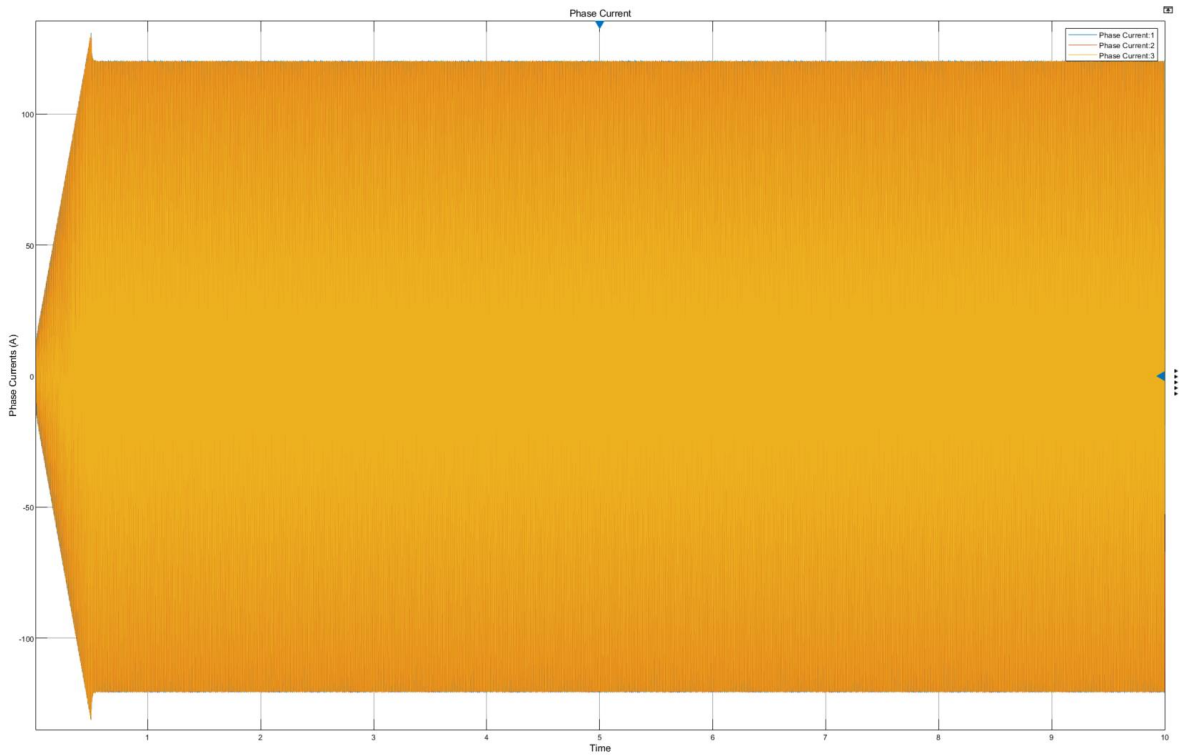


Figure 65: Phase Currents

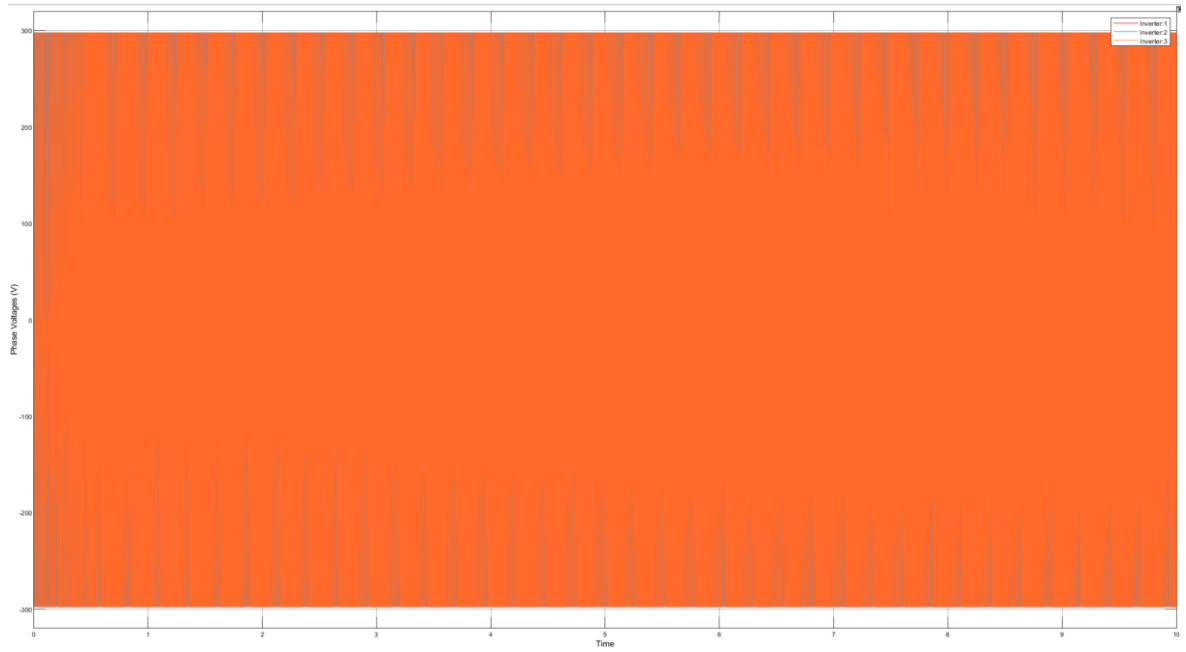


Figure 66: Phase Voltage

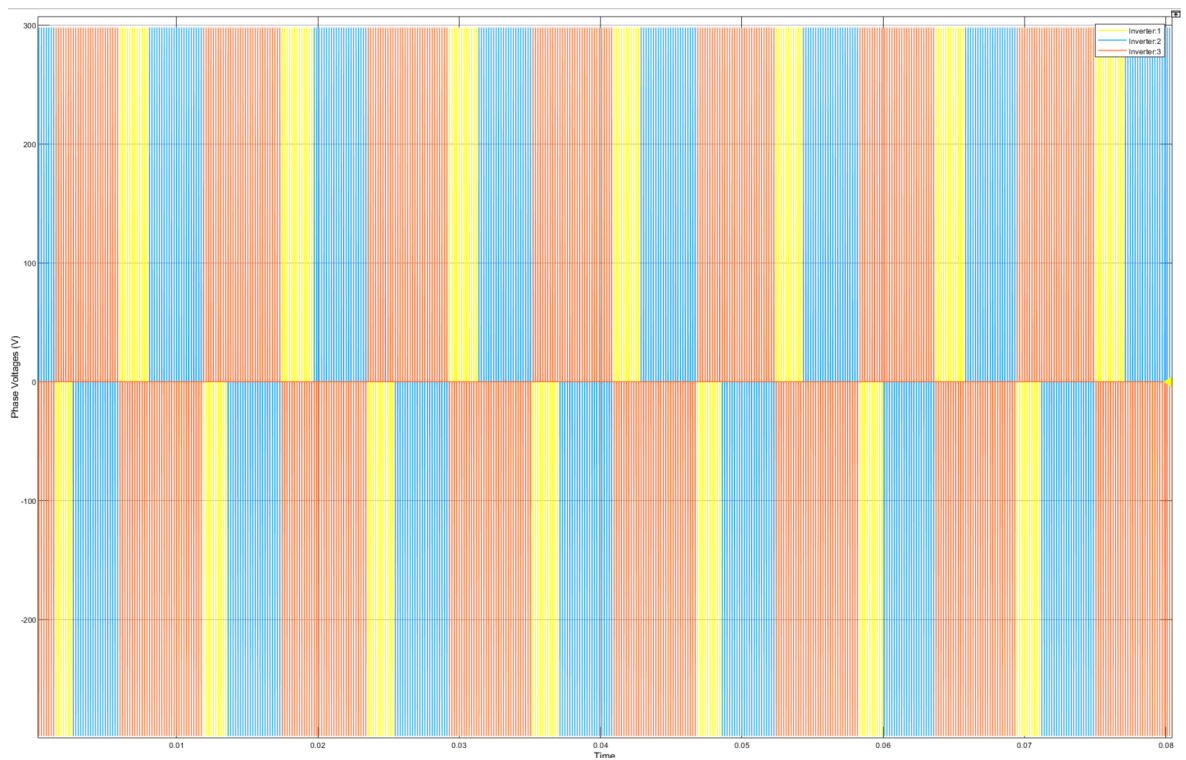


Figure 67: Detailed Square Waves from Inverter

Transient Analysis:

Case 1:

Unlike steady state analysis, transient includes variations in speed and the reference speed command is given as,

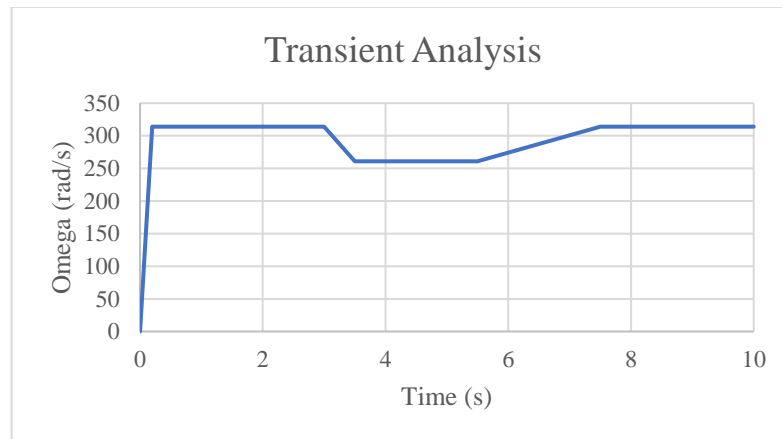


Figure 68: Transient Speed Command

For transient case, the inverter switching frequency is kept at a constant value of 5250Hz and the gain values were calculated based on that.

Inner Current Controller:

Proportional Gain: $K_P = 0.54151$

Integral gain: $K_I = 57.370$

Outer Speed Controller:

Proportional Gain: $K_P = 4.581$

Integral gain: $K_I = 75.564$

Sample Time: $3.031e^{-5}$ s

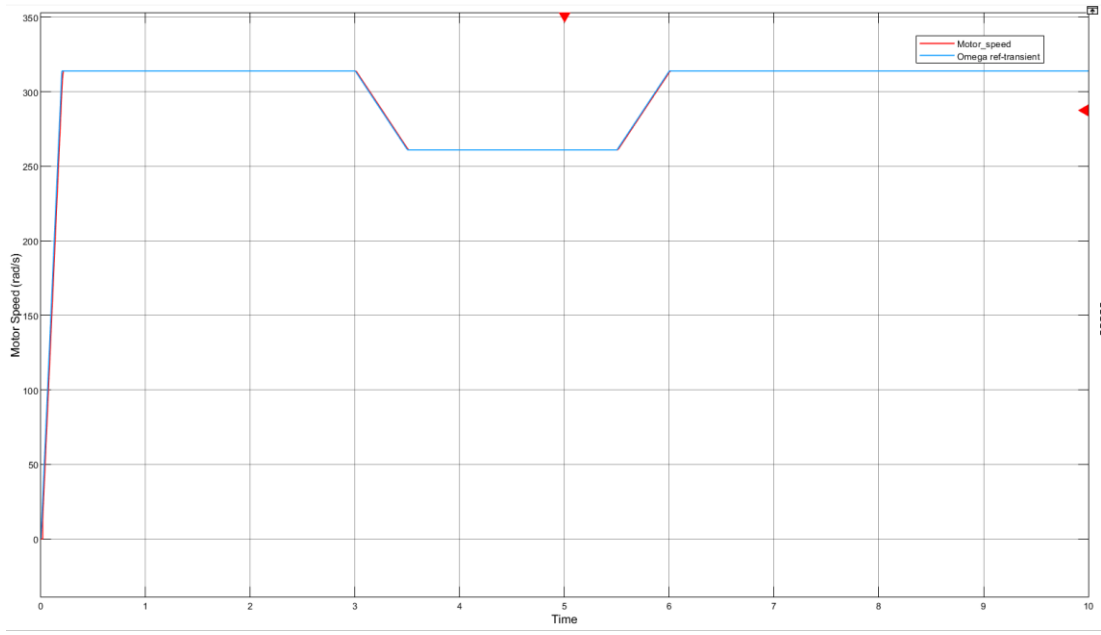


Figure 69: Motor Speed

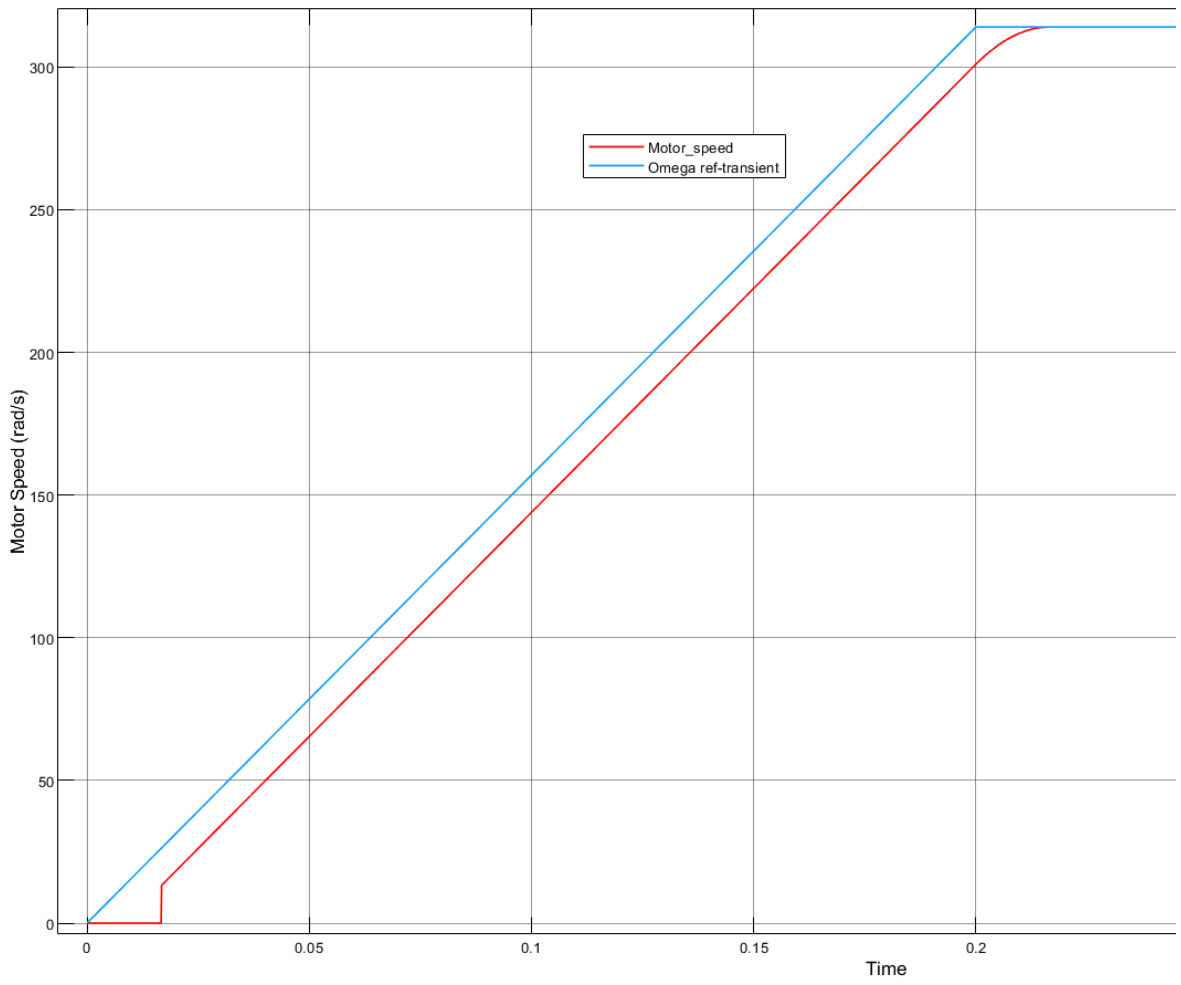


Figure 70: Detailed Motor Speed Result-Motor Start-up

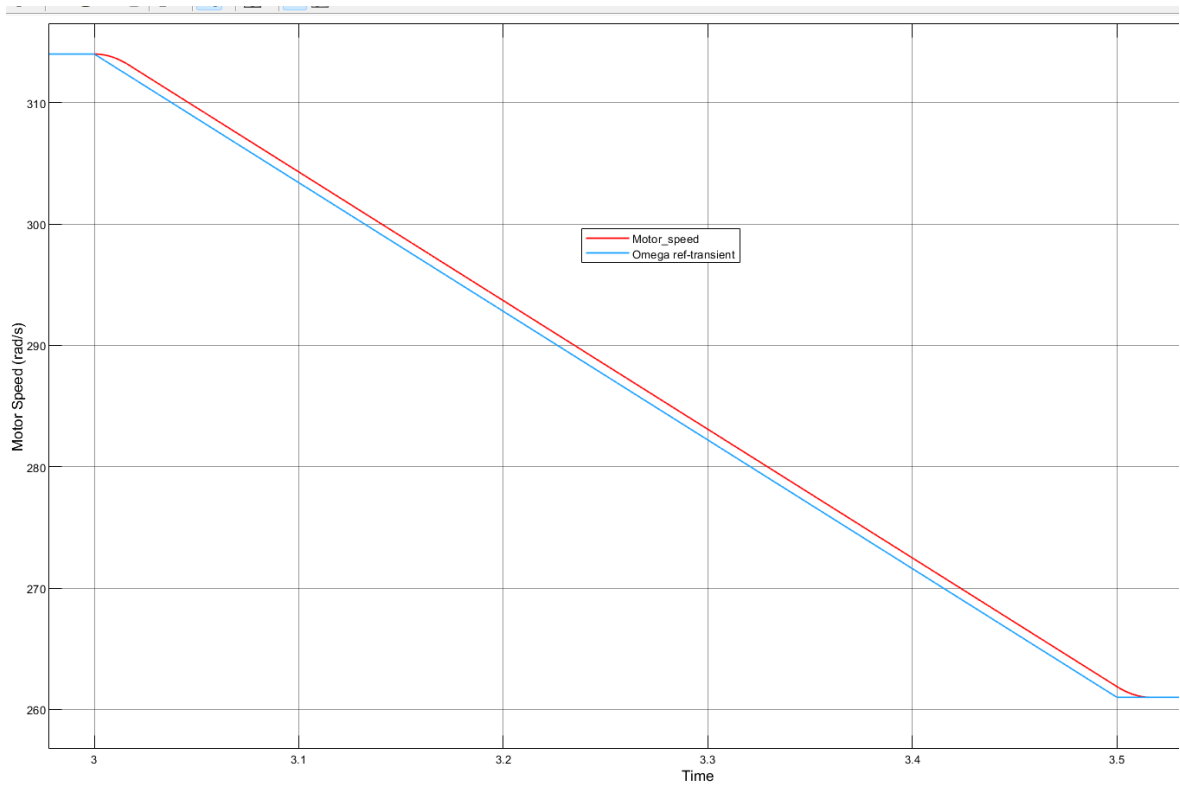


Figure 71: Detailed Speed Difference during the first speed reduction

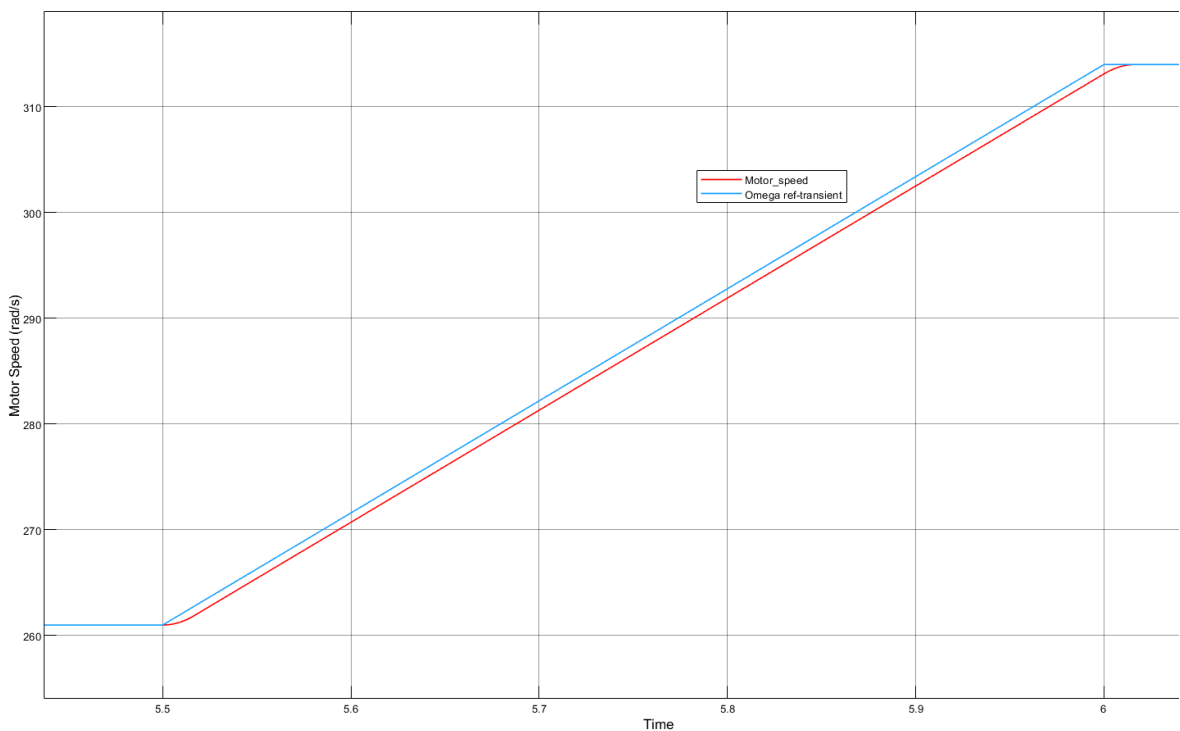


Figure 72: Detailed Motor speed difference while reaching the steady state

Figure 35,36 and 37 shows how the induction motor FOC algorithm acts during the transient reduction and increment of speed command. There was no major disturbance observed in the simulation.

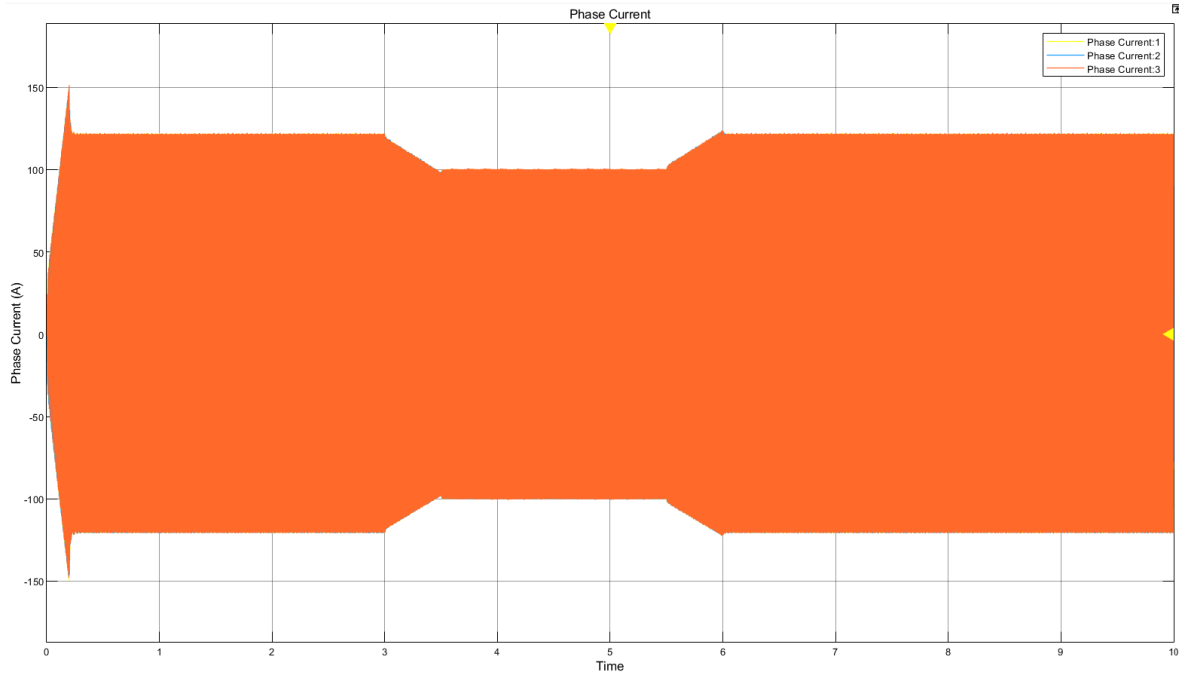


Figure 73:Phase Current

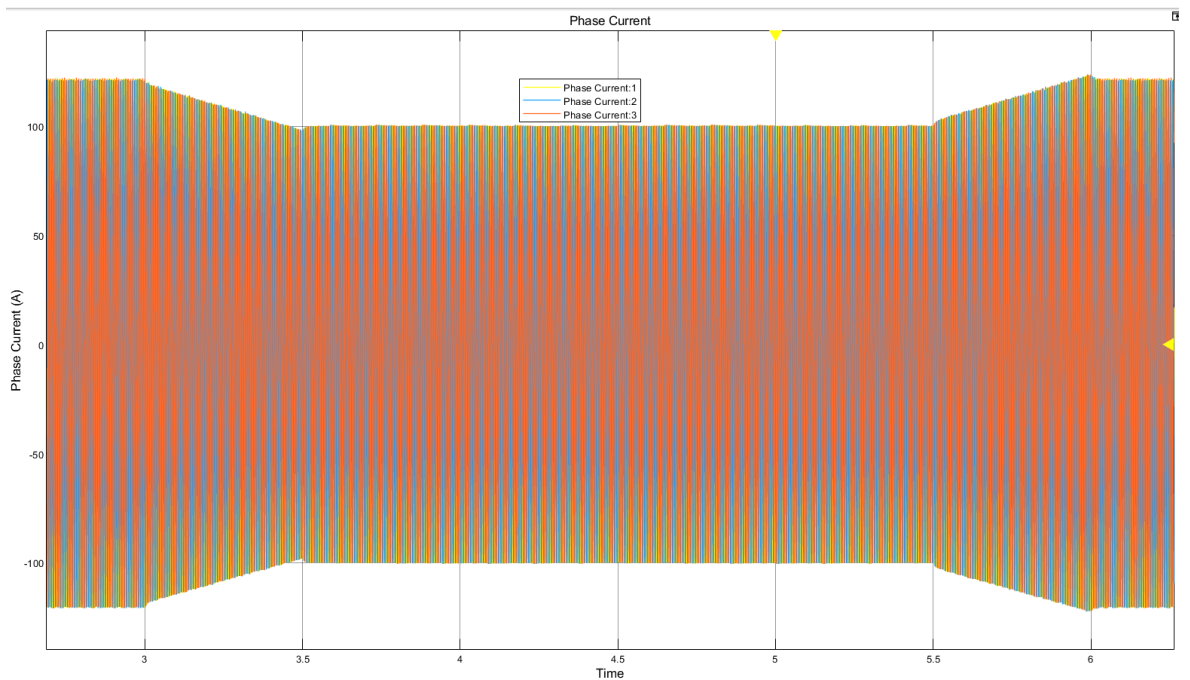


Figure 74:Detailed Image during the reduction and increment of speed

During the transient analysis, one of the points that was considered while selecting the switching frequency was the resulting phase current should not cross the maximum current (i.e) 250A throughout the simulation. While performing the iterations to find a suitable switching frequency, for this particular speed command, it was observed that the switching frequency should be less than 6kHz to get a stable output.

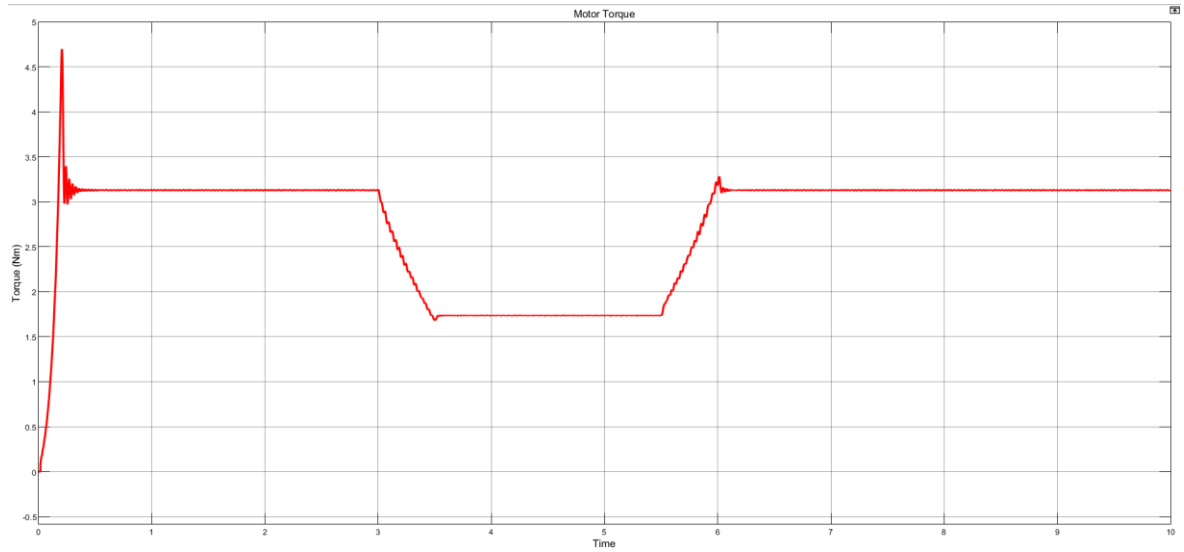


Figure 75: Torque

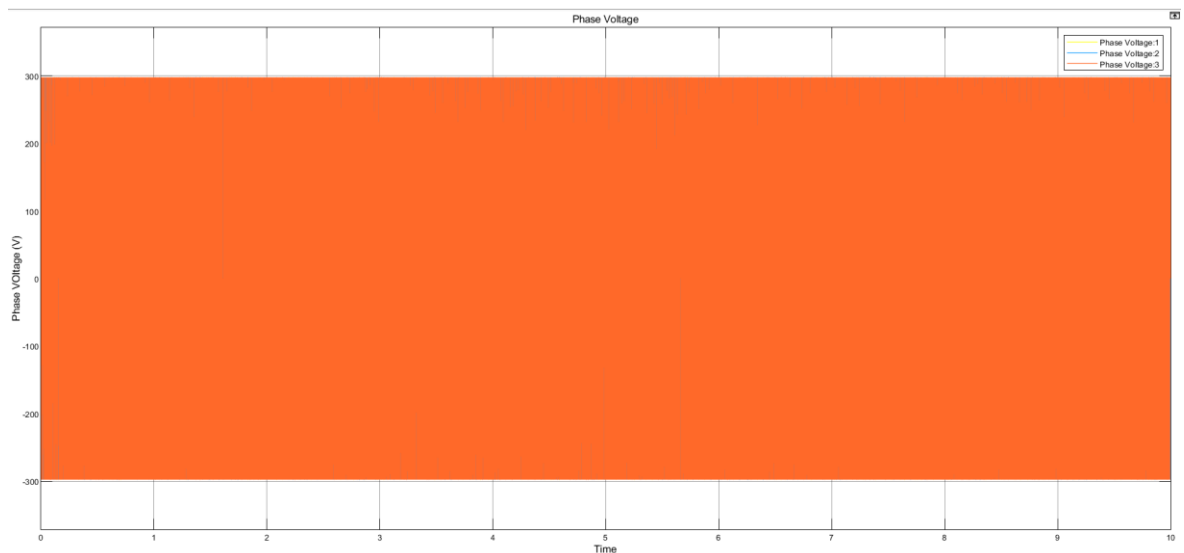


Figure 76: Phase Voltage

Case 2:

For the Final Simulation, the speed command was given in such a way that it has consecutive increment and reduction in speed.

For transient case, the inverter switching frequency is kept at a constant value of 7000Hz and the gain values were calculated based on that.

Inner Current Controller:

Proportional Gain: $K_P = 0.722$

Integral gain: $K_I = 69.827$

Outer Speed Controller:

Proportional Gain: $K_P = 6.108$

Integral gain: $K_I = 134.33$

Sample Time: $2.2736e^{-5}$ s

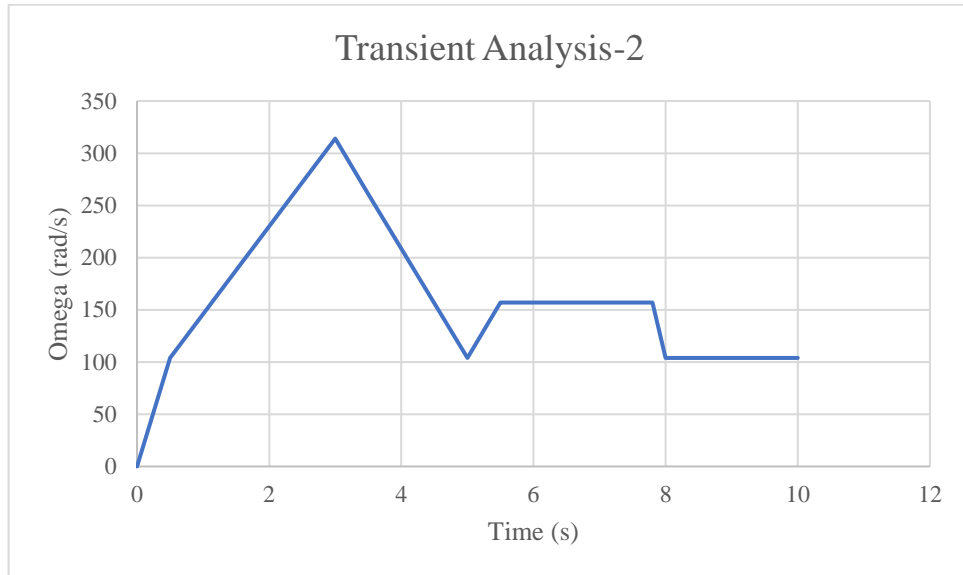


Figure 77: Speed Command for Transient Analysis-2

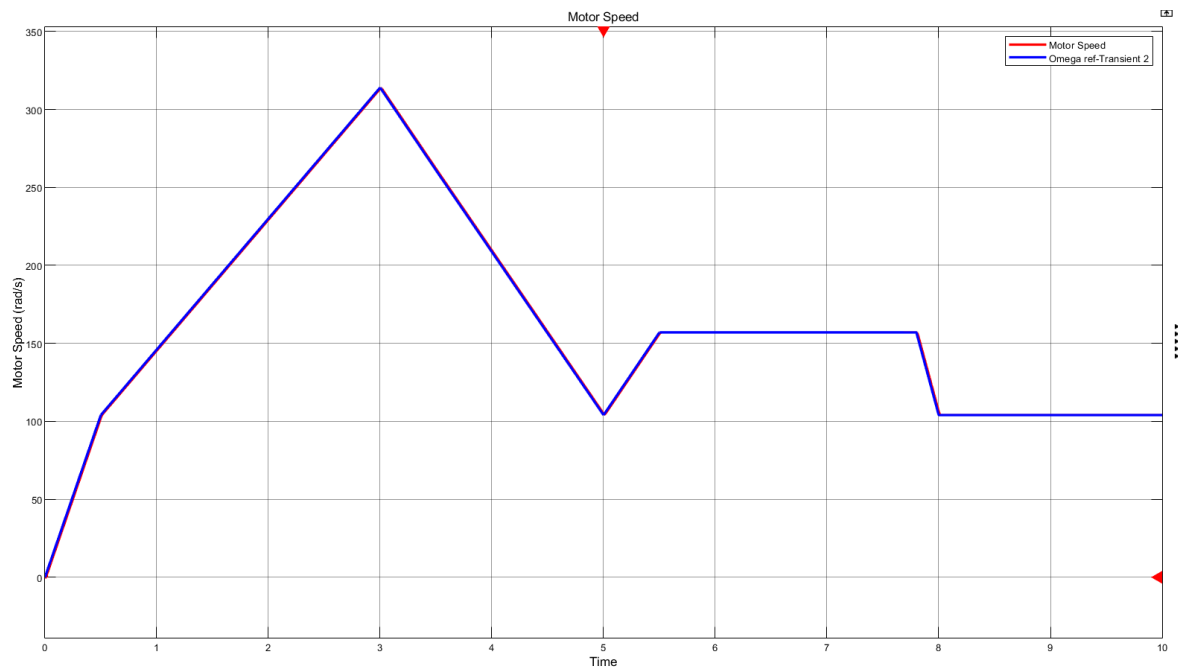


Figure 78: Motor Speed-transient -2

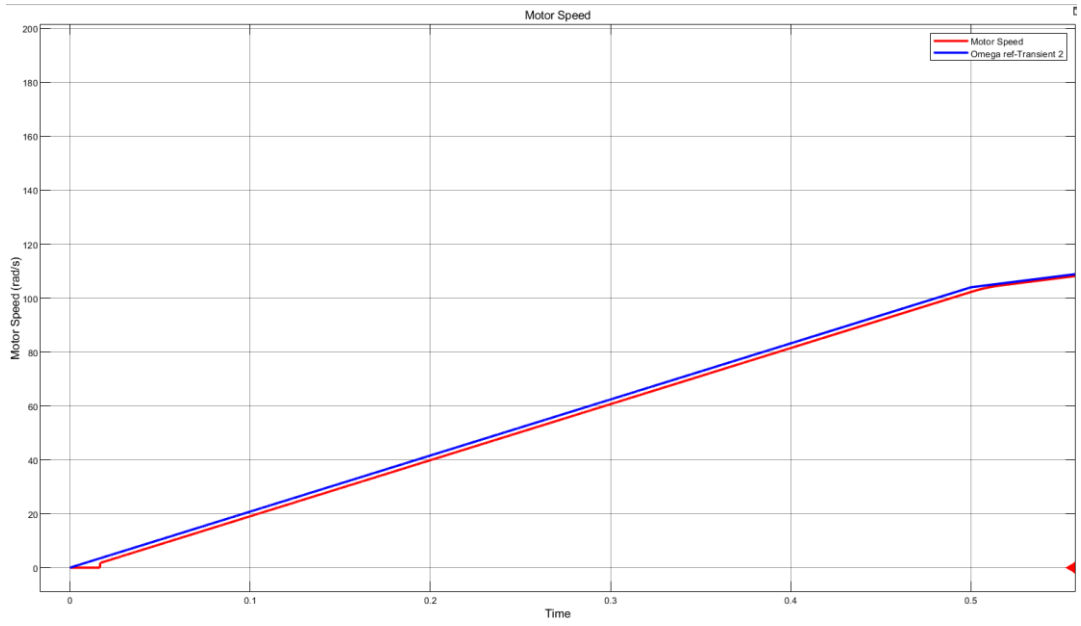


Figure 79: Detailed Picture of lag between speed reference and result

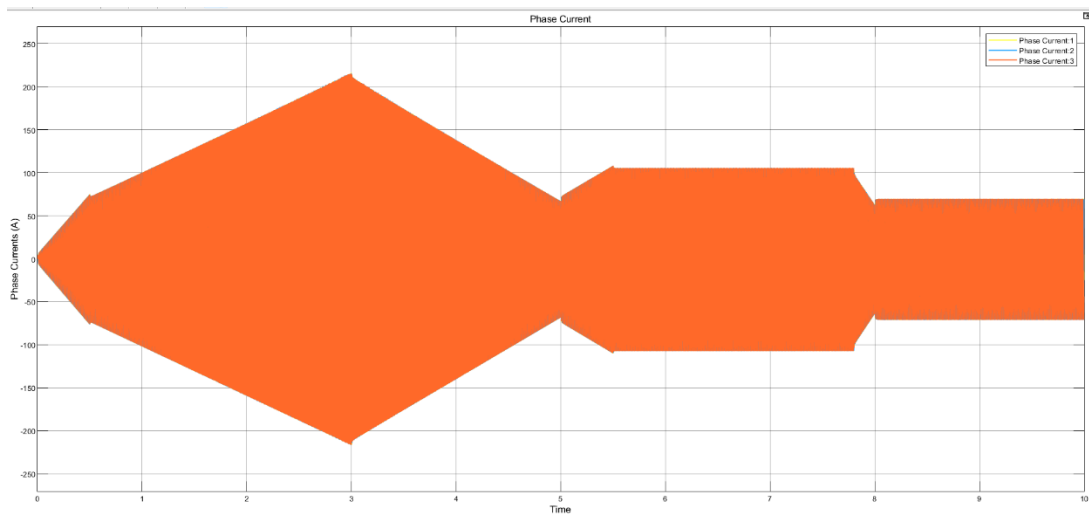


Figure 80: Phase Current

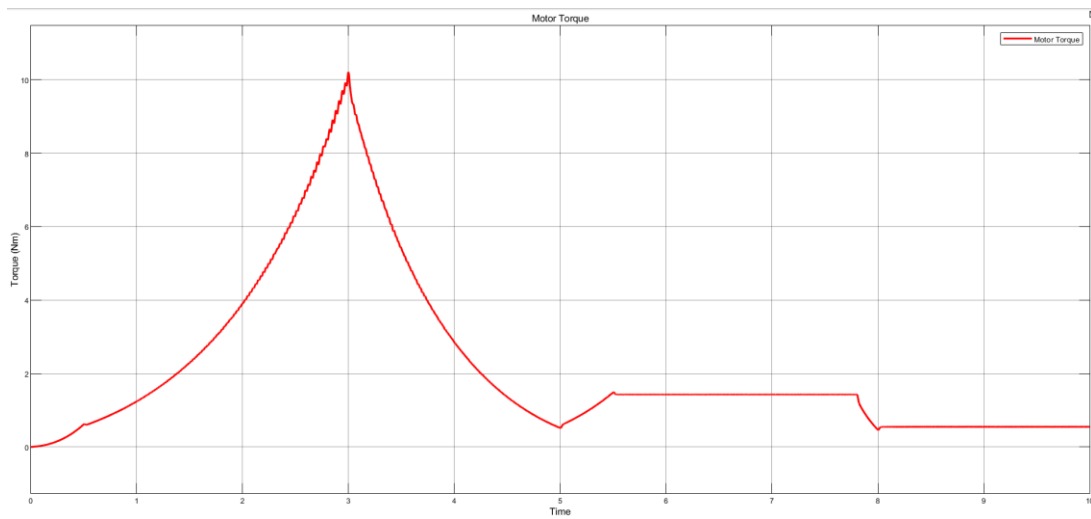


Figure 81: Torque

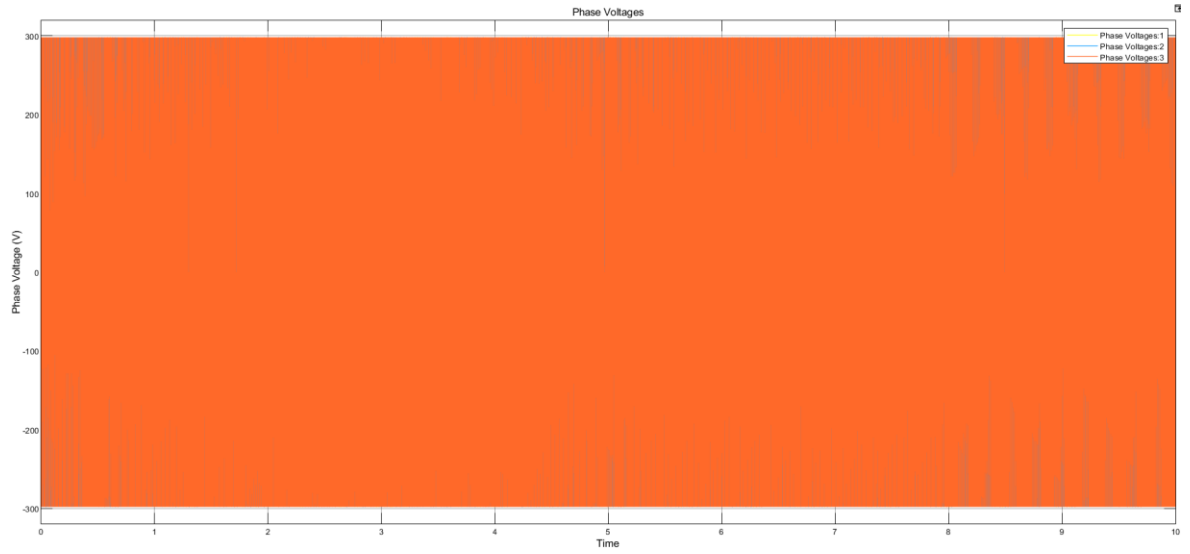


Figure 82:Phase Voltage

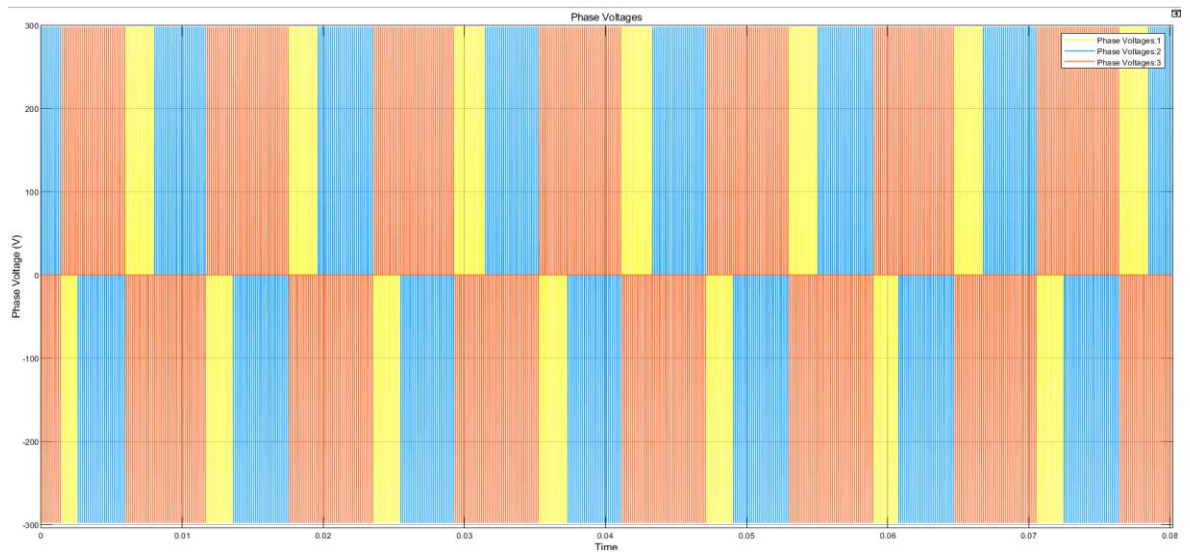


Figure 83:Resulting Square Wave

Conclusion

Basic theory of Induction motor and motor control have been studied and in the Simulink Platform simulations were performed and the results have been compared with the laboratory experimental values.

The magnitude of current during the start-up of the IM simulation depends on the reference speed profile. The starting currents are higher given that initial speed reference at 0 seconds is non zero, (i.e) by giving the speed reference as 314 rad/s at 0 seconds.

The current control is the crucial part is stabilizing the speed. For a more stable simulation, it is always preferred to choose current control bandwidth based on $1/20^{\text{th}}$ of inverter switching frequency. Here $1/20^{\text{th}}$ indicates that the current is sampled once every switching period.

Incorrect results can be expected when the sampling time is assumed incorrectly for speed measurement and theta measurement. As these variables determine the magnitude of the measured I_D and I_Q while converting from ab to dq stator current vectors for FOC. Overall, IFOC method proves to be useful in IM control

Further development of this topic can be performed by implementing Fuzzy logics and Genetic Algorithm which can accurately predict the gains for the current and speed control loops.

Alternate ways of motor control like DTC (Direct Torque Control) can also be employed and the motor can be tested to find the most efficient and performance driven motor control method

List of Abbreviations

- PWM – Pulse Width Modulation
- IGBT - Insulated Gate Bipolar Transistor
- FOC – Field Oriented Control
- CVH – Constant volts-Hertz
- PI – Proportional Integral
- IFOC – Indirect Field Oriented Control
- DTC- Direct Torque Control
- PID – Proportional Integral Derivative

Bibliography

1. A.Kumar, T. (2015). Direct Field Oriented Control of Induction Motor Drive. *2015 Second International Conference on Advances in Computing and Communication Engineering*, 219-223.
2. Awdaa M.A, O. A. (2021). A Comparative Study between V/F and IFOC Control for Three-Phase Induction Motor Drives. *Iop Conference Series: Materials Science and Engineering*, 2-13.
3. Bose, B. K. (2002). Chapter 2 AC Machines for Drives. In B. K. Bose, *Modern Power Electronics and AC Drives* (pp. 29-98). NJ Prentice Hall.
4. Electrical4U. (n.d.). *Construction of Three Phase Induction Motor*. Retrieved from Electrical4U: <https://www.electrical4u.com/construction-of-three-phase-induction-motor/>
5. Electrical4U. (n.d.). *Induction Motor Rotor*. Retrieved from Electrical4U: <https://www.electrical4u.com/induction-motor-rotor/#:~:text=Rotor%20as%20the%20name%20suggests,rotor%20is%20of%20two%20types%3A&text=Wound%20Type%20Rotor%20or%20Slip%20Ring%20Type%20Rotor>
6. Kim, S.-H. (2017). Chapter 2 - Control of direct current motors. In S.-H. Kim, *Electric Motor Control* (pp. 39-93). Elsevier.
7. Kim, S.-H. (2017). Chapter 6 - Current regulators of alternating current motors. In S.-H. Kim, *Electric Motor Control* (pp. 247-264). Elsevier.
8. Kim, S.-H. (2017). Chapter 7 - Pulse width modulation inverters. In S.-H. Kim, *Electric Motor Control* (pp. 265-340). Elsevier.
9. MathWorks Inc. (n.d.). *Power Electronics Control Design*. Retrieved from MathWorks Support: <https://www.mathworks.com/solutions/power-electronics-control/induction-motor-speed-control.html>
10. Mathworks. (n.d.). *Motor Control Blockset-Blocks*. Retrieved from Mathworks: https://www.mathworks.com/help/mcb/referencelist.html?type=block&s_tid=CRUX_topnav

11. Mohan, N. (2015). Induction Machine Equations in Phase Quantities: Assisted by Space Vectors. In N. Mohan, *Advanced electric drives: Analysis, control, and modeling using MATLAB/Simulink*. (pp. 6-26). John Wiley & Sons.
12. NI. (2020). *PID Theory Explained*. Retrieved from NI: <https://www.ni.com/cs-cz/innovations/white-papers/06/pid-theory-explained.html>
13. Ong, C.-M. (1997). Chapter 6- Three-Phase Induction Machine. In C.-M. Ong, *Dynamic Simulation Of Electric Machinery Using MATLAB/SIMULINK* (pp. 167-243). Prentice Hall.
14. Schofield, J. R. (1995). Direct torque control-DTC [of induction motors]. *IEE Colloquium on Vector Control and Direct Torque Control of Induction Motors*, 1/1-1/3.
15. Trzynadlowski, A. M. (2001). 4 - Power electronic converters for induction motor drives. In A. M. Trzynadlowski, *Control of Induction Motors* (pp. 55-92). Academic Press.
16. Trzynadlowski, A. M. (2001). 5 - Scalar control methods. In A. M. Trzynadlowski, *Control of Induction Motors* (pp. 93-105). Academic Press.